Spring 1-1-2010

Impact of the Rate of Heating on the Thermal Consolidation of Compacted Silt

Abdalla El Tawati
towati@yahoo.com

IMPACT OF THE RATE OF HEATING ON THE THERMAL CONSOLIDATION OF COMPACTED SILT

by

Abdalla El Tawati

B.S., University of Garyounis, 1997

A thesis submitted to the

Faculty of the Graduate School of the

University of Colorado in partial fulfillment

of the requirement for the degree of

Master of Science

Department of Civil and Environmental Engineering

2010

This thesis entitled:

Impact of the Rate of Heating on the Thermal Consolidation of Compacted Silt
written by Abdalla El Tawati
has been approved by the Department of Civil and Environmental Engineering

_____

Professor John McCartney (committee chair)

_____

Professor Dobroslav Znidarcic

_____

Professor Hon-Yim Ko

Date_____

The final copy of this thesis has been examined by the signatories, and we

Find that both the content and the form meet the acceptable presentation standards

Of scholarly work in the above mentioned discipline.

El Tawati, Abdalla (M.S. Civil Engineering, Department of Civil, Environmental, and Architectural Engineering)

Impact of the Rate of Heating on the Thermal Consolidation of Compacted Silt

Thesis directed by Professor John McCartney

ABSTRACT

This study involves an evaluation of the impact of the heating rate on the volume change of compacted silt. A temperature-regulated oedometer refurbished as part of this study was used to measure thermally induced volume changes. It was found that the impact of heating rates on the thermally induced volume change in soils lies in the difference between the drained and undrained behavior of soils. When a soil is heated in undrained conditions, the particles and water will expand at the same rate as the rate of heating. In addition, the difference in the coefficients of thermal expansion of the soil particles and the water during heating will result in the generation of excess pore water pressures. If drainage is allowed to occur, these excess pore water pressures will dissipate, leading to a time-dependent consolidation of the soil.

The dissipation of thermally induced excess pore water pressure was found to depend on the rate of heating. If the rate of heating is slow, the excess pore water pressures will be able to dissipate at a constant rate, leading to a corresponding decrease in volume. The rate of consolidation will be greater than the rate of thermal expansion of the soil particles and water. If a soil is heated quickly, the particles and water will expand much faster than the dissipation of excess pore water pressure. In this case, the thermally induced excess pore water pressures will be generated instantaneously and a consolidation process will occur afterward. In this case, the

amount of thermal consolidation was found to be greater than the amount of thermal expansion, leading to a greater net volume change than in the case of slow heating.

ACKNOWLEDGEMENT

The author wishes to thank Professor John Scott McCartney, for his assistance, inspiration, and enthusiasm throughout this research. Deserving of additional thanks for their insight, enthusiasm and assistance are: Professor Dobroslav Znidarcic, and Professor Hon-Yim Ko.

Table of Contents

List of Tables

List of Figures

1. INTRODUCTION

1.1. Motivation

Building foundations have recently been proposed for use as ground source heat pumps (GSHPs). These energy foundations are part of the effort in the United States to increase our energy efficiency by 20% over the next 20 years. GSHPs exchange heat with the subsurface soil and rock, which have a relatively steady temperature throughout the year compared with that of the outside air, in order to reduce the electricity demands for building heating and cooling (Brandl 2006). 71% of the electricity generated in the U.S. and 53% of its natural gas is consumed by commercial and residential buildings (EIA 2008). Buildings consume approximately 39% of the primary energy in the U.S., of which heating and building systems consume 20% of this fraction (EIA 2008). Despite their potential to address this building energy issue, temperature changes in the soil during energy foundation heat exchange processes may lead to irreversible volume changes (Campanella and Mitchell 1968). These volume changes can potentially result in movement of the foundation or changes in capacity.

1.2. Problem Statement

To address the temporal demands in heating and cooling on a daily basis, energy foundations may change in temperature at different rates. These different rates of heating and cooling may lead to different amounts of soil volume change. Specifically, a rapid increase in soil temperature will lead to the development of excess pore water pressure due to the difference in the coefficient of thermal expansion of the pore water and the mineral solids (Campanella and Mitchell 1968). The dissipation of this excess pore water pressure over time results in a volume change. The rate of temperature change may have a role in dictating the drainage condition of the heated soil, and consequently in the amount and type of volume change. Although several studies

in the literature have evaluated the ultimate changes in volume due to temperature changes, there have been relatively few studies on the impact of the rate of temperature change on the amount of soil volume change.

1.3. Objectives

This study involves evaluation of time rate of thermally induced volume change behavior in saturated compacted silt in a temperature controlled oedometer. In order to understand the impact of the rate of heating on the volume change behavior, the specific research objectives of this study are to:

i. Evaluate the mechanisms of thermal volume change in saturated soils and evaluate the impact of rate dependency.
ii. Refurbish and update a temperature-regulated oedometer device developed by McGinley (1983) for measurement of thermally induced volume change.
iii. Evaluate the isothermal compression curve of saturated, compacted silt to identify the preconsolidation stress and deformation properties.
iv. Perform heating tests for specimens with known stress history to understand the role of heating rate.

1.4. Scope

Chapter 2 includes a review of the mechanisms of thermally-induced volume change. Chapter 3 presents the geotechnical properties of the silt used in the experimental portion of this study. Chapter 4 includes a description of the experimental setup. Chapter 5 presents the experimental procedures for both the isothermal consolidation and thermal consolidation tests, including specimen setup. Chapter 6 includes a summary of the results, which are evaluated and discussed in Chapter 7. The conclusions of this study are summarized in Chapter 8.

2. LITERATURE REVIEW

2.1. Introduction

The volume change behavior of soils arising from changes in temperature is a topic which has been evaluated by many researchers. The motivation for early studies on the effect of temperature on soil behavior was related to the temperature change occurring within a soil sample during sampling, storage, and transportation to the laboratory. Consequently, most of the early research efforts concentrated on investigating the behavior of soils under temperature range up to 50°C **(**Gray 1936, Finn 1951, Paaswell 1967, Plum and Esrig 1969).

However, soils are subjected to a much higher levels of temperature in many different circumstances. Soil around buried high-voltage electric cables (Abdel-Hadi and Mitchell 1981) or oil and gas pipe lines (Slegel and Davis 1977) may be submitted to elevated temperatures. In nuclear waste disposal facilities, clay is used as a barrier material and exposed to an elevated temperature during a long period of time (Baldi et al. 1988). More recently, incorporation of heat exchangers into drilled shaft foundations induces cycles of heating and cooling to the surrounding soil. The growing interest in these applications has led, in the last decades, to the need to establish a thorough understanding of the thermomechanical behavior over a larger scale of temperature changes up to 100°C. In this regard, extensive research has been done on many different types of saturated fine-grained soils to investigate their response to the combined effects of stress and temperature as a host of geological information for such circumstances (Demars and Charles 1982, Baldi et al. 1988, Towhata et al. 1993, Cui et al. 2000, and others).

The main purpose of this chapter is to review the mechanisms of thermal-induced volume change, the experimental observations and main conclusions of different researchers and soils, and the analytical models that have been developed to explain the experimental observations.

This chapter will include a critical assessment of the experiments, focusing on discrepancies in the findings of different authors. Finally, the areas needing further research will be summarized.

2.2. Mechanisms of Temperature-Induced Volume Change

Before discussing the observations from the literature, the physical mechanisms which have been identified as sources of thermally-induced volume change in soils are reviewed. Thermally-induced volume change in water-saturated soils has been associated with three different mechanisms, which may occur simultaneously.

The first mechanism, identified by Campanella and Mitchell (1968), is the development of positive excess pore water pressure during a rapid increase in temperature. This increase in pore water pressure will occur in most soils, even when the soil is maintained under drained conditions. The excess pore water pressure results primarily from the difference in the coefficient of thermal expansion of the pore water and the mineral solids. Typical coefficients of linear thermal expansion for water and different soil minerals are summarized in Table 2.1. In general, water up to 20 times more for a given increase in temperature than most soil minerals.

Table 2.1: Linear coefficients of thermal expansion of water and common soil minerals and rocks

Material	Coefficient of linear thermal expansion, α ($\times 10^{-6}$/°C at 20 °C)
Water [a]	69
Muscovite [b]	10.6
Kaolinite [b]	11.9
Halloysite [b]	8
Quartz [c]	12
Calcite [c]	5
Marbles [c]	5.5

a From Lide 2010
b From McKinstry 1965 (values estimated assuming the expansion coefficients to be independent of temperature)
c From Lamond and Pielert 2006

The differential expansion between the water and soil particles will lead to an excess pore water pressure in the soil, which will dissipate as a function of time toward a drainage boundary. Specifically, as excess pore pressures develop, a pressure gradient is established producing a flow of pore water in or out of the soil until the excess pore water pressures have dissipated. Dissipation of this pressure results in a time-dependent volume change (decrease) of the soil as pore water flows out, resembling the primary consolidation behavior observed during a change in effective stress. The lower the soil's hydraulic conductivity, the longer the time required for the excess pore water pressure to dissipate.

The second mechanism described by Paaswell (1969) and Mitchell and Soga (2005) is the reduction in the shearing resistance at individual particle contacts due to an increase in temperature. An increase in temperature works as an activation energy which disrupts the bonding of the interparticle- adsorbed water layer. In other words, the heat causes a thermal agitation of the bond water atoms, enabling them to move out of the bond layer with greater ease. This ease of movement can be looked to as a decreased resistance to shear at the boundary layer. As a consequence, there is a partial collapse of the soil structure and a decrease in void ratio until a sufficient number of additional bonds are formed to enable the soil to carry the stresses at higher temperature. This is analogous to secondary compression under an increase in effective stress.

The third mechanism (Paaswell 1967) corresponds to the decrease in pore water viscosity under elevated temperatures. The variation in the viscosity of free pure water viscosity with temperature can be estimated using the following expression (Hillel 1998):

$$\mu_w = 0.00239138 - 0.00046575\ ln(T) \tag{2.1}$$

where μ_w is the viscosity of water (Pa.s), and T is temperature (°C). The viscosity as a function of temperature is summarized in Table 2.2. The lower viscosity is expected to result in a slight increase in the amount of volume change during heating due to less frictional losses during outflow of water from the soil.

Table 2.2: Change in viscosity of pure water with temperature (Hillel 1998)

Temperature, T (°C)	Viscosity, μ_w (Pa.s x10^{-3})
0	1.787
5	1.519
10	1.307
20	1.002
30	0.798
40	0.653
50	0.547

This decrease in viscosity leads to an increase in the permeability of soil and subsequently the rate at which thermal-induced volume change occurs, as described by Kozeny-Carman equation (Mitchell and Soga 2005):

$$k = K\left(\frac{\gamma_w}{\mu_w}\right) \tag{2.2}$$

where k is the hydraulic conductivity, K is the absolute or intrinsic permeability, and γ_w is the unit weight of water. As the pore water flows more readily through soils with a higher permeability, an additional decrease in volume may be expected during dissipation of the excess pore water pressure.

2.3. Experimental Evaluation of Thermal Volume Change Behavior of Soils

2.3.1. Categories of Experimental Studies on Temperature Effects on Soils

The experimental testing of the thermomechanical behavior of soils is based on combinations of the two loading parameters: thermal and mechanical. Hence, two types of loading paths may be distinguished in experimental testing programs that involve the evaluation of the thermal volume change behavior of soils: mechanical (isothermal), thermal (isobaric). Therefore, the experimental studies on temperature effects on soils can be classifies to two main categories based on the loading path.

The first category involves the effect of temperature on the conventional stress-induced consolidation of saturated soils. Research within this category has been devoted to investigating the effect of temperature on consolidation characteristics such as coefficient of consolidation, compressibility, permeability, and void ratio; and has involved performing isothermal consolidation tests which correspond to mechanical loading at a given constant temperature (Gray 1936, Finn 1951, Tidfors and Sällfors 1989, Eriksson 1989, Boudali et al. 1994).

The second category of the research on thermomechanical volume change behavior of soils concerned with investigating the behavior of a soil subjected to a temperature variation at constant stress. The research in this category is performed by running heating tests at various stress levels, i.e. isobaric thermal consolidation tests (Paaswell 1967, Campanella and Mitchell 1968, Plum and Esrig 1969, Baldi et al. 1988, Sultan et al. 2002, Cekerevac and Laloui 2004).

A third category may be recognized which involves performing both the thermal and mechanical loading. Studies within this category have been dedicated to investigating the behavior of soils subjected to variations in both temperature and stress. Though, the two loading paths are not imposed simultaneously, in order to permit distinguishing their effects (Cekerevac

et al. 2005, Cui et al. 2009). Therefore, most of the experimental works done within this category are classified here under one of the two main categories depending on the main feature of the thermal volume change being investigated.

2.3.2. Isothermal Volume Change of Saturated Soils

2.3.2.1 Effect of Temperature on the Coefficient of Consolidation

The work performed by Finn (1951) was mainly to investigate the effect of temperature on the coefficient of consolidation and, c_v, the coefficient of volume compressibility, m_v, and the void ratio, e. Compression tests were performed on remolded clay using a portable consolidometer at temperature range between 5 and 26.6°C. It was concluded that the coefficient of consolidation does not vary appreciably with temperature for temperature range of 21 to 26.6°C, but varies considerably with temperatures in the range of 5 to 21°C. McGinley (1983) carried out isothermal oedometer tests at temperature levels between 26.7 and 85°C on two types of remolded clay (Georgia Kaolin, PI = 19%, and Smectite, PI =89%). For the two types of soils tested, it was observed that the coefficient of consolidation, c_v, is affected by the temperature level. At the same void ratio, higher values of c_v corresponded with higher temperature levels.

2.3.2.2. Effect of Temperature on Compressibility

Finn (1951) observed that both void ratio and compressibility determinations are not affected by changes in temperature within the range adopted in his tests (21 to 26.6°C). Similar observations were made by Campanella and Mitchell (1968) at temperature range between 24.7 and 51.4°C. Campanella and Mitchell (1968) carried out isothermal triaxial consolidation tests at various temperature levels on saturated Illite clay and showed that the slope of the compressibility curves was independent of temperature (Fig. 2.1). Many researchers have subsequently confirmed this behavior (Plum and Esrig 1969, Tidfors and Sällfors 1989,

Cekerevac and Laloui 2004, among others). As shown in Fig. 2.1, the higher the temperature, the lower the void ratio at any given consolidation stress as the weaker soil structures at the higher temperatures would have to decrease in volume in order to carry the effective stress.

The observations of Sultan et al. (2002) on Boom clay were not in full agreement with the behavior noted by Campanella and Mitchell (1968). The results of Sultan et al. (2002) in Fig. 2.2 indicate that the compression curves of four samples heated to 100°C and cooled down to different temperatures and subsequently loaded to 6.37 MPa converged toward the same limit. It can be concluded from the observations of Sultan et al. (2002) that the thermal cycle of heating and cooling slightly decreases the compressibility at high levels of applied stress.

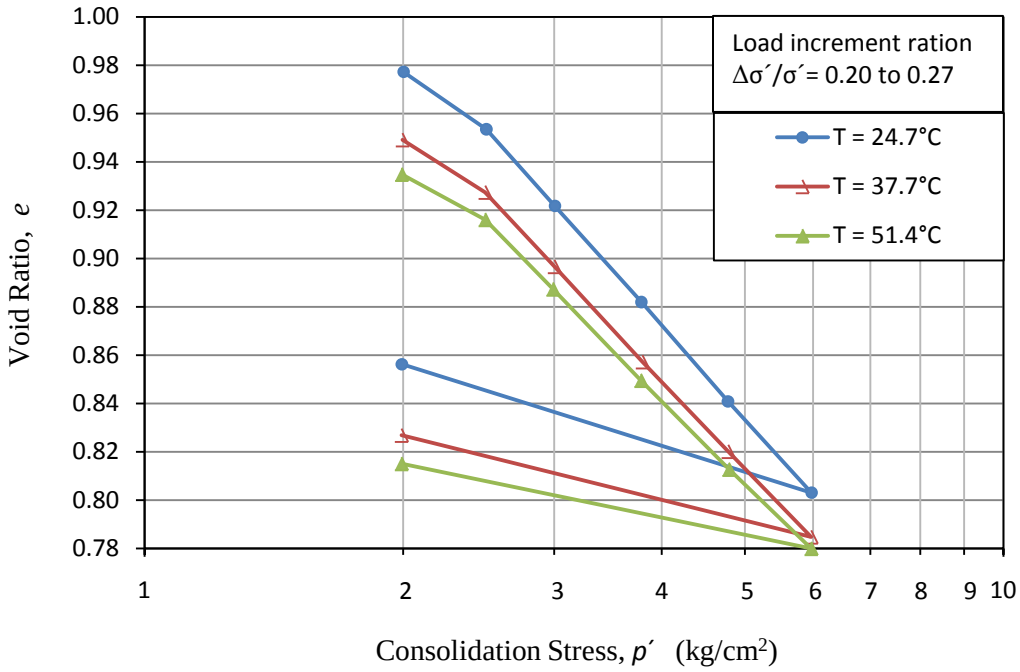

Fig. 2.1: Effect of temperature on the compressibility of saturated Illite (Campanella and Mitchell 1968).

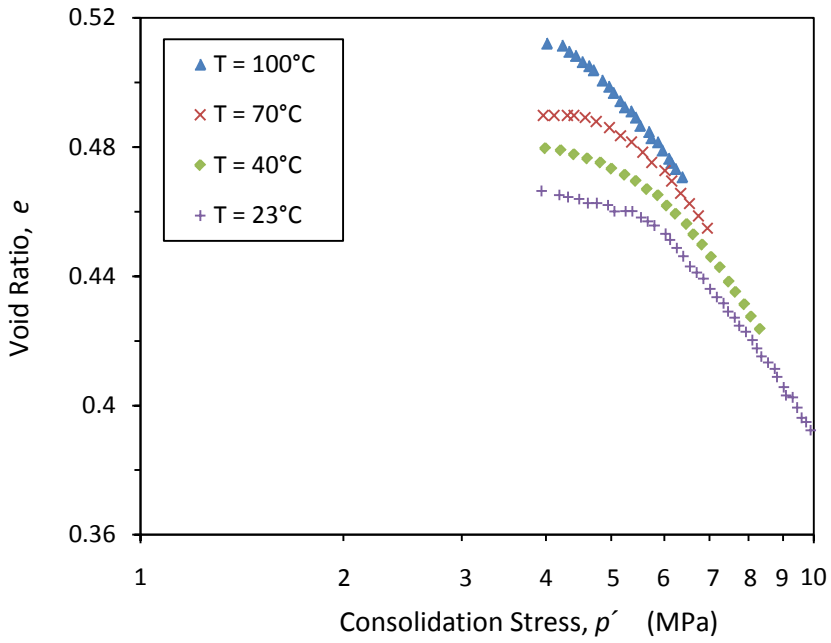

Fig. 2.2: Temperature effects on compressibility at high levels of applied stress (Sultan et al. 2002)

2.3.2.3. Apparent Changes in Stress History Due to Temperature Changes

2.3.2.3.1. Temperature Effects on Preconsolidation stress of Overconsolidated Soils

Many researchers have performed isothermal compression tests in which the soil was initially overconsolidated (Tidfors and Sällfors 1989, Eriksson 1989, Boudali et al. 1994, Cekerevac and Laloui 2004, and others). The samples were first loaded to a stress smaller than the preconsolidation stress, heated to different temperatures, and then loaded under a constant temperature. A decrease in preconsolidation stress as temperature increases has been observed. Tidfors and Sällfors (1989) performed isothermal oedometer tests between 7 and 50°C on five different intact clays and observed a linear decrease in the preconsolidation stress with temperature. Similar observations were reported by Boudali et al. (1994) for various medium plasticity clays (PI = 14 to 39%). Isothermal oedometer tests were carried out by Eriksson (1989) on samples of intact Lulea clay (PI = 60%) tested at temperature range between 5 and 55 °C. He observed a nonlinear decrease in the preconsolidation stress with temperature (Fig. 2.3).

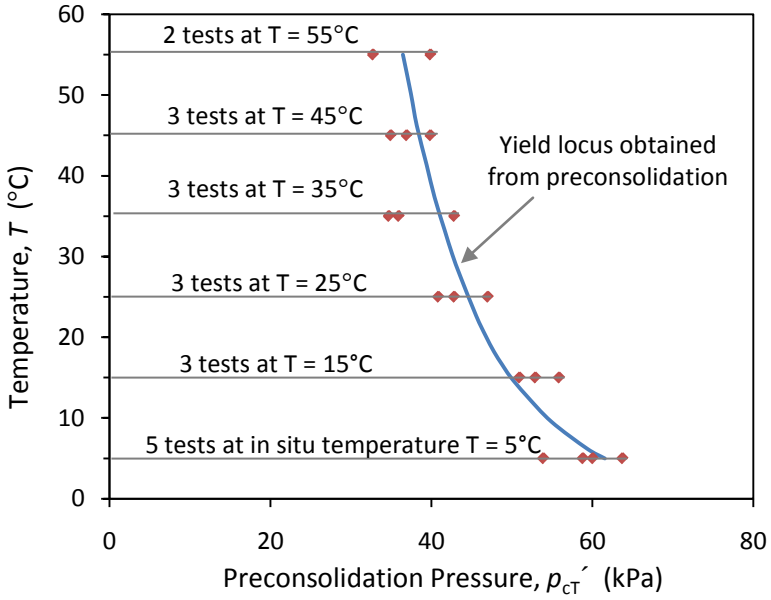

Fig. 2.3: Change in preconsolidation stress with temperature, obtained from isothermal oedometer tests (Eriksson 1989).

2.3.2.3.2. Temperature Effects on Preconsolidation stress of Normally Consolidated Soils

The observations made from tests in which the soil is heated in a normally consolidated state were different. Towhata et al. (1993) performed compression test on a remolded MC clay (Kaolinite, PI = 29%), where the sample was first loaded to a normally consolidated state at 160 kPa and then heated to 90°C. A subsequent isothermal loading at 90°C to 200 kPa revealed a little further contraction which implies a semi-overconsolidated behavior. Cui et al. 2000 reviewed the work of Sultan (1997) in which he checked the aforementioned behavior of the impact of temperature on the stress history of normally consolidated soils. Sultan (1997) carried out an isotropic compression test on a sample of intact clay. The sample was normally consolidated under 0.8 MPa at 20°C and then heated to 70°C. The heating resulted in a contraction, but a slight increase in the preconsolidation stress to 0.98 MPa was observed with subsequent loading at 70°C to 3 MPa (Fig. 2.4).

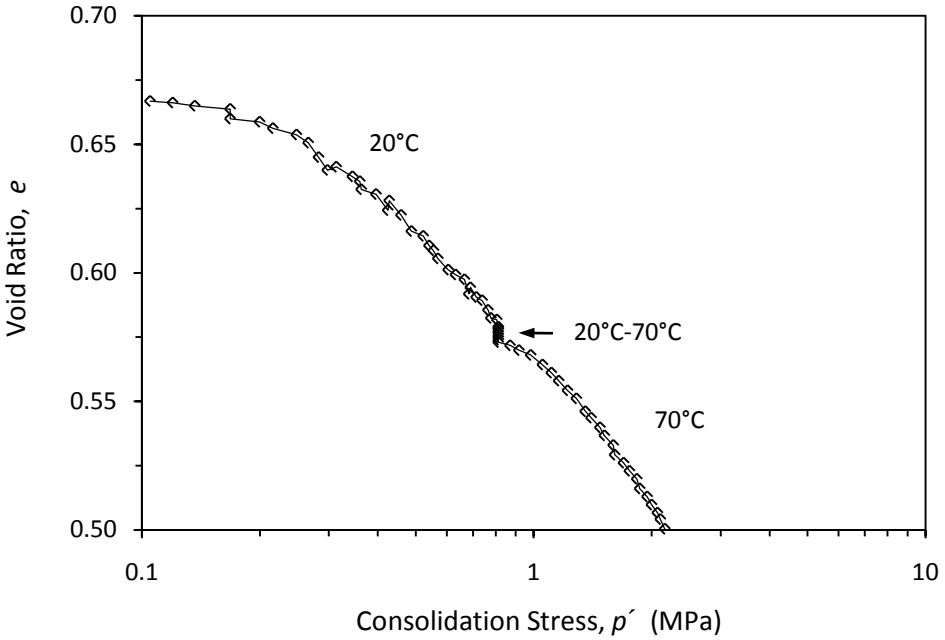

Fig. 2.4: Change in preconsolidation stress with temperature of Boom clay heated in a normally consolidation state (Sultan 1997).

2.3.2.3.3. Effect of Thermal Loading-Unloading Cycle on Preconsolidation stress

Plum and Esrig (1969) investigated the effect of heating to 50°C and then recooling to 24°C on the volume change behavior of Illite clay in a normally consolidated state. Subsequently, the soil was further loaded and submitted to a similar thermal cycle. This cycle of heating and cooling has caused the soil to behave as if it were overconsolidated (Fig 2.5). In other words, the thermal cycle leads to an increase in the preconsolidation stress. After each cycle, the compression curve remains parallel to the former curve, but was displaced toward a higher pressure by the overconsolidation effect, evidence of a thermal hardening effect. The concept of thermal hardening was confirmed by Sultan et al. (2002) by performing isotropic compression tests on four samples of Boom clay. Samples were normally consolidated at 4 MPa and then heated to 100°C. The samples were subsequently cooled down to different temperatures (100, 70, 40 and 23°C) and loaded up to 6.37 MPa (Fig. 2.6). The thermal cycle induces a hardening phenomenon since that the stress at which yield occurs increases as cooling

temperature decreases (i.e. as the thermal cycle range increases). In conclusion, Literature data show an increase in the preconsolidation stress of normally consolidated soils with heating. A further increase in preconsolidation stress was observed with subsequent cooling (see Fig 2.6).

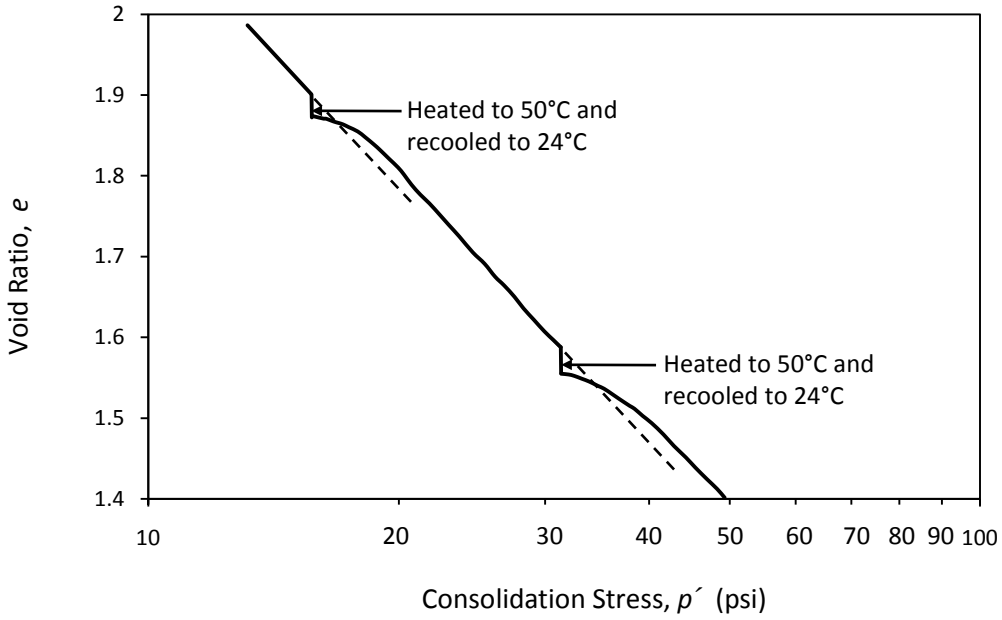

Fig. 2.5: Effect of heating and cooling on the volume change behavior of NC Illite clay; thermal hardening effect (Plum and Esrig 1969)

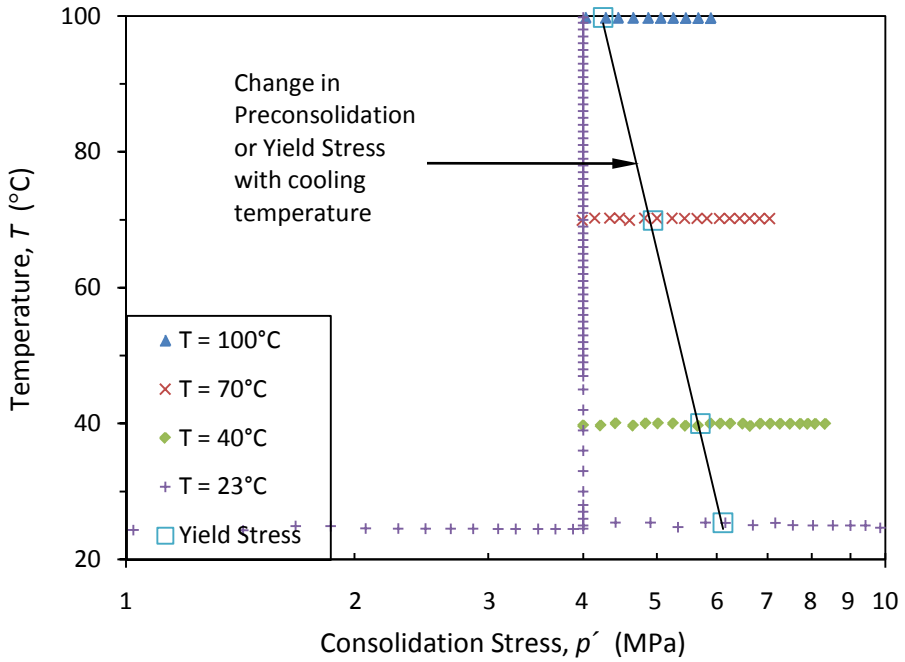

Fig. 2.6: Temperature effects on the stress history of NC Boom clay; hardening induced by thermal cycle (Sultan et al. 2002)

2.3.3. Non-Isothermal Volume Change of Saturated Soils

The volume change of soils is closely related with the drainage conditions. If a soil is heated in undrained conditions, it will expand in volume due to the thermal expansion of the soil and water. The differential expansion of the water and soil particles will result in pore water pressures. Uchaipichat and Khalili (2009) observed the relative changes in volume of a compacted silt during undrained heating [Fig. 2.7(a)] as well as corresponding positive excess pore water pressure generation [Fig. 2.7(b)]. Regardless of whether the soil specimen is normally or over consolidated, it will expand and generate positive pore water pressures during an undrained heating test. During expansion, Uchaipichat and Khalili (2009) observed that the specimen travels along the unloading-reloading curve for the soil [Fig. 2.7(c)].

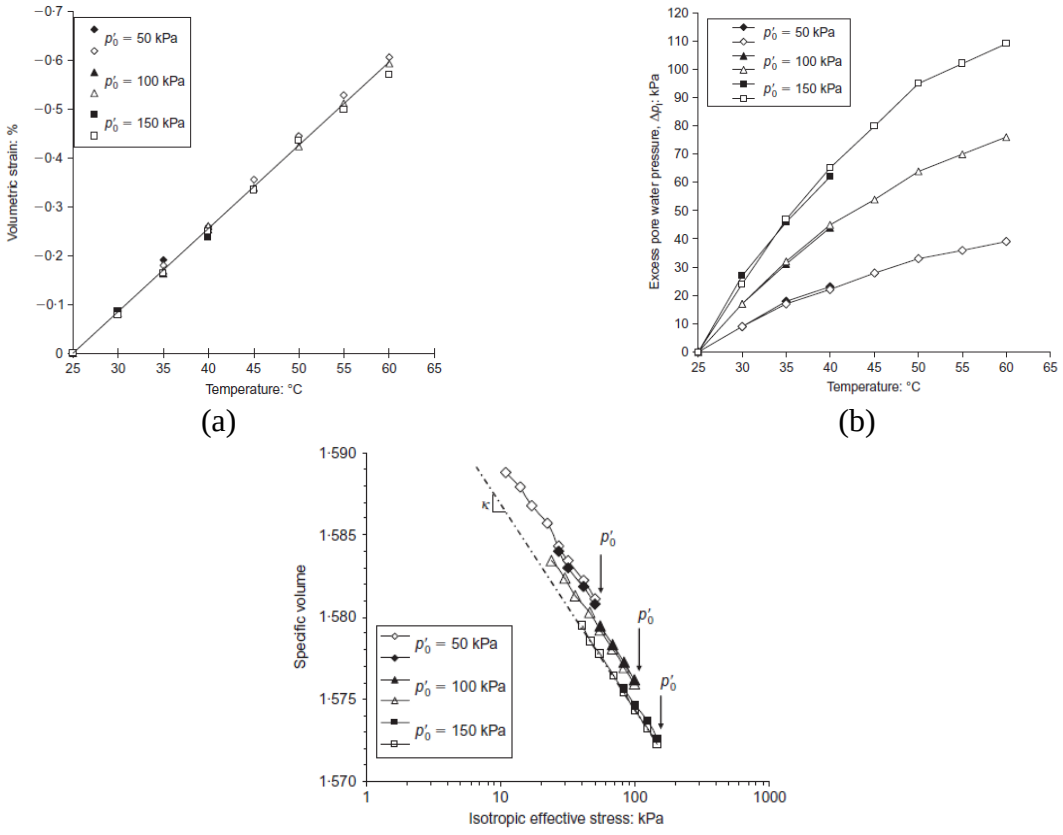

Fig. 2.7: Thermal effects on undrained compacted silt: (a) Volume change; (b) Pore water pressure generation; (c) State space

Several studies have investigated the thermally induced volume change of soil in drained conditions. Paaswell (1967) was among the first researchers who carried out heating tests under a constant stress in a rigid ring oedometer. He observed that the curves of thermal volume change as a function of time were similar to those obtained from conventional consolidation test, leading to the concept of thermal consolidation. Campanella and Mitchell (1968) performed similar tests in an isotropic (triaxial) compression cell and presented a detailed study of the thermal dilation of the soil constituents.

Campanella and Mitchell (1968) observed a good analogy between temperature-induced and stress-induced volume changes, and suggested that a thermal cycle may be equivalent to overconsolidation (i.e. Mechanical loading and unloading effect). Fig. 2.8 illustrates the response to a thermal loading-unloading cycle at constant isotropic stress of normally consolidated Illite clay. During heating, a non-linear contraction can be observed. In contrast, a relatively linear behavior results in expansion under cooling. The behavior over the whole cycle indicates the irreversibility of strain due to thermal loading which is representative of thermal hardening. Campanella and Mitchell (1968) explained this behavior in terms of irrecoverable physico-chemical adjustment in the structure of soil, needed to carry the applied effective stress. This can be interpreted as the soil undergoing densification, i.e. overconsolidated behavior, even though there was no change in the effective stress. Similar conclusion has been reached formerly by Paaswell (1967) and this phenomenon has been subsequently confirmed by other authors as previously discussed in Section 2.3.2.3.3 (Plum and Esrig 1969, Towhata et al. 1993).

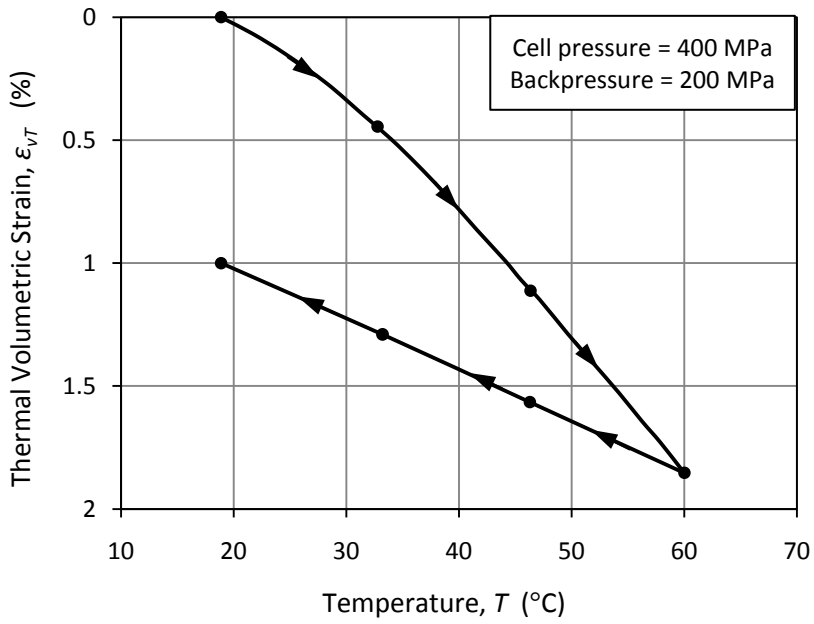

Fig. 2.8: Effects of temperature variation on a saturated Illite under constant isotropic compression (Campanella& Mitchell 1968)

2.3.3.1. Effect of Stress History on the Thermal Volumetric Strain

Review of the literature data shows that the overconsolidation ratio has an effect on the contracting/expanding nature of the volume change of a sample heated under a constant stress. Depending on the stress history and temperature range, the soil exhibited either a volume increase (large OCR values) or a volume decrease (small OCR values). Plum and Esrig (1969) performed heating tests on remolded Illite clay (PI = 84%) between 24 and 50°C at different OCR values. Fig. 2.9 shows the change in thermal strains with OCR values, where contraction is considered as positive. A thermal contraction was observed in the normally consolidated state and as the OCR increases this contraction decreases to no volume change occurs at OCR value of 1.7. In addition, by examining the slope of the curve in Fig. 2.8, which represents the change of thermal strain with OCR value, one would expect a thermal expansion to take place for OCR values higher than 1.7.

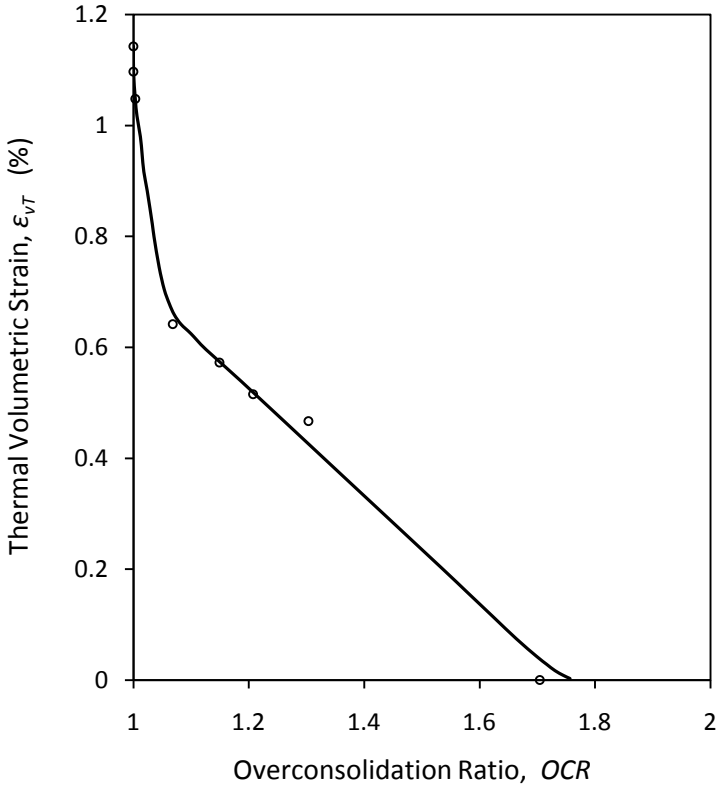

Fig. 2.9: Effect of overconsolidation ratio on volume change of Illite heated from 24°C to 50°C (Plum and Esrig 1969)

Baldi et al. (1988) reported similar observations on remolded Pontida silty clay (PI = 12.9%). The samples were consolidated isotropically under a pressure of 2.5 MPa and the thermal strains were subsequently examined under different constant pressures (i.e. different OCR values). Thermal strains were found to depend on OCR value (stress history) and temperature. Contractile strains were observed at low values of OCR and dilative strains were observed at high values of OCR, as observed in Fig. 2.10. Many other researchers have confirmed this behavior (Sultan et al. 2002, Cekerevac and Laloui 2004, Cui et al. 2009). In addition, Baldi et al. (1988) observed that the tendency to contraction increases as temperature increases; for OCR = 1, the contraction phase is observed from the beginning of heating; for OCR = 2.5, an initial dilation phase is followed by a contracting phase at 60°C; for OCR = 12.5, the dilation phase is prevailing with a probable contraction occurring at a temperature higher

than 100°C. Hence, the temperature at which the thermal volume change behavior passes from an expansion to a contraction increases as OCR increases. This phenomenon has been subsequently confirmed by other authors (Towhata et al. 1993, Sultan et al. 2002). Fig. 2.11 shows the variation of the transition temperature with OCR value for Boom clay as observed by Baldi et al. (1988) and Sultan et al. (2002).

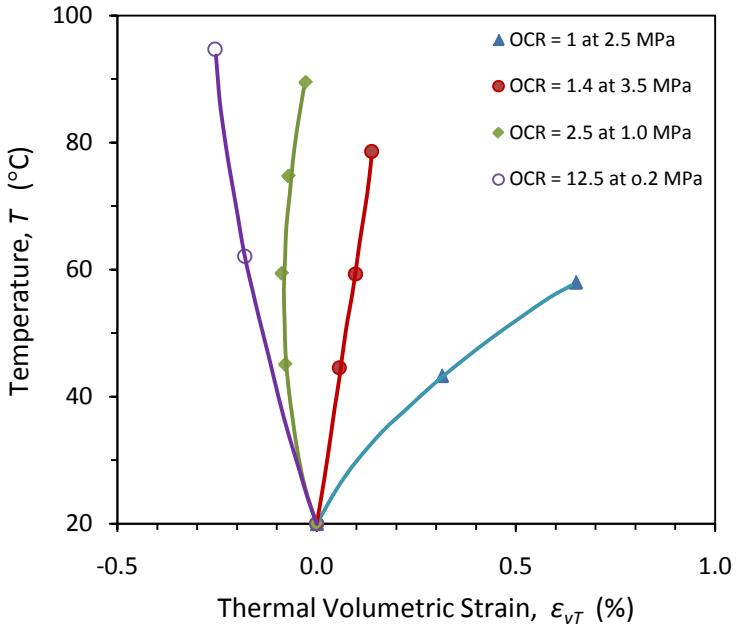

Fig. 2.10: Effect of OCR and temperature on the thermal volume change of remolded Pontida clay (Baldi et al. 1988)

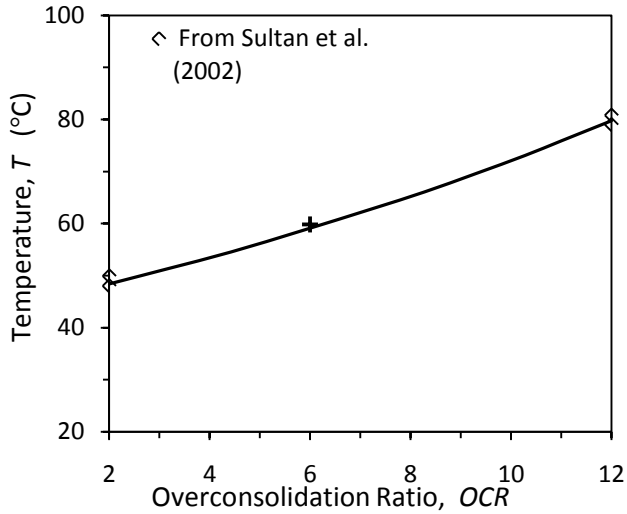

Fig. 2.11: Change of the temperature of the thermal expansion/contraction transition with OCR values for Boom clay

2.3.3.2 Elasto-Plasticity Concepts in Non-Isothermal Volume change

As previously discussed in Section 2.3.3, Campanella and Mitchell (1968) observed thermal permanent (i.e. plastic strains) volume reductions on normally consolidated Illite clay after cyclic changes of temperature (see Fig. 2.8). Demars and Charles (1982) observed with six different natural marine soils that the irrecoverable thermal volume reduction of normally consolidated samples subjected to a temperature cycle (25°C to 50°C to 25°C) under a constant stress was independent of the stress and was directly related to soil plasticity.

Irrecoverable volume reduction is also exhibited by overconsolidated soils (Demars and Charles 1982). For overconsolidated soils, the effect of temperature cycling on volume change behavior depends, in addition to soil plasticity, on stress level expressed in terms of the overconsolidation ratio (OCR); smaller irrecoverable volume decreases were observed at larger OCR values. It has been noticed that, for a given increase in temperature, the reduction in a soil volume is smaller for higher overconsolidation ratios and then tends to dilation (see Fig. 2.10).

The thermal strains after cooling are essentially reversible as demonstrated in Fig. 2.12 (Campanella and Mitchell 1968). It is of interest to notice that, in Fig. 2.12, the irrecoverable reduction in volume is large only during initial heating. Subsequent permanent volume decreases in further heating cycles were small and occurred only at the high temperatures. Again, this temperature-history effect is similar to the stress-history effect on volume change involving virgin compression, unloading, and reloading.

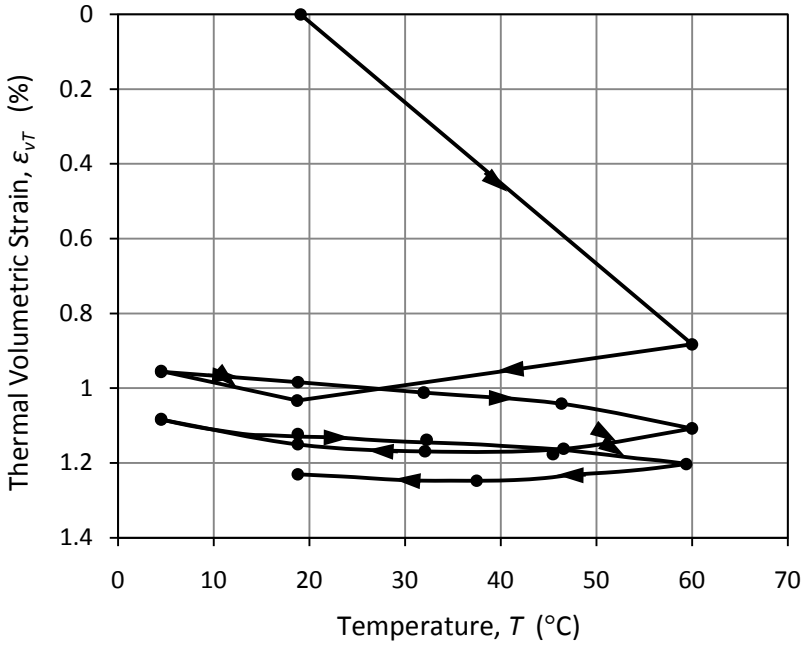

Fig. 2.12: Effect of temperature cycles on the thermal volume change behavior of saturated Illite clay (Campanella and Mitchell 1968).

2.3.4 Time-Dependent Thermomechanical Volume Change Behavior of Saturated Soils

Cui et al. (2009) investigated the time-dependent behavior of Boom clay under both thermal and mechanical loading. For this purpose, mixed heating and loading tests were performed by following various loading or heating paths and various loading or heating rates (constant rate or in steps). The time-dependent behavior was investigated by examining the volumetric strain rate coefficient, ($d\varepsilon_v$ / *dlogt*), at constant effective pressure and constant temperature (i.e. after the loading or heating is stopped). They observed showed a significant time-dependent behavior through the observation of a significant effect of stress and temperature on the volumetric strain rate coefficient.

Cui et al. (2009) also looked into the effect of loading rate and heating rate on the (time-dependent) volume change behavior. They related the volume change under constant stress/temperature after slow-rate loading/heating stages to creep, where part of the consolidation would have been achieved during the constant slow-rate loading/heating. However, in the case of

fast loading/heating tests, the data by Cui et al. (2009) lacked the pore pressure measurements in the soil sample, which were needed in order to distinguish consolidation and creep from the total volume change with time.

2.4. Analytical Models for Thermal Volume Change of Soils

Many models have been developed to describe the behavior of saturated fine-grained soils under temperature changes, such as effective stress changes, pore-water pressure changes, and changes in volume of the soil. The objective of these models is to predict the engineering behavior of the soil medium under a change in the environmental temperature.

The first conceptual model for strain response of soil to elevated temperature was given by Campanella and Mitchell (1968) who predicted the volume change of a saturated soil submitted to an increase in temperature by considering the thermal properties of free water. The thermal volumetric strain of a linear elastic material can be estimated using the coefficient of thermal expansion, as follows:

$$\Delta\varepsilon_v = \alpha\,\Delta T \tag{2.3}$$

This equation can be used to predict the thermal expansion of water ΔV_w having an initial pore water volume V_w during a temperature increment ΔT, as follows:

$$\Delta V_w = \alpha_w\, V_w\, \Delta T \tag{2.4}$$

where α_w is the coefficient of volumetric thermal expansion free water. The change in volume of the mineral solids due to temperature change can be expressed using the following expression:

$$\Delta V_s = \alpha_s\, V_s\, \Delta T \tag{2.5}$$

where α_s is the volumetric coefficient of thermal expansion of mineral solids. If a saturated specimen is free to drain at constant effective stress, the volume of water drained from the sample due to a temperature change is:

(2.6) $$(\Delta V_{DR})_{\Delta T} = (\Delta V_w)_{\Delta T} + (\Delta V_s)_{\Delta T} - (\Delta V_m)_{\Delta T}$$

where $(\Delta V_m)_{\Delta T}$ is the change in volume of the soil specimen due to a temperature change, and volume increases are considered positive. Combining Eqns. 2.1, 2.2 and 2.3, the following equation can be obtained:

(2.7) $$(\Delta V_{DR})_{\Delta T} = \alpha_w V_w \Delta T + \alpha_s V_s \Delta T - (\Delta V_m)_{\Delta T}$$

The corresponding volumetric strain ε_v during a drained heating test is obtained by subtracting the volume due to the thermal expansion of water and solids from the volume of drained water, giving the following expression:

(2.8) $$\varepsilon_v = \frac{-(\Delta V_m)_{\Delta T}}{V} = \frac{[(\Delta V_{DR})_{\Delta T} - (\alpha_w V_w + \alpha_s V_s)\Delta T]}{V}$$

In undrained conditions, this change in volumetric strain will lead to a change in volume. However, this model is only suitable for normally consolidated soils which generate positive pore water pressures. The previous model is based on two hypotheses. The first is that the coefficient of thermal expansion of the soil skeleton is constant and negative if an increase in temperature causes a decrease in volume of the soil structure. The second is that clay water expands as pure water does at atmospheric pressure as pointed out earlier. Both assumptions

were experimentally validated in the range of relatively high water content and low effective stresses (Campanella and Mitchell 1968).

Baldi et al. (1988) performed drained heating testes at various constant and relatively high effective stresses on clays of low water contents. They concluded that the thermal expansion of adsorbed water in these clays is significantly lower than that of free water. Unlike the expression of Campanella and Mitchell (1968), which assumes a constant value for α_w and does not take into account the influence of water pressure on water thermal expansion, Baldi et al. (1988) gave α_w as a function of temperature (T) and pressure (p) as follows:

$$\alpha_w = \alpha_o + (\alpha_1 + \beta_1 T) \ln mp + (\alpha_2 + \beta_2 T) (\ln mp)^2 \tag{2.9}$$

where α_i, β_i and m are imperial parameters.

Baldi et al. (1988) accounted for the effects of adsorbed water using the double-layer theory and took into consideration the effects of temperature and pressure on the volume change of the adsorbed water. Considering that there is no free water in low-porosity clays, Baldi et al. (1988) obtained the following expression for the thermal volumetric strain:

$$\varepsilon_v = \frac{[(\Delta V_{DR})_{\Delta T} - (V\, \Delta v_a\, S_s\, \rho_d\ +\ \alpha_s\, V_s)\, \Delta T]}{V} \tag{2.10}$$

where Δv_a is the volume of expelled adsorbed water per unit surface of the clay mineral due to a unit temperature variation, S_s is the specific surface of the mineral particle, and ρ_d is the dry unit weight of the soil. The two theories on the thermal expansion of the clay-water system presented above were evaluated by Delage et al. (2000) using slow heating tests on samples of Boom clay (IP = 50%). Experimental data of volume changes were compared (Fig. 2.13) with those

obtained using the expressions of Campanella and Mitchell (1968) (Eqn. 2.8) and Baldi et al. (1988) (Eqn. 2.10). Delage et al. (2000) concluded that the simpler model of Campanella and Mitchell (1968) was satisfactory for describing the volume change of Boom clay in a heating test, especially, when considering the influence of pore water pressure on the thermal expansion of water.

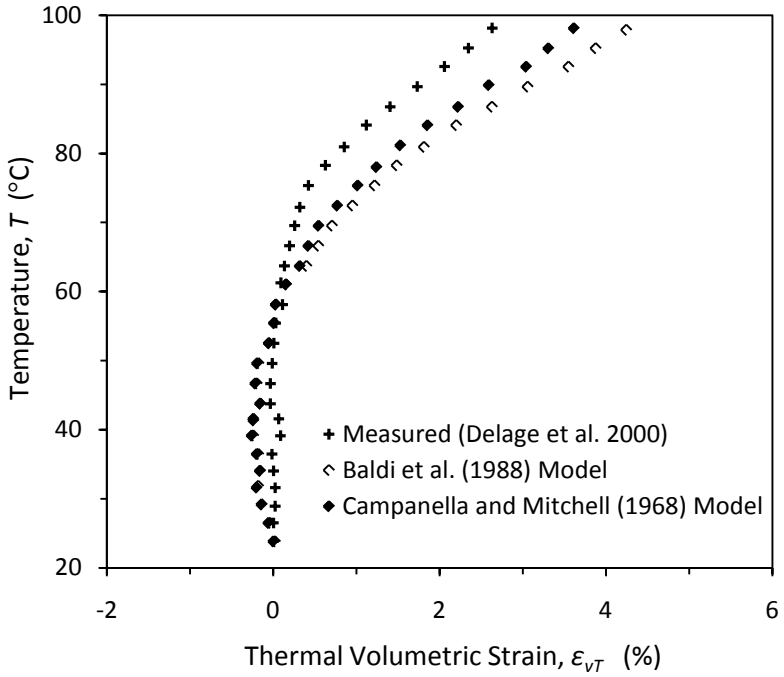

Fig. 2.13: Comparison between the predicted and measured thermal volumetric strains (Delage et al. 2000)

3. SOIL PROPERTIES

3.1. Introduction

Statically compacted silt was used as the test material in this study. The soil was obtained from the Bonny dam in Yuma County, Colorado. At the site, Bonny silt was passed through a ½-inch screen before being transported to the Graduate Geotechnical Engineering Laboratory at the University of Colorado, Boulder. Evaluation of the technical literature indicates that the effect of elevated temperature changes on silts has only been investigated in a single study (Uchaipichat and Khalili 2009). However, evaluation of the behavior of silt during freezing indicates that it may have significantly different behavior from sands and clays (Konrad and Morgenstern 1980). This chapter includes a summary of the physical properties of Bonny silt, including the Atterberg consistency limits, grain-size distribution, specific gravity, and compaction properties.

3.2. Atterberg Limits

The Atterberg limits, including the liquid limit, plastic limit, and plasticity index, were defined for Bonny silt in accordance with ASTM D 4318. The Atterberg limits are summarized in Table 3.1. The silt can be considered to have low plasticity, and can be classified as ML soil (inorganic silt or silt with sand) according to the Unified Soil Classification System (ASTM D 2487).

Table 3.1: Index properties and activity of Bonny silt

Liquid Limit, LL	25
Plastic Limit, PL	21
Plasticity Index, PI	4
Activity, A	0.29

Table 3.1 also includes the activity (A) calculated for the soil, defined as

(3.1) $$A = \frac{PI}{\%\ by\ weight\ of\ clay\text{-}size\ fraction}$$

The Activity of 0.29 for Bonny silt indicates that it does not contain significant clay minerals. Accordingly, temperature effects on soil volume change behavior are expected to arise due to thermal properties of free water and soil particles, rather than diffuse double layer effects (Mitchell and Soga 2005).

3.3. Particle-Size Analysis

The quantitative determination of the distribution of particle sizes in Bonny silt was obtained in accordance to ASTM D 422. The distribution of particle sizes larger than 75 μm (retained on No. 200 sieve) was determined by sieving, while the distribution of particle sizes smaller than 75 μm was determined by a sedimentation process, using a hydrometer. The particle-size distribution curve is shown in Fig. 3.1, while Table 3.2 summarizes the particle size distribution characteristics.

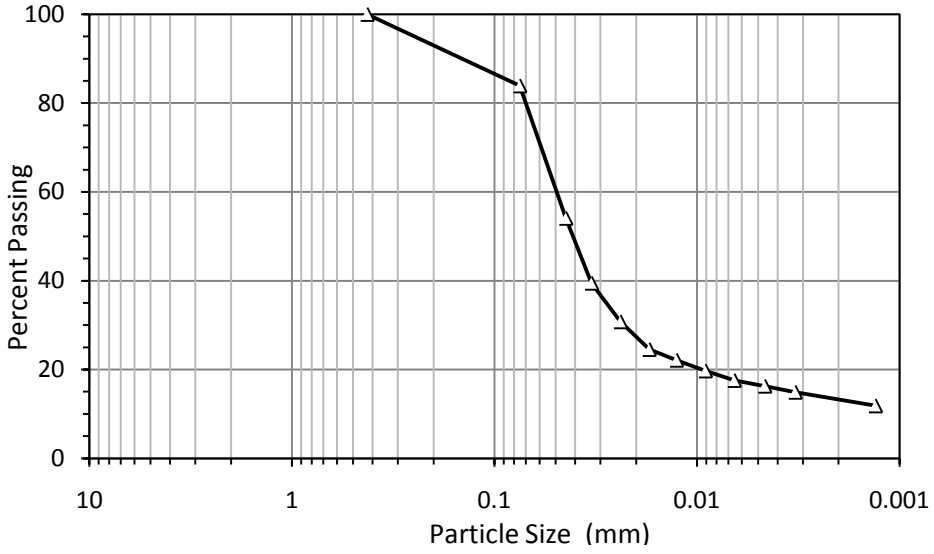

Fig. 3.1: Particle-size distribution curve for Bonny silt

Table 3.2: Physical properties of Bonny silt

Physical Property	Bonny Silt
Specific Gravity	2.63
Particle-Size Data	
D_{10}	< 0.0013 mm
D_{30}	0.022 mm
D_{50}	0.039 mm
% Passing No. 200 Sieve	83.9%
% Clay size	14%
% Silt size	69.9%
% Sand size	16.1%
Thermal Conductivity	1.4 W/m°C

3.4. Specific Gravity

The specific gravity of soil solids, G_s, is defined as the ratio of the mass of a unit volume of soil solids to the mass of the same volume of gas-free distilled water at 20°C. The specific gravity is often needed for various calculations in soil mechanics, involving weight-volume relations. The value of G_s for most natural soils falls within a range of 2.6 to 2.9. For Bonny silt, the specific gravity of solids was determined by means of a water pycnometer in accordance to ASTM D 854, which covers the determination of the specific gravity of soil solids that pass the 4.75-mm (No. 4) sieve. The test result is included in Table 3.2.

3.5. Compaction Properties

The standard Proctor test was performed according to ASTM D 698 to define the relationship between water content and dry unit weight (i.e., compaction curve) for Bonny silt. The standard Proctor compaction curve for Bonny silt is presented in Fig. 3.2. The optimum water content, w_{opt}, and the maximum dry unit weight, $\gamma_{d,max}$, are summarized in Table 3.3.

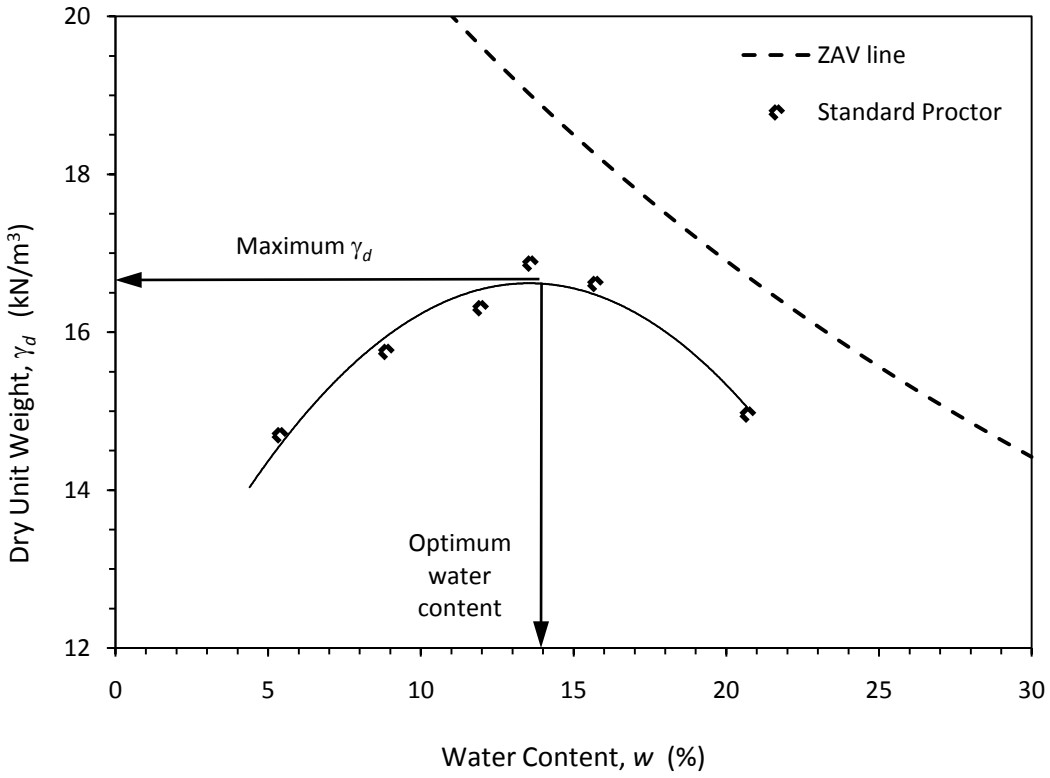

Fig. 3.2: Standard Proctor compaction curve for Bonny silt

Table 3.3: Compaction data for Bonny Silt

Property	Value
Standard Proctor Test	
Max. Dry Unit Weight	16.7 kN/m^3
Optimum Water Content	14%

4. EXPERIMENTAL SETUP

4.1. Introduction

This chapter describes aspects of the temperature-regulated oedometer used in this study to evaluate the thermomechanical response of compacted silt to different rates of temperature change. The device was designed by McGinley (1983) but was refurbished and updated by the author within the framework of this research project. Fig. 4.1 shows a photograph of the temperature-regulated oedometer system. It consists of three main components: the pressure cell, the mechanical loading system, and the heating system. The setup includes instrumentation to measure relevant variables, include a load cell to measure the axial load, a linearly variable displacement transformer (LVDT) to measure axial displacement, a pressure transducer to measure pore water pressure at the bottom of the specimen, and several thermocouples to measure the temperature of the specimen and cell water. Each of the main components and the instrumentation are discussed in detail in the following sections.

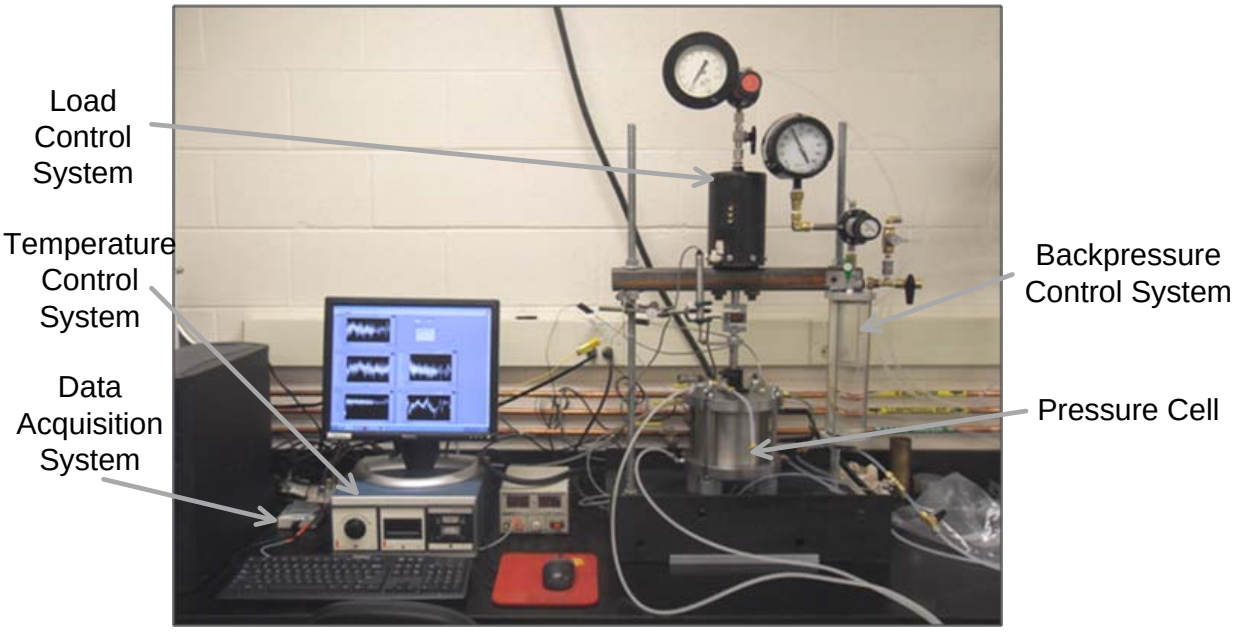

Fig. 4.1: Temperature-regulated oedometer system

4.2. Pressure Cell

A schematic drawing of the pressure cell is shown in Fig. 4.2. All of the main components of the cell were made of stainless steel (TYPE 316) to resist corrosion, withstand high pressures, and permit high temperature ranges. Because all of the components consist of the same metal, they will have a similar coefficient of thermal expansion, which helps minimize differential displacement of the cell components during temperature changes.

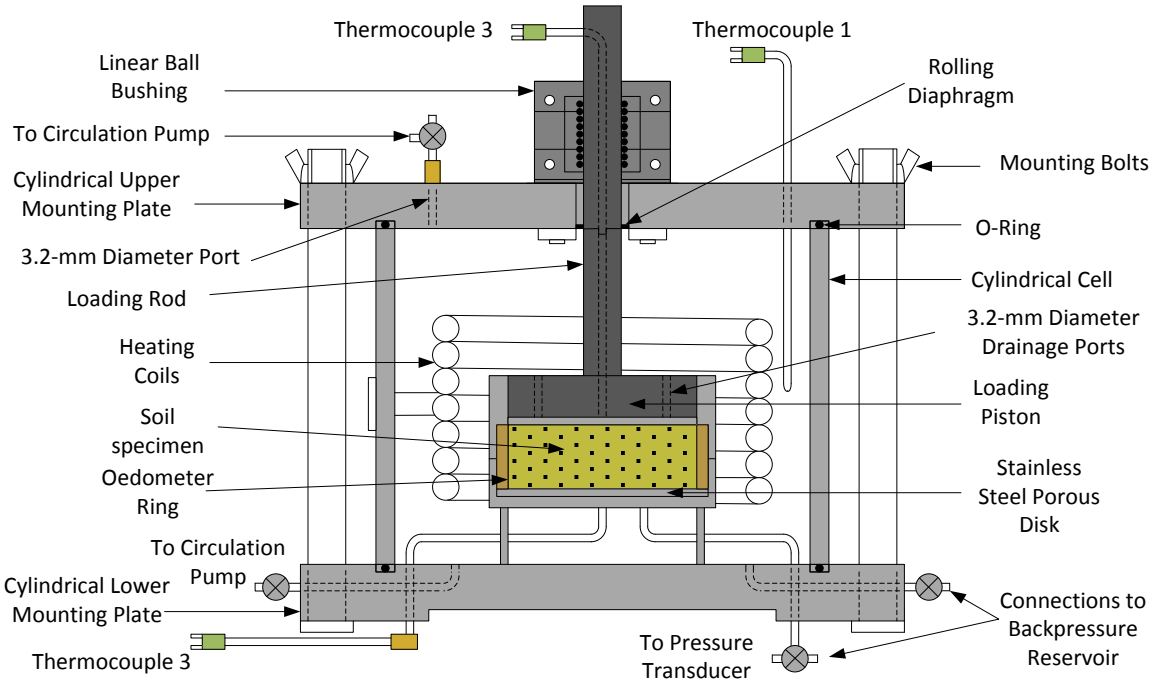

Fig. 4.2: Schematic of the pressure cell

The oedometer itself is held within the pressure cell which has a diameter of 153 mm and a height of 127 mm. Two circular plates, 25.4-mm thick each, encompass the top and bottom sides of the pressure cell and connected together to four feet base through 12.7-mm diameter bolts, as shown in Fig. 4.3. At the interface between the pressure cell wall and mounting plates, two ethylene-propylene “O”-rings are placed in order to provide a leak-proof for the cell water. Coils for temperature control are integrated into the main cylinder body, and will be discussed in detail in Section 4.4 of this chapter. The pressure cell includes several ports for cell pressure

control and instrumentation access. A loading piston is used to apply mechanical loads and measure displacements on the specimen. The piston is connected to a loading rod which passes out of the pressure cell, sealed by a Bellofram rolling diaphragm. It is maintained vertical using a linear guide bushing.

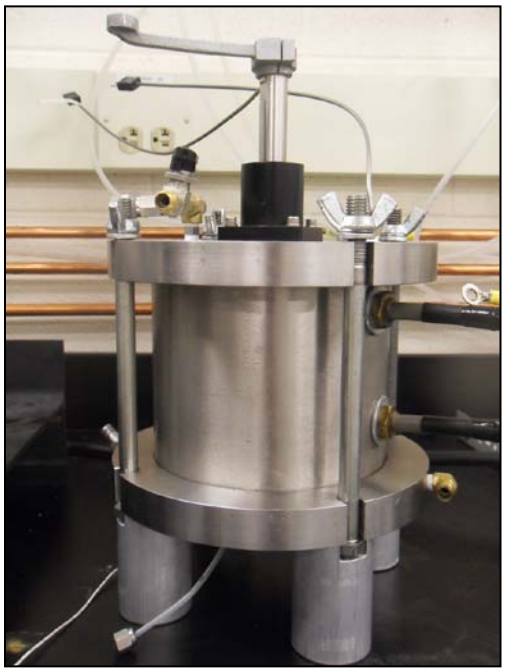

Fig. 4.3: Assembled pressure cell

The soil specimen is held within a cylindrical consolidation ring which has a diameter of 83 mm, a height of 25.4 mm, and a thickness of 3.2 mm. The consolidation ring and the specimen can be freely removed from the setup as an integral piece for compaction, weighing, and measurement of the final mass. The goal of the oedometer is to have a single drainage boundary condition, with free drainage from the top of the specimen and no drainage from the bottom of the specimen. This goal permits measurement of pore water pressure at the bottom of the specimen. To achieve this goal, the consolidation ring is placed on a steel porous disc resting atop a solid steel pedestal. The pedestal is outfitted with a thermocouple in the center, and a port at a radial distance of 25 mm connected directly to a pore water pressure transducer outside of

the pressure cell. A raised lip around the outside of the pedestal contains an ethylene-propylene "O"-ring which is used to provide a hydraulic seal between the consolidation ring and the pedestal. A collar having the same inside diameter as the consolidation ring is placed on top of the consolidation ring. The collar is outfitted with the same type of "O"-ring seal as used in the pedestal. The collar is used to assist compaction of the soil specimen, and to permit swelling of the specimen above the extents of the consolidation ring. The collar extends above the specimen a distance equal to the thickness of the loading piston plate, which also helps ensure alignment of the loading piston. The loading piston consists of a steel porous disc attached to a cylindrical steel plate, attached rigidly to the loading rod. Two 3.2-mm ports through the cylindrical steel plate permit free drainage of water from the specimen. Any backpressure applied to the pressure cell is applied directly to the specimen.

The assembled pedestal, consolidation ring, and collar are shown in Fig. 4.4. To help reducing friction between the consolidation ring and the travelling loading piston, the inner surface of the ring was coated with green Teflon paint.

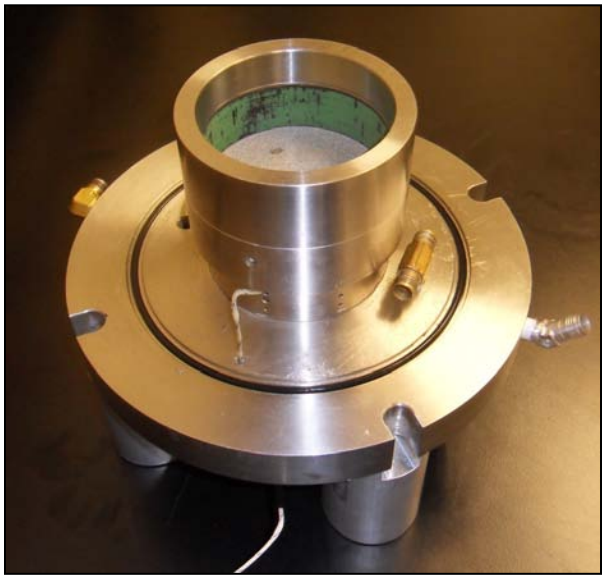

Fig. 4.4: Base plate, specimen ring, collar, and bottom porous disk

4.3. Mechanical Loading System.

The axial load is applied to the specimen through a 83 diameter, 17.8-mm thick loading piston. A picture of the top of the pressure cell and the loading piston is shown in Fig. 4.5. The loading piston is attached to a 12.7-mm diameter rod which extends out of the cell through a linear ball bushing. The linear ball bushing is used to ensure the alignment of the loading rod to prevent the loading piston from binding with the inner walls of the consolidation ring. A high-temperature and corrosion-resistant ethylene-propylene rolling diaphragm is installed at the entrance of the loading rod in the upper cell plate to ensure a continual seal against leaking of cell water as the shaft moves into or out of the cell. A target for the LVDT is mounted to the top of the loading rod as shown in Fig. 4.5.

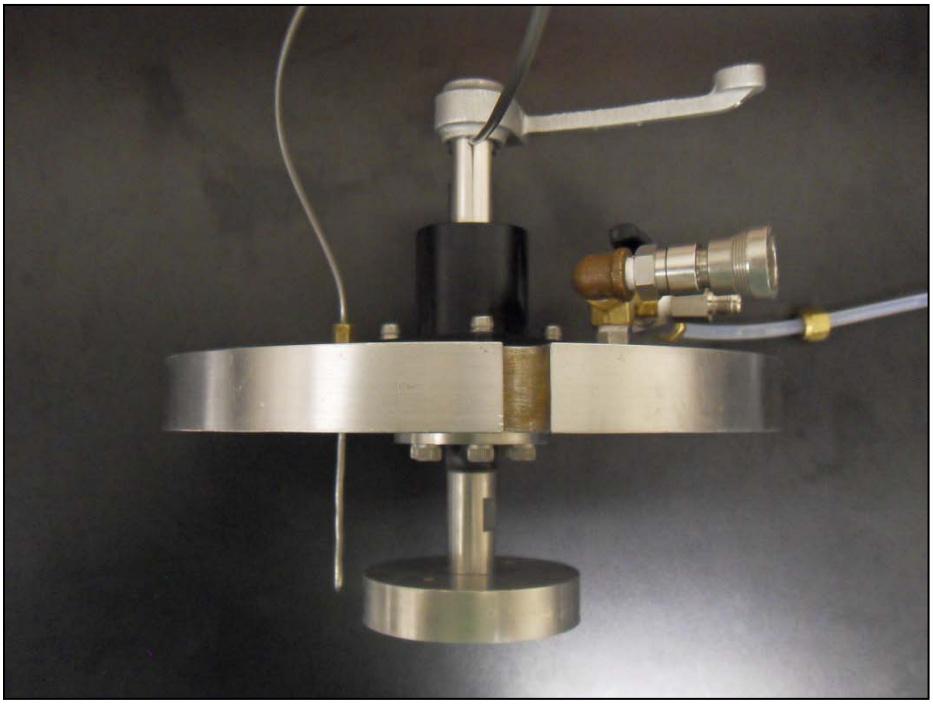

Fig. 4.5: The loading piston, loading rod, and linear ball bushing

A pneumatic air cylinder shown in Fig. 4.6 was used to generate the static axial load applied to the specimen. The air cylinder is double-acting, standard diaphragm air cylinder

manufactured by Bellofram Precision Controls from Marsh Bellofram Group of Companies of Newell, WV. The cylinder has an effective area of 10323 mm^2, a stroke of 94 mm, with an operating range up to 1000 kPa. The pressure delivered to the air cylinder is controlled by a Fairchild Model 10 air pressure regulator attached to an 830 kPa compressed air supply. The operating range of the pressure regulator is 35 to 2070 kPa. The amount of pressure generated by the air cylinder is monitored using a Master Test pressure gauge attached to the pressure regulator. The pressure gauge is manufactured by Marsh Instruments Company and it has an operating range of 0 to 690 kPa.

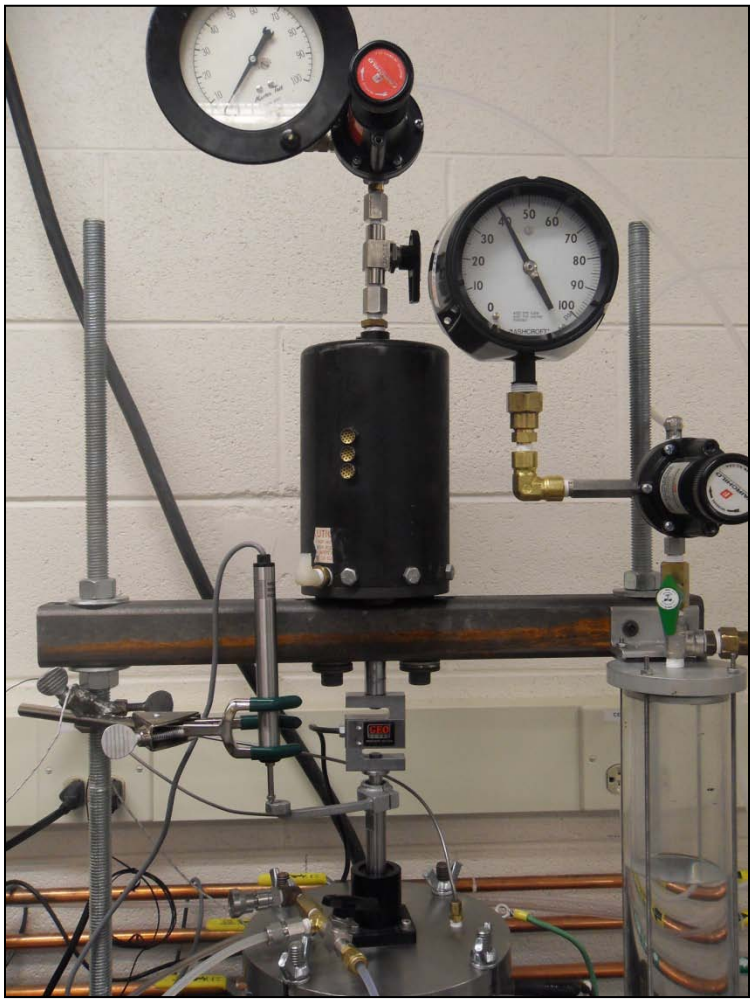

Fig. 4.6: The diaphragm air cylinder, pressure regulator, and pressure gauge

The Brainard-Kilman E-210, S-type load cell shown in Fig. 4.7 was used for measuring the axial force. The load cell requires an excitation voltage of 10V DC and operates in a load range up to 2.2 kN, with an accuracy of ±0.44 kN. The load cell is mounted to the bottom of the air cylinder rod and bearing on the loading piston.

Fig. 4.7: Load cell used to measure the axial load applied to the specimen

Axial deformations of the soil specimen during mechanical or thermal loading are measured using a linear variable deformation transformer (LVDT). The LVDT used in this study was a Brainard-Kilman model E-312. Fig. 4.8 shows the LVDT and the mechanical core shaft. The LVDT provides voltage output proportional with the displacement of the mechanical shaft. The operating linear displacement range of the LVDT is from 0 to 50 mm, with a sensitivity of 0.025 mm.

Fig. 4.8: LVDT model E-312 used to measure the axial deformations

4.4. Pore Water Pressure Measurement

Precise measurement of the development and dissipation of pore water pressure is an essential and crucial part of the experimental setup. Such measurement is greatly influenced by the selection of materials in the oedometer. Consequently, several precautions were taken to ensure accurate pore water pressure measurements. All water line connections have been constructed of stainless steel back and front Swagelok ferrule-type fittings to prevent possible leaks. In addition, Whitney ball stainless steel valves have been used at several points in the water line system to regulate the direction of water flow. The use of stainless steel in all components enhances the accuracy of the pore water pressure measurements as thermal expansion of the metal will cause a change in pressure within the pipes.

The backpressure applied to the water in the pressure cell is controlled using the backpressure reservoir shown in Fig. 4.9. A Fairchild Model 10 air pressure regulator with an operating range of 35 to 2070 kPa is used to pressurize the water within the backpressure

reservoir and the pressure cell. An in-line Ashcroft Dura-gauge pressure gauge, with an operating range of 0 to 690 kPa is utilized to measure the applied air pressure.

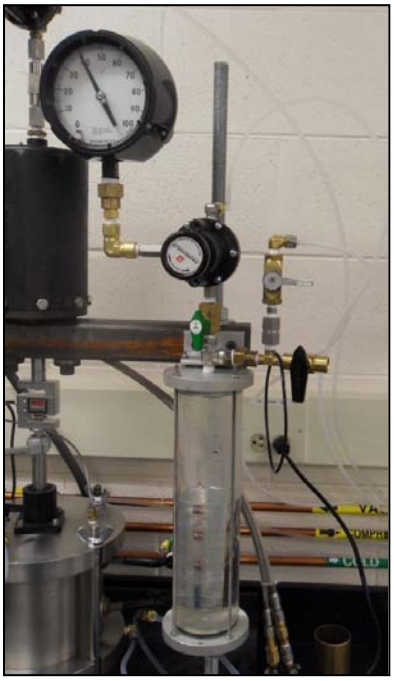

Fig. 4.9: Closed, glass pressure reservoir

The water inside the pressure reservoir is de-aired using a high vacuum supplied by a Precision Scientific vacuum pump (Model DD-100), shown in Fig. 4.10. The vacuum pump has a pumping speed of 4 CFM and can apply a vacuum of up to 85 kPa.

Fig. 4.10: Scientific vacuum pump, Model DD-100

The pore water pressure was measured at the bottom of the specimen during testing using a pore water pressure transducer. A schematic of the pore water pressure transducer connection to the specimen is shown in Fig. 4.2. The pore pressure transducer used in this study is a Brainard-Kilman E-124 model (Fig. 4.11). It requires an excitation voltage of 10V DC. The pressure transducer is enclosed in a stainless steel enclosure which has an air flushing system. The operating range for the pressure sensor is from 0 to 1036 kPa.

Fig. 4.11: Pressure Transducer model E-124 used to measure pore water pressure

The load cell, pressure transducer, and LVDT were all monitored using a National instruments NI 9219 module shown in Fig. 4.12. This data acquisition system is small in size and can be used to monitor up to four instruments. It can be connected to the computer directly through a USB connection.

Fig. 4.12: A National Instruments data-logger NI 9219

The data-logger and the instrumentation were supplied with current from a DC variable power supply PS1502AU shown in Fig. 4.13. The power supply has an output voltage range of 0 to 15 V DC and a maximum output current of 2A.

Fig. 4.13: DC variable power supply PS1502AU

4.5. Heating System

The temperature regulated oedometer device has the capability of regulating and monitoring the temperature of testing specimen. An independently working heating system was incorporated into the device especially for this reason. Three essential requirements were established for the heating system:

1. The heating system should work independently of the other parts of the device;
2. The heating system should induce a uniform temperature field in the cell;
3. The heater should be as close as possible to the specimen in order to ensure a better temperature control.

A schematic drawing of the temperature-regulated oedometer system that includes the heating system is shown in Fig. 4.14. The main components of the heating system are the heater, the temperature control unit, and the circulation pump.

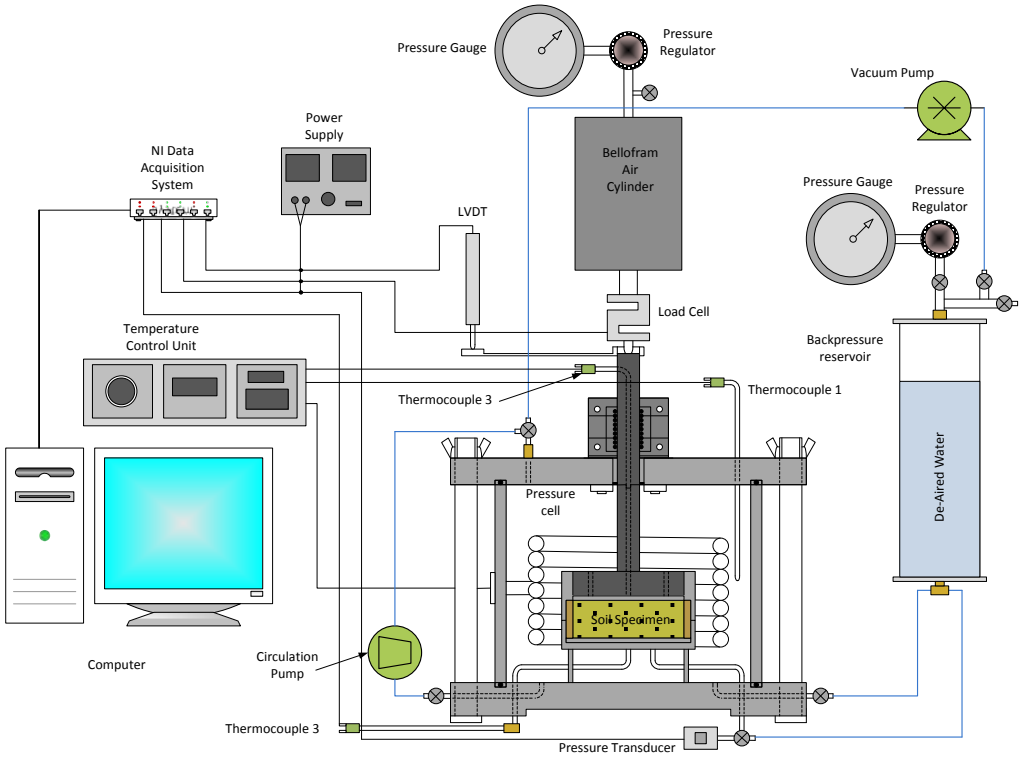

Fig. 4.14: Schematic drawing of the temperature-regulated oedometer system

In order to maintain a consistent temperature of the testing environment and to obtain an efficient control of the specimen temperature, the environmental temperature was changed by regulating the temperature of the de-aired water sealed within the pressure cell. A tubular coiled heater (Fig. 4.15), manufactured by Watlow Electronics with a total capacity of 4500 watt, was introduced around the sample inside the pressure cell in order to increase the temperature of the cell water. The fact that the heater completely surrounds the specimen, as shown in Fig. 4.15, contributes to imposing a uniform temperature change along the circumference of the specimen. This makes monitoring of the changes in temperature of the specimen easier.

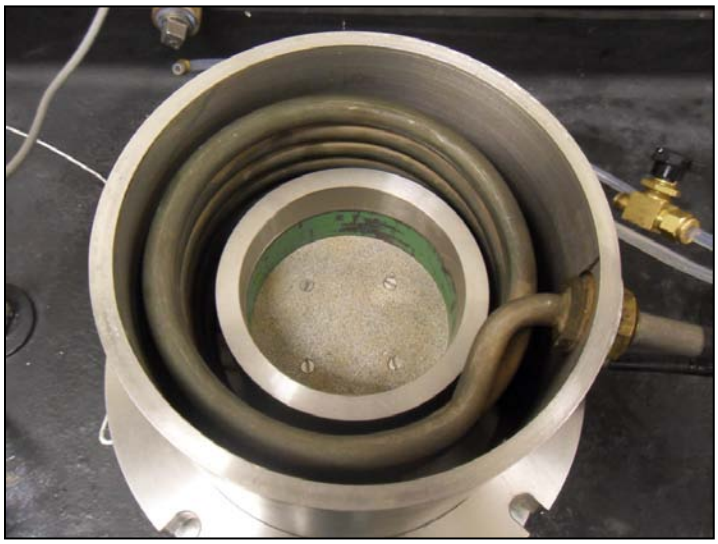

Fig. 4.15: Tubular coiled heater

The amount of temperature accomplished by the coiled heater is monitored through the temperature-controlling unit, which also gives the temperature-regulated oedometer system the capability of regulating the temperature of the testing environment. Fig. 4.16 shows a photograph of the temperature-controlling unit. The heater is driven and controlled by means of a manually operated electronic temperature regulator. The temperature regulator is also produced by Watlow Electronics and has an analog set control. The regulator provides an adjustable proportional band

and is field selectable for an automatic on-of mode or control with an adjustable cycle time. It allows temperatures up to 205°C with an accuracy of ±1/2°C. The rate of heating produced by the temperature regulator depends on the amount of temperature increment applied; the larger the increment the higher the rate of heating. In order to achieve higher rates of heating, larger temperature increments should be applied in stepwise fashion so that the temperature regulator increases the heating rate to reach to the target temperature. Lower rates of heating can be achieved by applying temperature increment in very small divisions. Each small division is allowed to equilibrate before applying the next division. The environmental temperature of the temperature-regulated oedometer device is measured by 3 thermocouples and monitored in a Watlow digital temperature indicator, in conjunction with a thermocouple switch. The digital temperature indicator, shown in Fig. 4.16, has an operating range of -190 to 870°C, with an accuracy of about ±1/2°C.

To improve the temperature control of the feedback loop in the temperature control unit, a circulation pump was used to homogenize the water temperature within the pressure cell. Water was circulated utilizing an AC motor-driven gear pump (model PQM-1 from Greylor Company), shown in Fig. 4.17. The pump has an operating range of temperature up to 85°C.

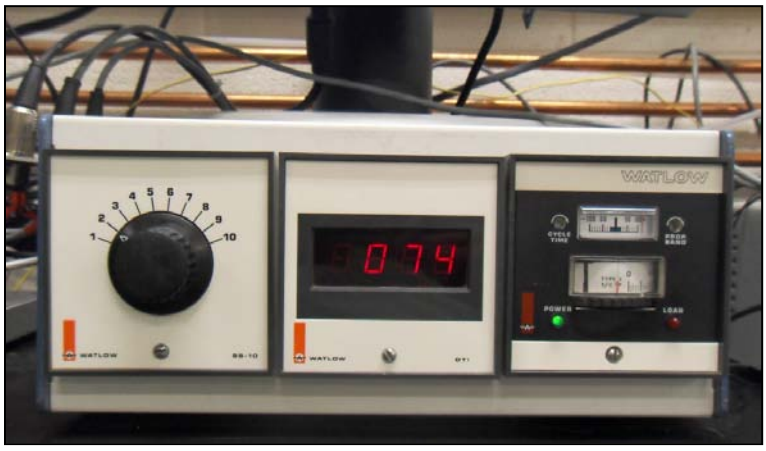

Fig. 4.16: Temperature-controlling unit

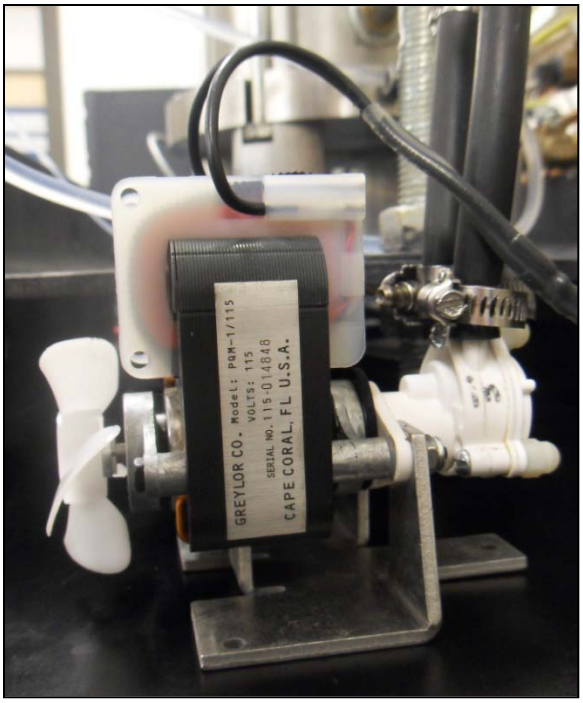

Fig. 4.17: Circulation pump

4.6. Temperature Measurement

Three tip-sensitive thermocouples were used to measure the temperature of the specimen and of the cell water. Thermocouple number 1 is situated within the TRO cell close to the coiled heater as shown in Fig. 4.14. This thermocouple back-feed the coiled heater as it is directly wired to the temperature regulator, which in turn is wired to the heater. Utilizing this thermocouple, the temperature regulator cycles the heater in order to accurately maintain the desired temperature. Thermocouples number 2 and 3 are used to measure the temperature at the top and bottom of the specimen, respectively. Thermocouple number 2 extends through the loading rod so that it can measure the temperature at the face of the loading piston (see Fig. 4.14). Thermocouple number 3 was constructed through the pedestal holding the specimen ring to measure the temperature at the bottom of the specimen (see Fig. 4.2). It was believed that placement of the thermocouples within the soil specimen would disturb the consolidation process. To minimize any likelihood of

disturbing the specimen, both thermocouples 2 and 3 were specifically designed so that they do not extend beyond the upper and lower porous disks.

Thermocouples 1 and 2 are 3.2-mm diameter, stainless steel sheathed Type J thermocouples. They are manufactured by Watlow Electronics with an operating range of -73 to 538°C, and an accuracy of about ±1/2°C. Thermocouples 1 and 2 are connected to the digital temperature indicator to provide a continued temperature monitoring within the cell water and at the top of the specimen. Thermocouple 3 is a type K flexible thermocouple produced by Omega, with an operating range of -50 to 250°C, and an accuracy of about ±1/2°C. A continual monitoring and recording of the temperature measurement at the bottom of the specimen is provided by thermocouple 3 as it is directly connected to the data acquisition system.

5. PROCEDURES

5.1. Setup Preparation

5.1.1. De-airing of Water in the Backpressure Reservoir

Before preparing the specimen, the backpressure reservoir described in Section 4.4 was filled with water from an elevated water tank connected to the bottom of the backpressure reservoir. The valve at the tube line connecting the backpressure reservoir to the elevated water tank was then closed. Next, the water inside the backpressure reservoir was subjected to a vacuum of 85 kPa. The high vacuum is supplied by a vacuum pump connected to the top of backpressure reservoir (see Fig. 4.14). The purpose of applying a high vacuum is to de-air the water inside the backpressure reservoir. This is significant in that the de-aired water of the backpressure reservoir is the supply that provides the pressure cell with water. Filling the pressure cell with de-aired water helps minimize air within the temperature-regulated oedometer system, facilitating saturation of the specimen. The water in the backpressure reservoir was placed under high vacuum for few hours.

5.1.2. Specimen Preparation

All soil specimens evaluated in this study were prepared in an identical manner in order to allow comparison of the compiled results obtained from the experimental program. The same procedure was followed in all tests for specimen compaction and placement, and all specimens were tested in saturated conditions.

The target compaction conditions were 17% gravimetric water content (wet of optimum), and 13.9 kN/m^3 dry unit weight. The soil was moisture-conditioned and stored in sealed 5-gallon buckets (Fig. 5.1). To moisture condition the soil, water was added to a known weight of soil until reaching the target water content.

Fig. 5.1: Moisture conditioning of soil

Static compaction was used to prepare the soil specimens in this study, as it was found to result in nearly identical initial soil conditions. The tools used in the compaction process are shown in Fig. 5.2.

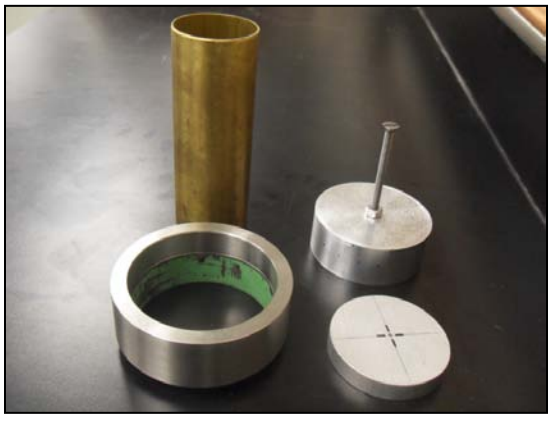

Fig. 5.2: Static compaction tools

The moisture-conditioned soil was placed into the consolidation ring [Fig. 5.3(a)] in order to reach a target dry unit weight of 13.89 kN/m^3. The specimen was placed in two lifts such that the final height was slightly greater than the consolidation ring. The soil was then statically compacted inside the consolidation ring by applying a constant force from the air cylinder, as shown in Fig. 5.3(b). The collar was placed around the consolidation ring during compaction.

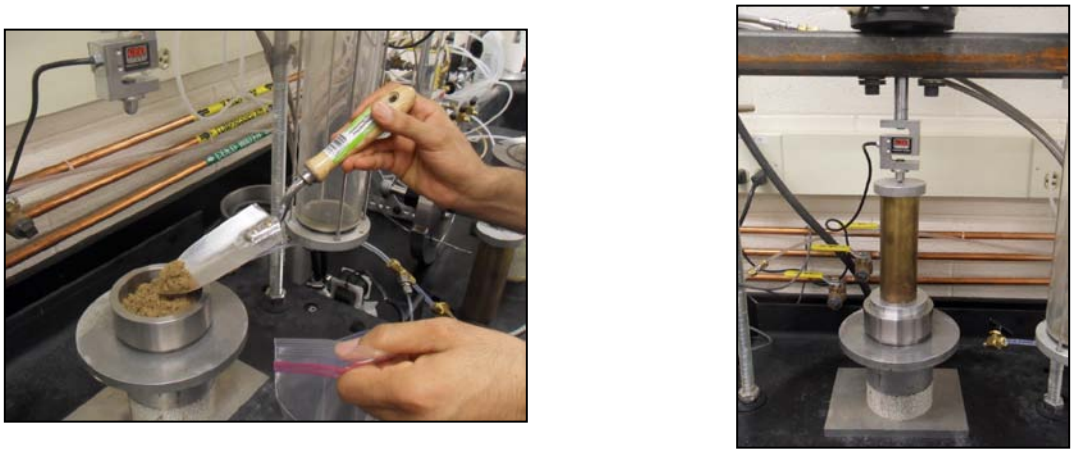

(a) **(b)**

Fig. 5.3: Compaction of Bonny silt: (a) Pouring the soil into the consolidation ring; (b) Application of static load

The soil specimen was compacted in two lifts of equal thickness to reach a uniform soil density. For each lift, the soil was compressed to a thickness of 12.7 mm under a static load of 300 kPa. The interface between the layers was scarified (Fig. 5.4) to minimize the formation of a weak zone within the specimen. After compaction, the consolidation ring containing the specimen was separated from the collar. The specimen was then trimmed and weighed to calculate the actual initial unit weight. The compacted specimen contained in the consolidation ring is shown in Fig. 5.5. At least two samples were obtained for measurement of water content following ASTM D 2216.

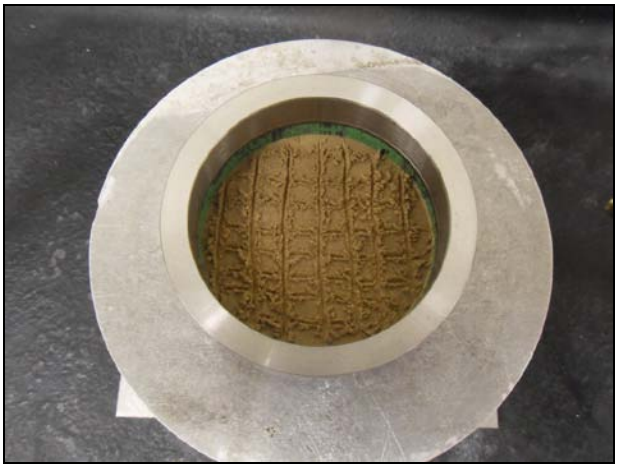

Fig. 5.4: Scarified interface between the two compaction layers

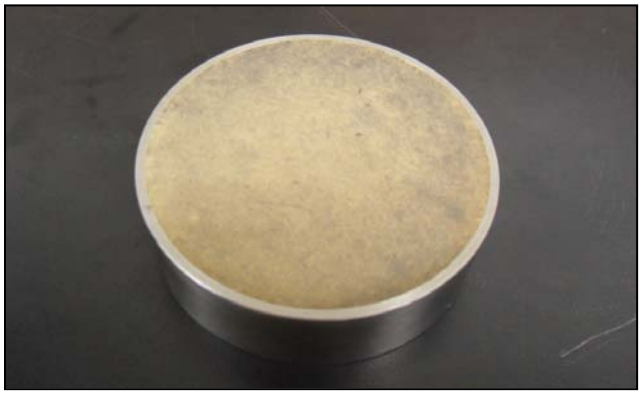

Fig. 5.5: Compacted Bonny silt specimen

5.1.3. Setup of Oedometer Device

The compacted soil specimen was placed in the temperature-regulated oedometer, and the following steps were performed:

1. The upper and lower porous stones were first completely flushed with de-aired water to eliminate possible air bubbles and to prevent a change in water content of the specimen.
2. Filter paper was then situated on top of the lower porous disk to prevent possible intrusion of the soil into the lower disk and the “O”-ring was placed around the inner surface of the raised lip (see Fig. 5.6).

3. The consolidation ring containing the specimen was then put in place inside the pressure cell as shown in Fig. 5.7.
4. The cylindrical collar was then fitted on top of the consolidation ring and a second piece of filter paper was then placed on top of the specimen in order to prevent intrusion of soil grains into the pores of the upper porous disk (Fig. 5.8).
5. The cylindrical cell, piston, sealing O-rings, and upper mounting plate were put in place, and the assembly was sealed to the base plate with four connecting bolts.

Once the pressure cell was sealed, all instrumentation were put in place and connected to the data acquisition system, and tubing and wiring were secured to the temperature-regulated oedometer system. After checking the functionality of all components, including the LabView program and instrumentation, a small seating load (equivalent to about 6.5 kPa) was applied to the specimen to prevent possible swelling of the specimen during the saturation process.

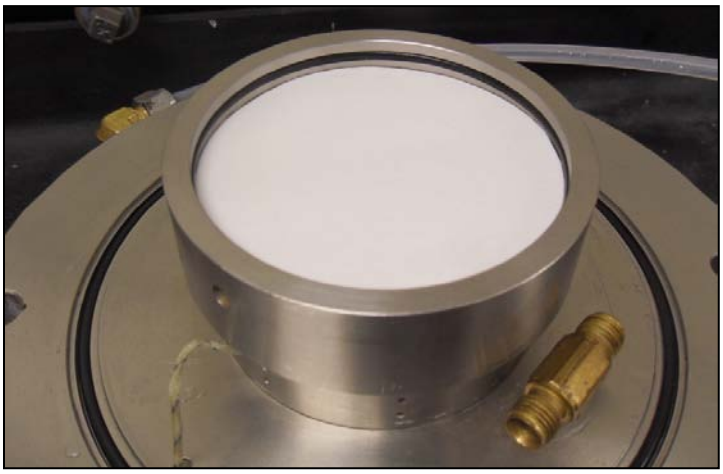

Fig. 5.6: Lower filter paper and "O"-ring surrounding the consolidation ring

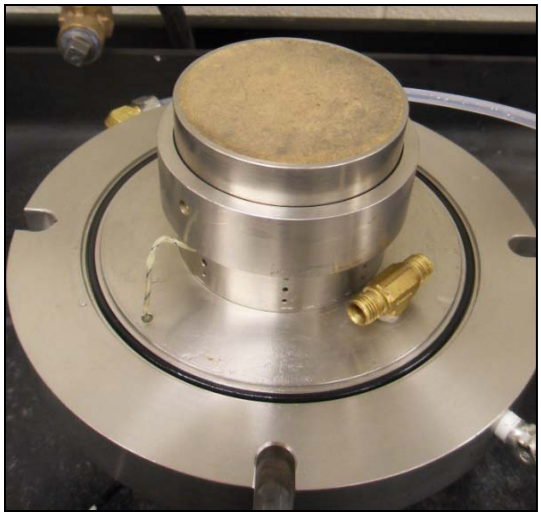

Fig. 5.7: The consolidation ring containing the specimen inside the pressure cell

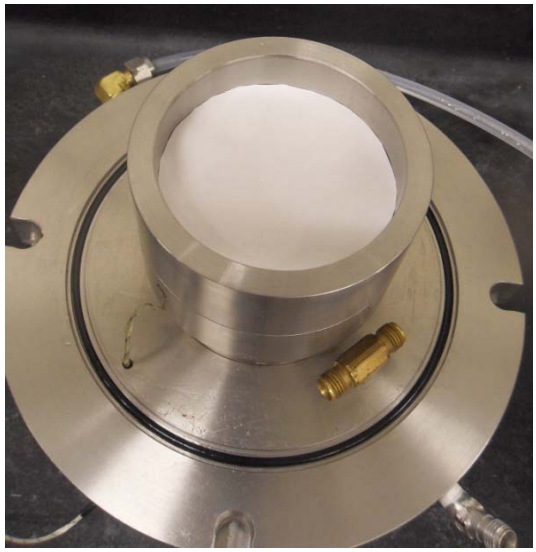

Fig. 5.8: Upper filter paper inside the cylindrical collar

5.1.4. Soil Specimen Saturation Procedures

After application of the setting load to the specimen, a vacuum of 80 kPa was applied to the top of the pressure cell. The purpose of applying the vacuum is to replace the air inside the pressure cell and the specimen itself with vacuum to better saturate the specimen. The vacuum was allowed to act for a sufficient period of time to ensure pulling as much air as possible out of

the pressure cell as well as of the specimen. The de-aired water supplied from the backpressure reservoir was then allowed to seep into the specimen from the bottom of the specimen (see Fig. 4.14), while maintaining vacuum on top of the pressure cell. Allowing the de-aired water to substitute the vacuum in the specimen voids is an efficient means to saturate the specimen.

After saturation of the specimen, the vacuum valve leading to the pressure cell was closed, and the pressure cell was filled with de-aired water from the backpressure reservoir. The de-aired water within the pressure cell and all water lines was then subjected to a backpressure of 40 psi for approximately 24 hours prior to testing. The connection to the backpressure reservoir was maintained in open conditions throughout the duration of the test to permit free drainage out of the top of the specimen during application of mechanical or thermal loading. The purpose of using the backpressure is twofold. First, the backpressure serves as an additional means to further ensure complete saturation of the specimen by leading to dissolution of any air bubbles which might still be trapped in the water inside the specimen or within the rest of the system. Secondly, the backpressure is considered as an initial value of the pore water pressure.

The cell backpressure, which is the pressure acting on top of the specimen through the ports in the loading piston, is the initial reference pressure. Thus, any developed or dissipated pore water pressure is going to be the difference between the pore water pressure measured at the undrained bottom boundary of the specimen and the initial reference pressure. An additional axial force equivalent to the force resulted from the application of the cell backpressure on the cross sectional area of the loading rod, was simultaneously applied from the air cylinder, in order to avoid pushing the loading piston up outside the pressure cell.

5.2. Testing Procedures

After the oedometer device was assembled and the specimen was subjected to backpressure following the procedures described above, mechanical or thermal tests were performed. The mechanical test performed in this study is referred to as an isothermal consolidation (IC) test, while the thermal test performed in this study is generally referred to as a thermal consolidation (TC) test. The thermal consolidation tests were performed to evaluate the impact of heating rate, including thermal consolidation tests TC1, TC2, and TC3 which are performed at different heating rates. The main goal of the IC and TC tests is to infer the pore water pressure and volume change responses during either mechanical or thermal loading.

5.2.1. Machine Deflections

The thermal deformation of the oedometer elements due to heating during thermal consolidation tests were calibrated and taken into account in measuring the thermally induced volume change of the specimens. The temperature change and corresponding change in height measured by the LVDT are shown in Fig. 5.9(a) and 5.9(b), respectively. The thermal vertical dilation of the oedometer apparatus is shown in Fig. 5.9(c). The measured vertical displacements during thermal consolidation tests were corrected using the slope shown in this figure. Specifically, for any change in temperature imposed on the soil specimen, a volume change equal to $\Delta T/2000$ was subtracted from the measured LVDT reading.

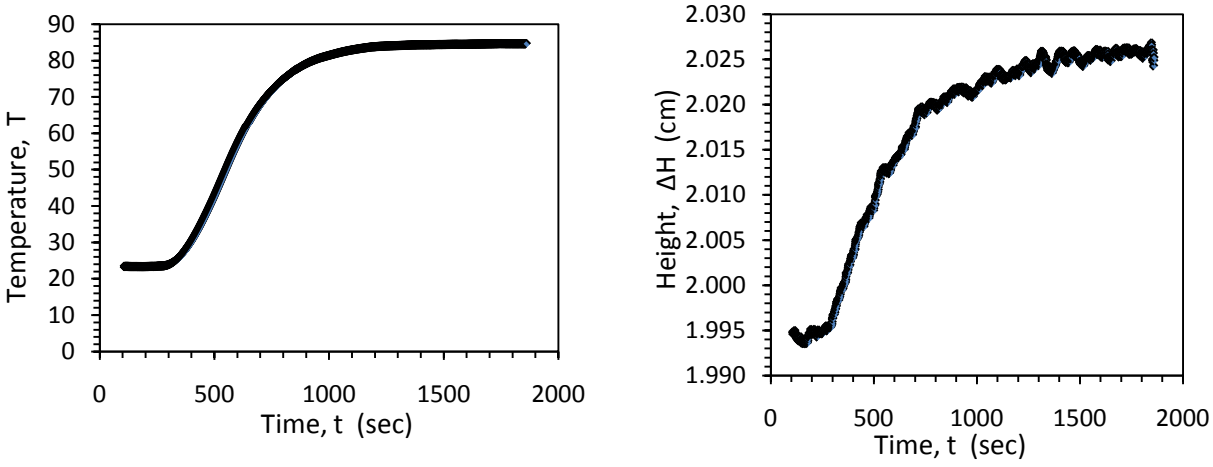

(a) (b)

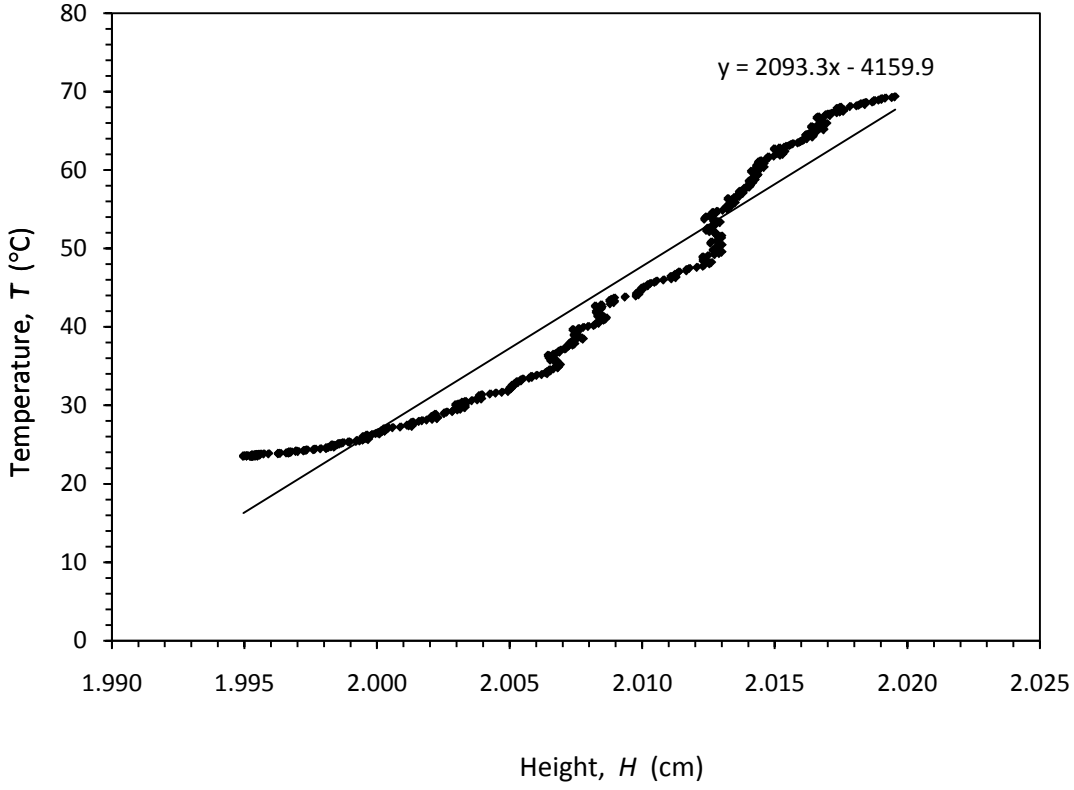

(c)

Fig. 5.9: Thermal machine deflections of the thermal oedometer apparatus

5.2.2. Isothermal Consolidation (IC) Test Procedures

An incremental consolidation (IC) test was performed to infer the preconsolidation stress under ambient temperature. This is necessary to infer the initial overconsolidation ratio for the compacted soils in the thermal consolidation tests. As mentioned in Chapter 2, the stress history of the soil quantified by the overconsolidation ratio has an impact on the contracting/expanding nature of the volume change of a sample heated under a constant stress.

A schematic of the procedures followed in the isothermal consolidation (IC) test is shown in Fig. 5.10. The specimen was subjected to increments of total stress at an ambient temperature of 24 °C. This was the same ambient temperature for all tests. Following the recommendations of ASTM D2435, the highest stress applied to the specimen is intended to be equal or greater than 4 times the preconsolidation stress of the soil. Each of the stress increments was allowed to act upon the specimen until the specimen had completed the primary consolidation phase. After equilibration under the final stress increment, an additional cycle of unloading-reloading was imposed on the specimen to better characterize the recompression characteristics of the compacted soil. The vertical deformations and excess pore water pressure dissipation were continuously monitored and recorded during the entire duration of the testing period using the LVDT and pore water pressure transducer, respectively.

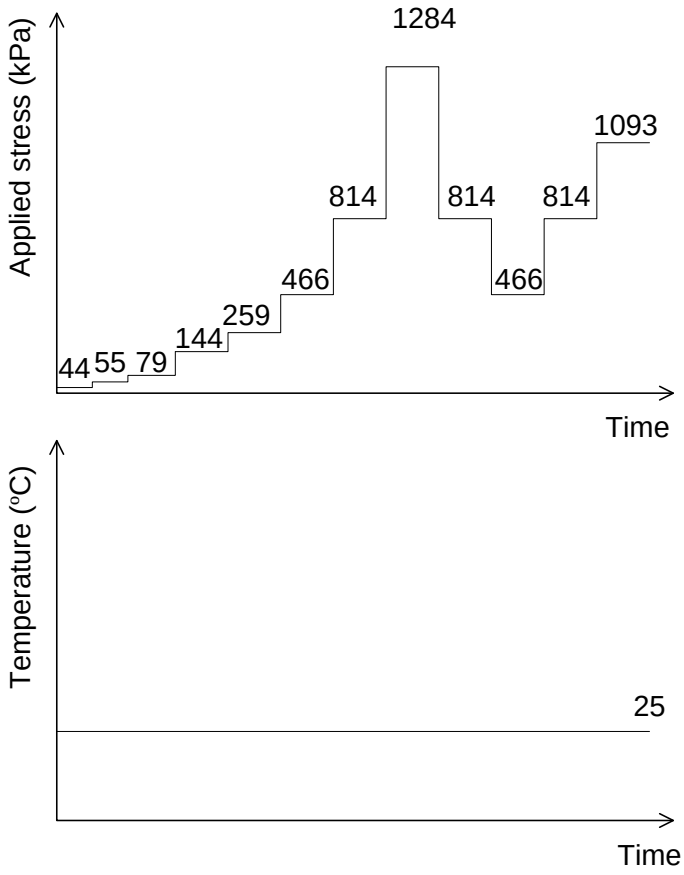

Fig. 5.10: Schematic of the procedures for the Isothermal Consolidation (IC) Test

5.2.3. Thermal Consolidation (TC) Test Procedures

Three thermal consolidation (TC) tests were performed in this study on compacted specimens of Bonny silt under constant stress. The first was performed after completion of the last reloading stage of the IC test shown in Fig. 5.10, while the other two were performed on different specimens. The purpose of the first test was to characterize the volume change of the silt during heating and cooling, while the other two tests were performed to characterize the role of the rate of heating on the magnitude of thermally induced volumetric strain of the compacted silt. After each of the TC tests, the specimens were unloaded and removed from the temperature-regulated oedometer, weighed, oven dried, and reweighed for the determination of the final water content, w_f, and weight of soil solids, W_s.

5.2.3.1 Thermal Consolidation (TC1) Test Procedures

Upon completion of the last reloading increment, the specimen in the IC test described in Fig. 5.10 was subjected to a thermal loading-unloading cycle as additional stages to investigate the effect of the thermal cycle on the volume change behavior of an overconsolidated specimen. The goal of this test was to evaluate the magnitude of thermally induced volumetric strain during heating and cooling. The procedures of the TC1 test are shown in Fig. 5.11. The specimen was heated in two stages at a heating rate of 2.72°C/min to an ultimate temperature of 65.6 °C. The heating increments applied to the specimen with the initial and final target temperatures are shown in Table 5.1.

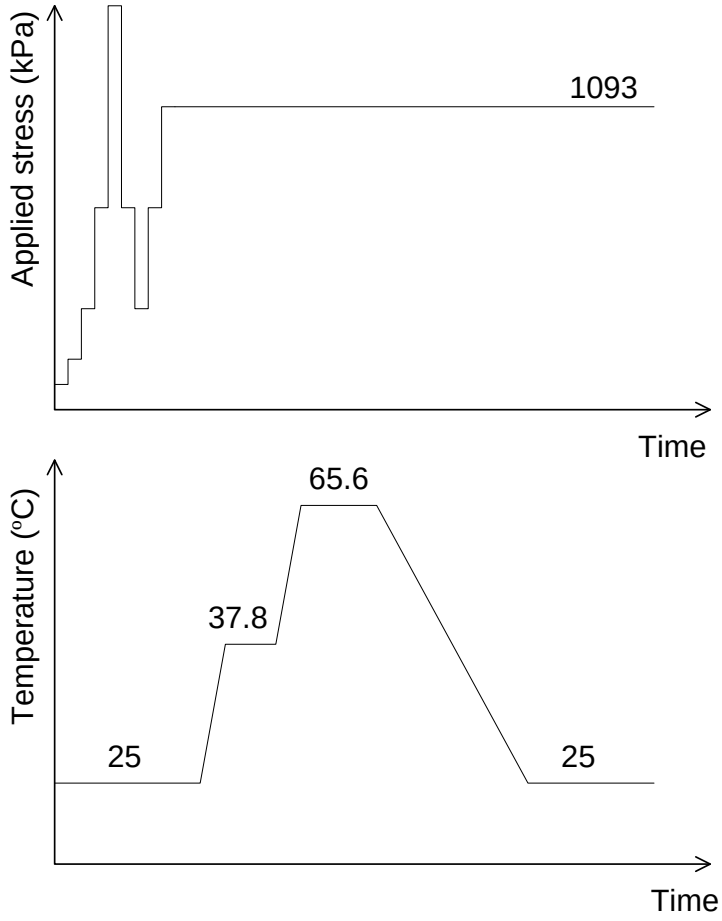

Fig. 5.11: Schematic of the procedures for the thermal consolidation (TC1) test

Table 5.1: Summary of thermal consolidation test (TC1) procedures

Thermal increment/decrement	Target heating rate (°C/min)	Target temperature (°C)	
		Initial	Final
1	2.72	ambient	37.8
2	2.72	37.8	65.6
3	-	65.6	ambient

5.2.3.2 Thermal Consolidation (TC2) Test Procedures

A schematic of the procedures followed in the thermal consolidation (TC2) test is shown in Fig. 5.12. The specimen was consolidated under a stress level corresponding to an OCR of 1.2, which was maintained constant throughout the duration of the test. After the load has stabilized, a heating increment was applied to the specimen at the highest rate permitted by the temperature regulator for that specific temperature increment. The highest possible rate of heating was achieved by applying the temperature increment in stepwise fashion as previously explained in Section 4.5. An average rate of heating of 2.72°C/min was set as a target for each heating increment. After equilibration of the axial deformation under the first heating increment, the specimen was subjected to a second thermal loading increment applied at the same rate. The process was repeated for several additional thermal loading increments. The heating increments applied to the specimen with the initial and final target temperatures are shown in Table 5.2. After equilibration under the last thermal increment, the specimen was allowed to cool to the room temperature of 24 °C. The vertical deformations exerted by the specimen, along with any changes in the specimen pore water pressure were continuously measured during the duration of the testing period using the LVDT and the pressure transducer, respectively.

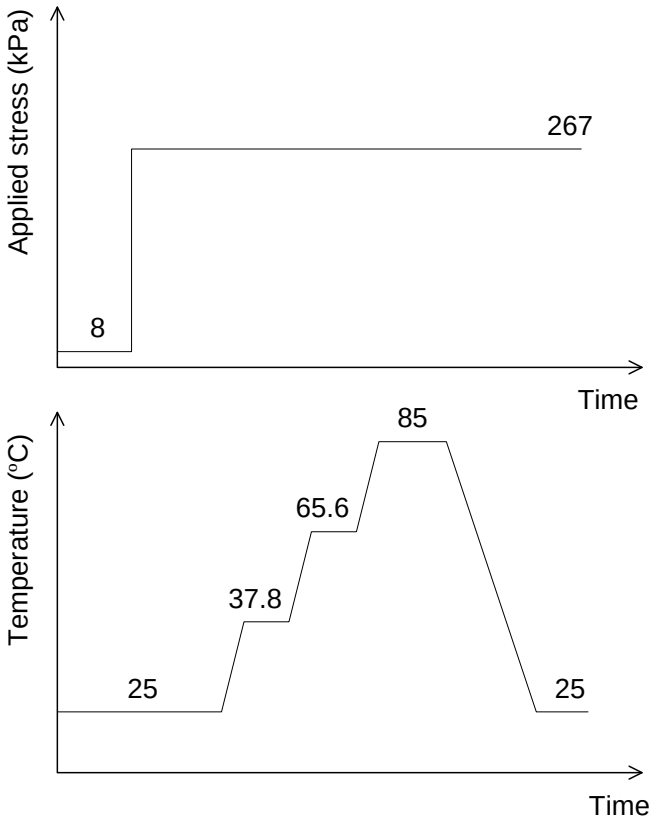

Fig. 5.12: Schematic of the procedures for the thermal consolidation (TC2) test

Table 5.2: Summary of the thermal consolidation test (TC2) procedures

Thermal increment/decrement	Target heating rate (°C/min)	Target temperature (°C)	
		Initial	Final
1	2.72	ambient	37.8
2	2.72	37.8	65.6
3	2.72	65.6	85
4	-	85	ambient

5.2.3.3 Thermal Consolidation (TC3) Test Procedures

A schematic of the procedures followed in the thermal consolidation (TC3) test is shown in Fig. 5.13. The specimen was consolidated under the same stress as in TC2 test in order to allow a comparison of the results. This stress was then held constant throughout the duration of

the test period, while increments of temperature change were successively applied to the specimen at the lowest rate possible by the temperature regulator (0.14°C/min). As previously explained in Section 4.5, the rate of heating during each heating increment was lowered to the lowest rate possible by applying the target increment in very small divisions, 1.4°C each. Each small division was allowed to equilibrate for 10 min before applying the next division.

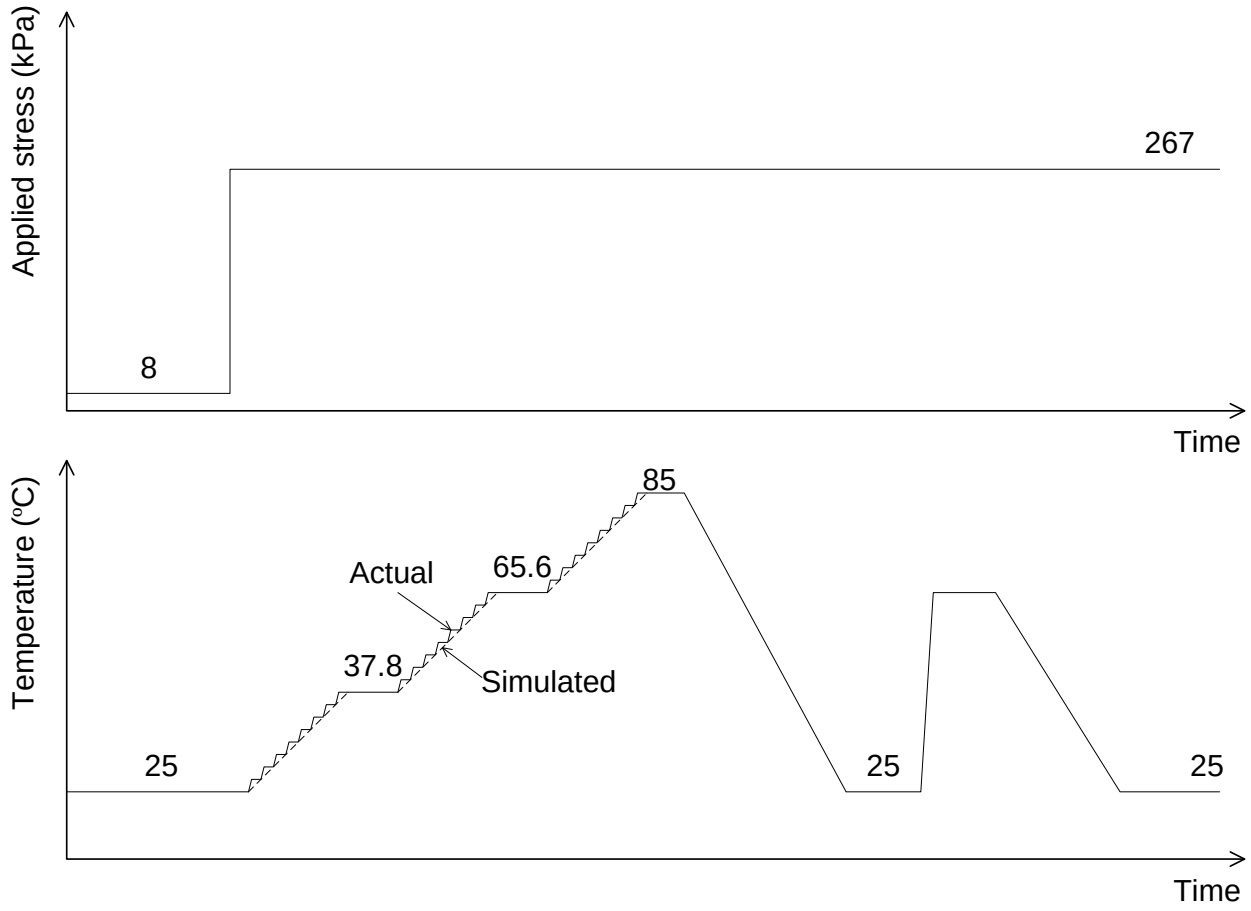

Fig. 5.13: Schematic of the procedures for the thermal consolidation (TC3) test

Table 5.3 summarizes the heating increments applied to the specimen with their initial and final target temperatures. As in TC2 test, each heating increment was allowed to act on the specimen until the axial deformations measured by the LVDT stabilized. At the end of the last heating increment, the specimen was cooled to the room temperature. The specimen was then subjected to an additional loading increment at a rate of 5.5 °C/min. This high rate was achieved

by applying a large temperature increment of 41°C in stepwise fashion. This large increment causes the regulator to work harder to achieve the target temperature. The specimen was then cooled to the ambient temperature.

Table 5.3: Summary of the thermal consolidation (TC3) test procedures

Thermal increment/decrement	Target heating rate (°C/min)	Target temperature (°C)	
		Initial	Final
1	0.14	ambient	37.8
2	0.14	37.8	65.6
3	0.14	65.6	85
4	-	85	ambient
5	5.5	ambient	65.6
6	-	65.6	ambient

6. RESULTS

6.1. Overview

Isothermal and thermal consolidation tests were performed on three compacted Bonny silt specimens in order to evaluate the impact of the rate of temperature change on their volume change behavior. A description of the different tests is shown in Table 6.1, along with a summary of the initial conditions of the soil specimens. It can be notice from Table 6.1 that the initial void ratio for the thermal consolidation (TC1) test is considerably different from those of the thermal consolidation (TC2) test and the thermal consolidation (TC2) test, and all of them are different from the isothermal consolidation (IC) test. These differences in initial void ratios are mainly due to differences in the stress history. The IC test was carried out on a normally consolidated specimen, while in the thermal consolidation tests, the specimens were brought to an OCR of 1.2. The specimen in the TC1 test was initially in the recompression curve (i.e. the preconsolidation stress is higher than that of the two other thermal consolidation tests).

Table 6.1: Summary of tests

Test name	Specimen number	Test description	e_c	w_c	e_i
IC	1	Isothermal consolidation	0.865	17.3	0.855
TC1	1	Thermal consolidation with an average heating rate of 2.72°C/min	N/A	N/A	0.504
TC2	2	Thermal consolidation with an average heating rate of 2.72°C/min	0.861	17.2	0.724
TC3	3	Thermal consolidation with an average heating rate of 0.14°C/min followed by an average heating with a heating rate of 5.5°C/min	0.836	17	0.737

Note: e_c: compaction void ratio
w_c: compaction water content
e_i: initial void ratio

Measurements of the response of the compacted silt specimens to the different paths of mechanical or thermal loading followed in these tests are presented in this chapter, focused on evaluation of the impact of different rates of heating. The soil's response is presented in terms of changes in void ratio and pore water pressure. The void ratio at the end of each thermal or mechanical loading increment was calculated using the following steps:

1. The height of the soil solids, H_s, was first calculated using the following relationship:

(6.1) $$H_s = \frac{H_i}{1 + e_i}$$

where H_i is the initial height of the specimen, and e_i is the initial void ratio.

2. The void ratio at any time during the test, e, was calculated from the height of soil solids and the measured height of the specimen using the phase diagram as follows:

(6.2) $$e = \frac{H}{H_s} - 1$$

6.2. Isothermal Consolidation (IC) Test

The mechanical loading and unloading paths followed in the isothermal consolidation (IC) test are represented by the solid lines shown in Fig. 6.1. The main purpose of this test is to infer the preconsolidation stress of the compacted silt at ambient temperature. Although the static compaction pressure was measured, estimation of the preconsolidation stress of the silt after saturation is difficult because of the contribution of the matric suction in the unsaturated silt during compaction. The test was carried out under a constant average temperature of 23.5 °C.

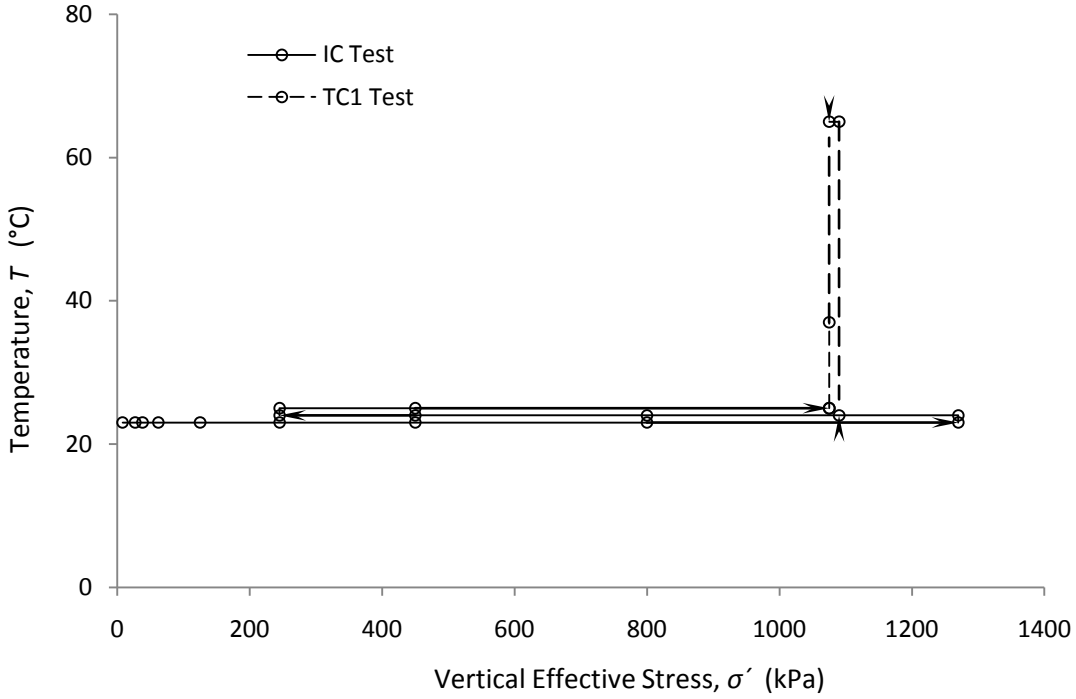

Fig. 6.1: Loading and heating paths followed in tests on specimen 1 (IC and TC1 tests)

Table 6.2 summarizes the calculated void ratio at the end of each mechanical loading or unloading step. Plot of the void ratio versus effective stress is shown in Fig.6.2. Evaluation of the compression curve indicates that the preconsolidation stress was approximately 300 kPa.

Table 6.2: Summary of results for IC test

Increment/decrement	Initial stress (kPa)	Final stress (kPa)	Void ratio
1	8	44	0.850
2	44	55	0.847
3	55	79	0.837
4	79	144	0.804
5	144	259	0.747
6	259	466	0.667
7	466	814	0.573
8	814	1284	0.487
9	1284	814	0.524
10	814	466	0.567
11	466	259	0.594
12	259	466	0.571
13	466	1093	0.504

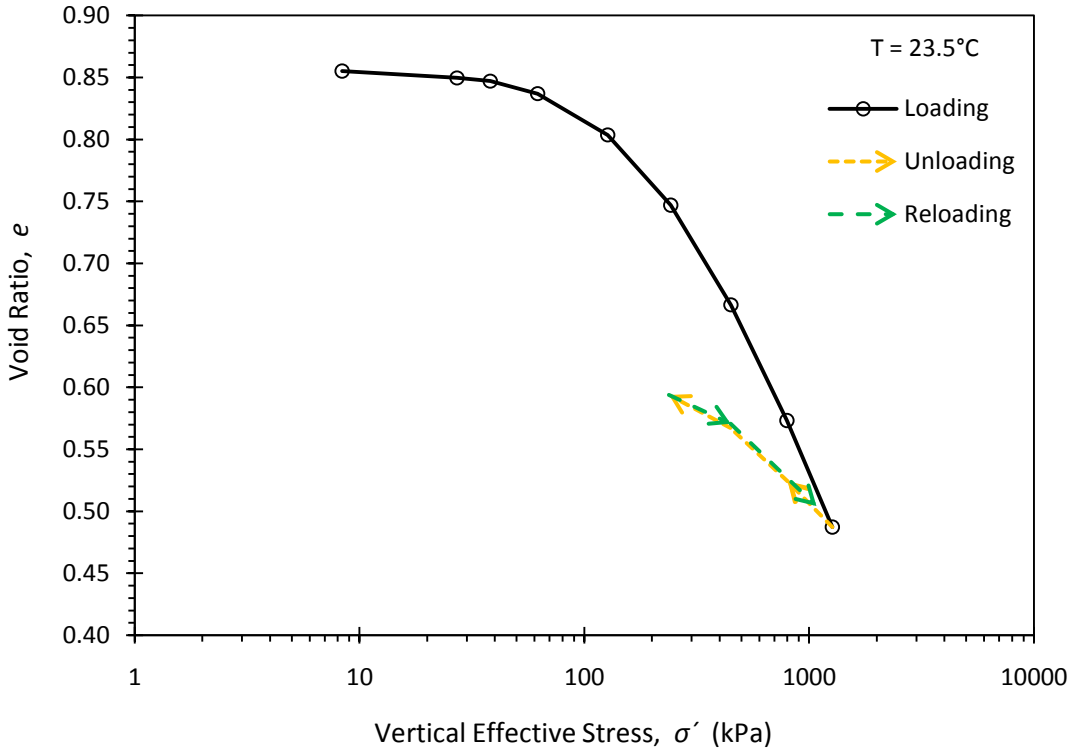

Fig. 6.2: Variations in void ratio with effective stress at 23.5°C for IC test

6.3. Thermal Consolidation (TC1) Test

The goal of this test was to evaluate the ultimate changes in volume of the silt during heating and cooling, without emphasis on the rate of heating. The dashed lines in Fig. 6.1 represent the thermal loading paths followed in the thermal consolidation (TC1) test. The test was carried out at the end of the isothermal consolidation (IC) test under an effective stress of 1093 kPa at which point the soil has an overconsolidation ratio (OCR) value of 1.2. The vertical effective stress as measured by the load cell throughout the test period is presented in Fig. 6.3. The change in measured temperature of the specimen with time for the TC1 test is shown in Fig. 6.4.

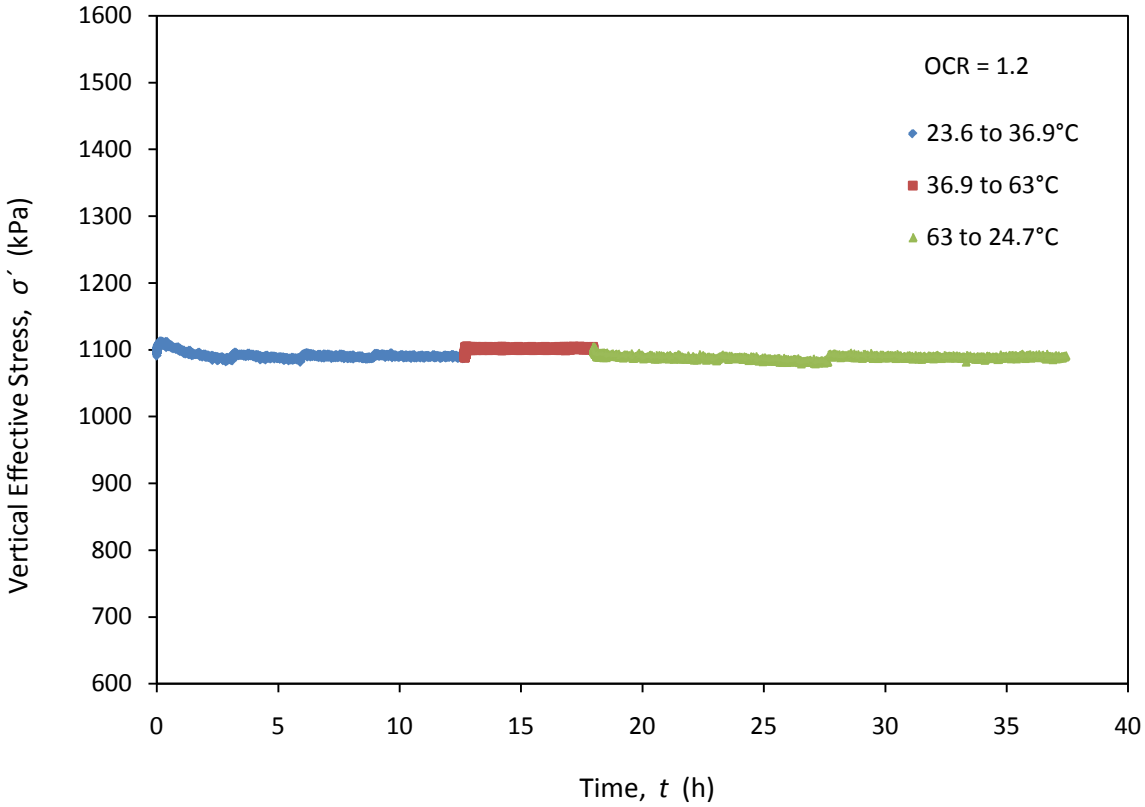

Fig. 6.3: Vertical Effective Stress versus time for TC1 test

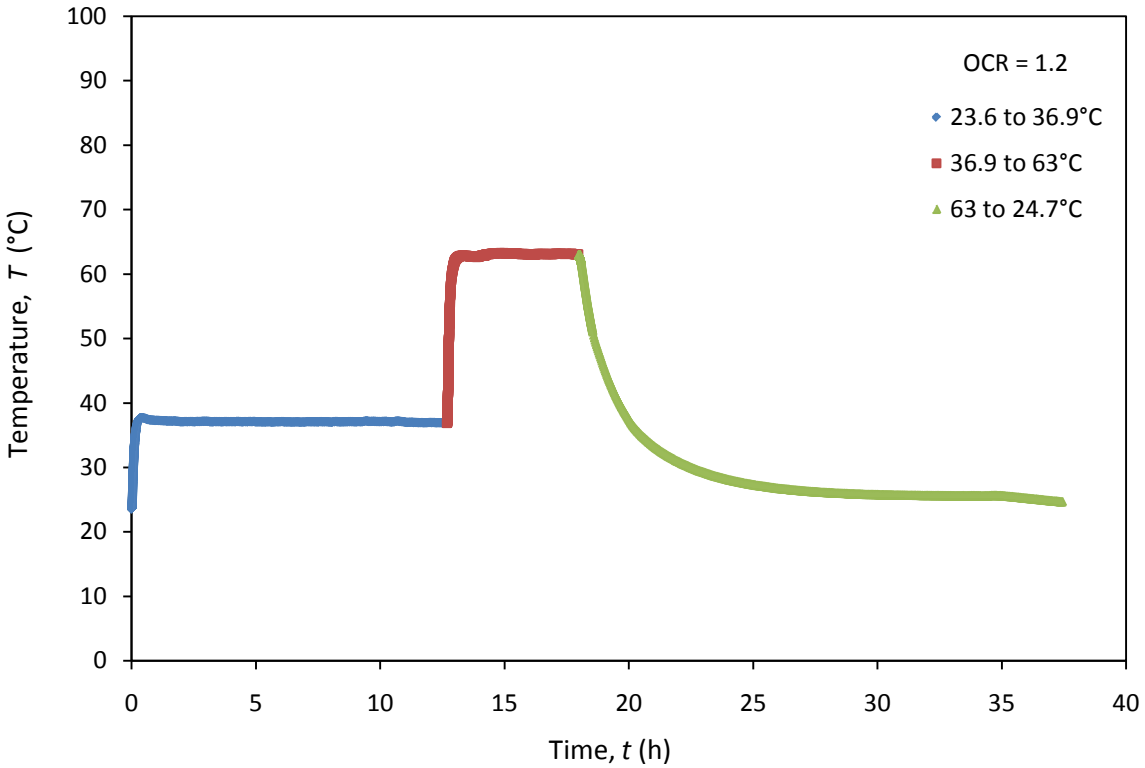

Fig. 6.4: Temperature versus time for TC1 test

The compiled data from the TC1 test in the form of a plot of specimen height versus time is shown in Fig. 6.5, while a plot of the corresponding changes in pore water pressure is presented in Fig. 6.6. In each heating increment, an initial contraction was observed which followed by a relatively slight dilation, resulting in a net decrease in specimen height (Fig. 6.5). The first increment of heating led to a percentage decrease in height of 0.34%, while the second increment in temperature led to a relatively larger contraction of the specimen of about 0.45%. These observations can be expected for a slightly overconsolidated specimen (similar behavior to normally consolidated soils as discussed in Section 2.3.3.1). A negligible net change in the specimen height was noted upon cooling of the specimen to room temperature. The excess pore water pressures during each heating increment show a very rapid increase in pore water pressure, which dissipated relatively quickly. This rapid dissipation of the excess pore water pressure likely occurred due to two reasons. First, the hydraulic conductivity of Bonny silt is relatively high compared to most of the other soils evaluated in thermo-mechanical testing. Second, the rate of heating was not instantaneous (2.72 °C/min), so the pore water pressure in the specimen did not increase instantaneously as would be expected in a conventional consolidation test during application of a load increment. In fact, the rate of dissipation was faster than the rate of heating. More accurate measurements of the generation and dissipation of the excess pore water pressure were not possible because the smallest time interval for data collection in the National Instruments CompacDAQ system is 0.6 seconds.

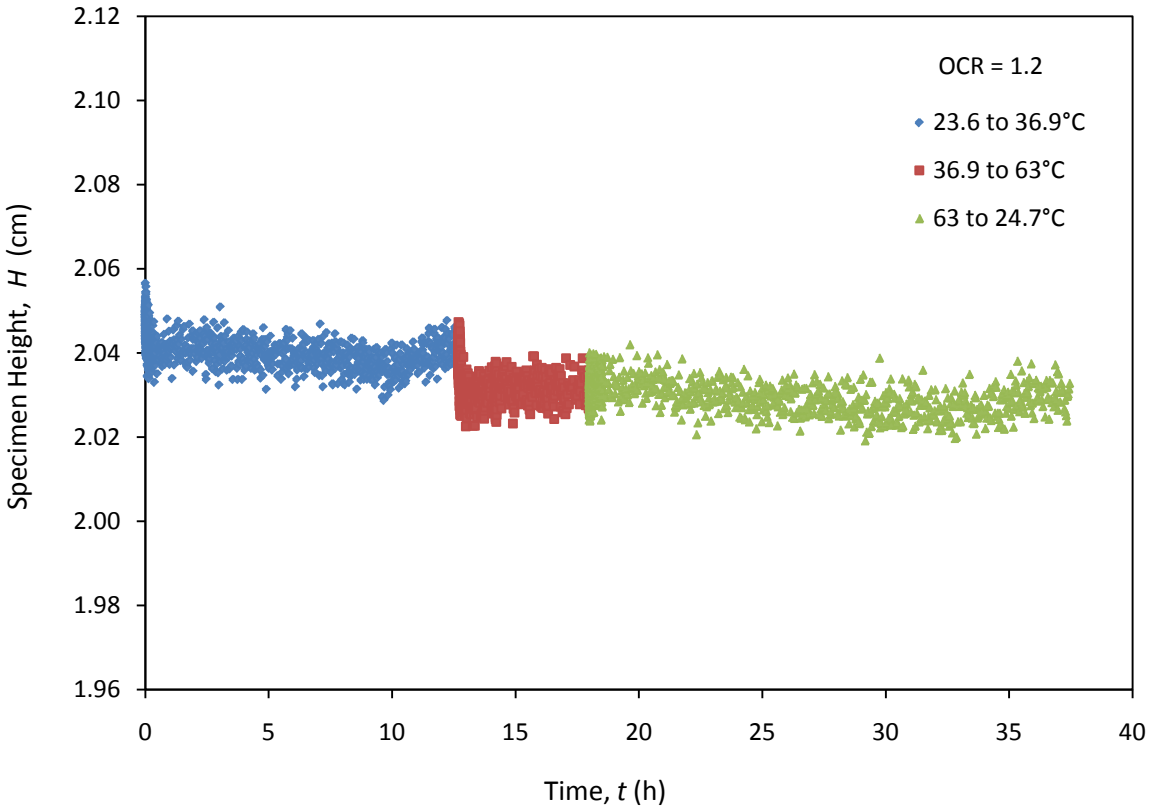

Fig. 6.5: Specimen height versus time for TC1 test

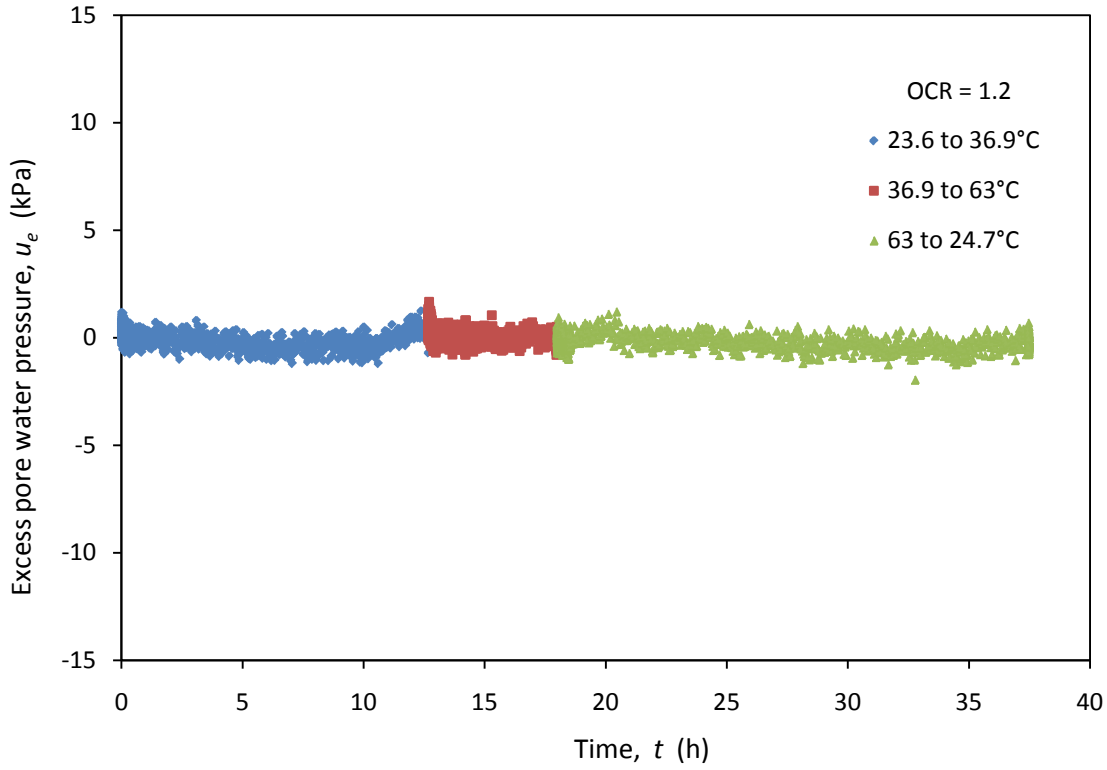

Fig. 6.6: Changes in excess pore water pressure with time for TC1 test

The void ratios at the end of each thermal increment are summarized in Table 6.3. The initial and final values of the measured temperatures for each increment as well as the actual rates of heating are also presented in Table 6.3. The target values of the final temperature and the target heating rates are also listed in Table 6.3 for comparison purposes. A plot of the variation of void ratio with temperature is presented in Fig. 6.7. This figure shows a contraction upon heating, which is expected for a slightly overconsolidated soil. The net change in specimen height after cooling was negligible.

Table 6.3: Summary of results for TC1 test

Thermal increment/decrement	Heating rate (°C/min)		Initial temperature (°C)	Final temperature (°C)		Void ratio
	Target	Measured		**Target**	Measured	
Initial Stress	**N.A.**	**N.A.**	**N.A.**	**N.A.**	**N.A.**	0.504
1	**2.72**	1.61	23.6	**37.8**	36.9	0.499
2	**2.72**	3.31	36.9	**65.6**	63	0.492
3	-	-	63	-	24.7	0.492

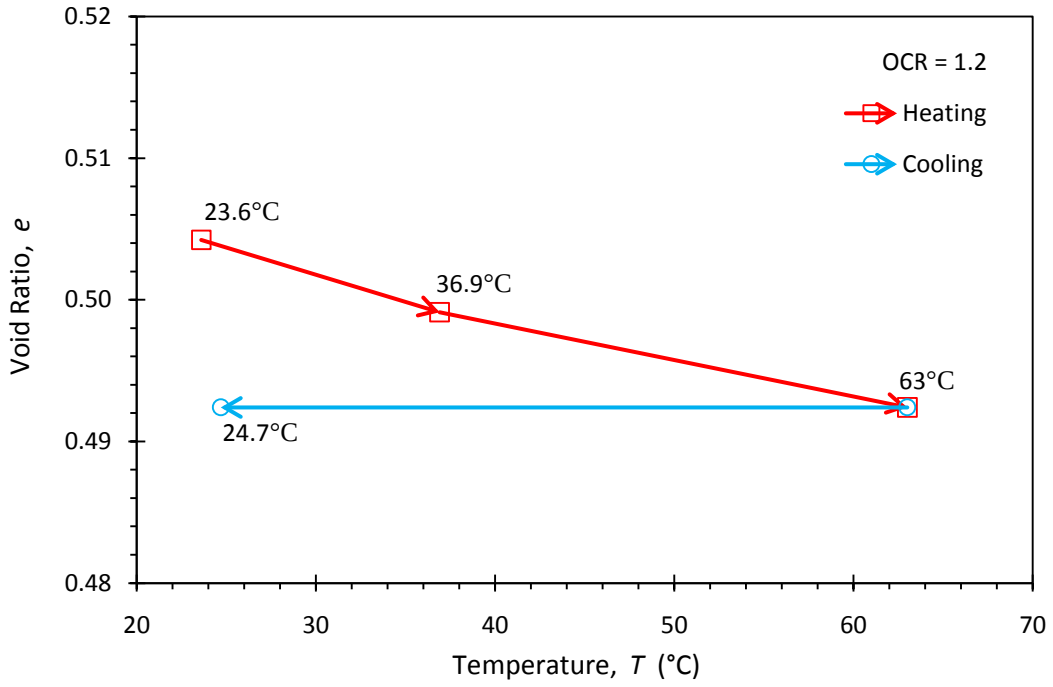

Fig. 6.7: Variations in void ratio with temperature at OCR = 1.2 for TC1 test

6.4. Thermal Consolidation (TC2) Test

The thermomechanical loading paths followed in the thermal consolidation test (TC2) is shown in Fig. 6.8. The test was carried out under an effective stress of 267 kPa at which point the soil has an overconsolidation ratio (OCR) value of 1.2. The vertical effective stress as measured by the load cell throughout the TC2 test period is presented in Fig. 6.9. The change in measured temperature of the specimen with time for the TC2 test is shown in Fig. 6.10.

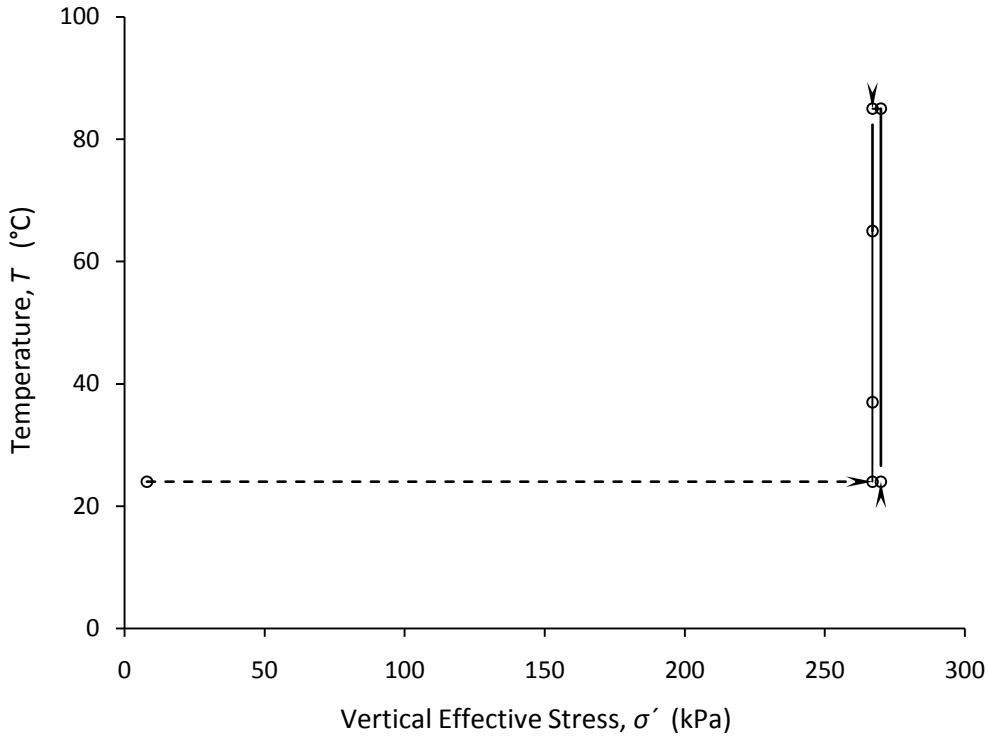

Fig. 6.8: Loading and heating paths followed in the thermal consolidation (TC2) test

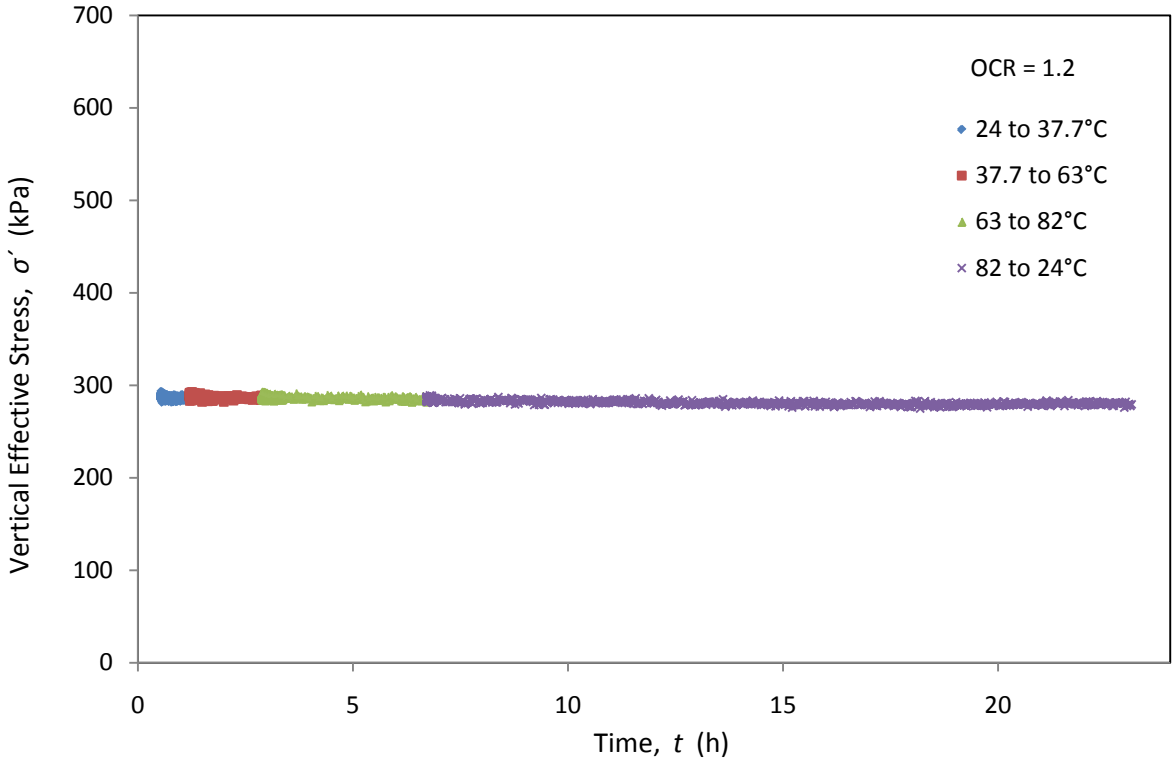

Fig. 6.9: Vertical Effective Stress versus time for TC2 test

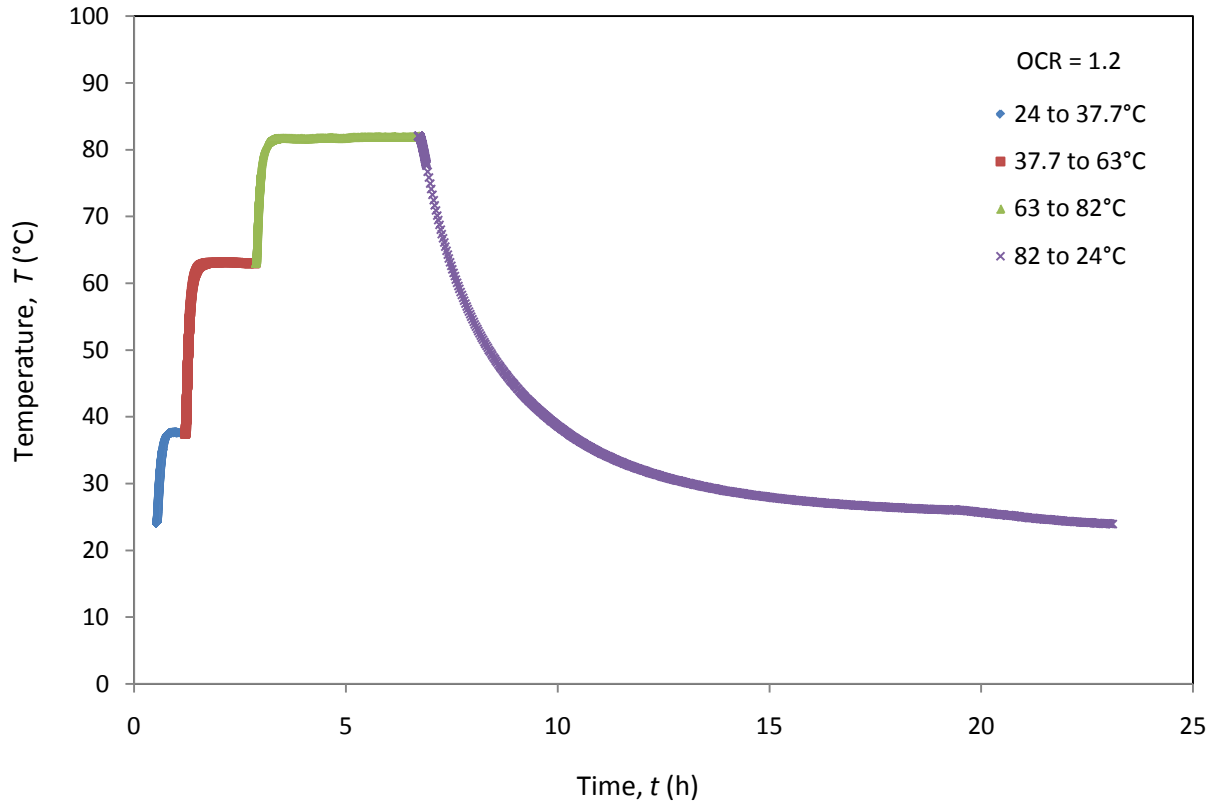

Fig. 6.10: Temperature versus time for TC2 test

The compiled data from the test in terms of changes in specimen height and pore water pressure with time are presented in Fig. 6.11 and Fig. 6.12, respectively. Similar to the TC1 test, considerable net decreases in volume were noted during heating. During each heating phase, a decrease in volume was noted, after which a slight expansion occurred. However, the magnitudes of changes in height are relatively small, within the accuracy of the LVDT. The percentage net decreases in specimen height were 0.5%, 0.73%, and 0.46% for the first, second, and third heating phases, respectively. A negligible net change in volume of the specimen was noted upon cooling. The pore water pressure shows a significant increase in pore water pressure after each heating increment, which dissipated relatively quickly (Fig. 6.12).

Table 6.4 summarizes the target and measured temperatures at the beginning and the end of each temperature rise increment. The target and actual rates of heating are also summarized in the same table. The target heating rates were not achieved in the first and the third heating increments because these two increments were not large enough to cause the heater to output the desired target rates. The relationship between the heating rate and the increment of loading was observed after analysis of the data. The temperature increments were limited by the maximum temperature of 85 °C permitted by the circulating pump. The calculated void ratios at the end of each thermal increment are summarized in Table 6.4. Plot of the void ratio versus temperature is shown in Fig.6.13. A contraction was noted at the end of each heating phase, followed by a negligible net change in volume after cooling.

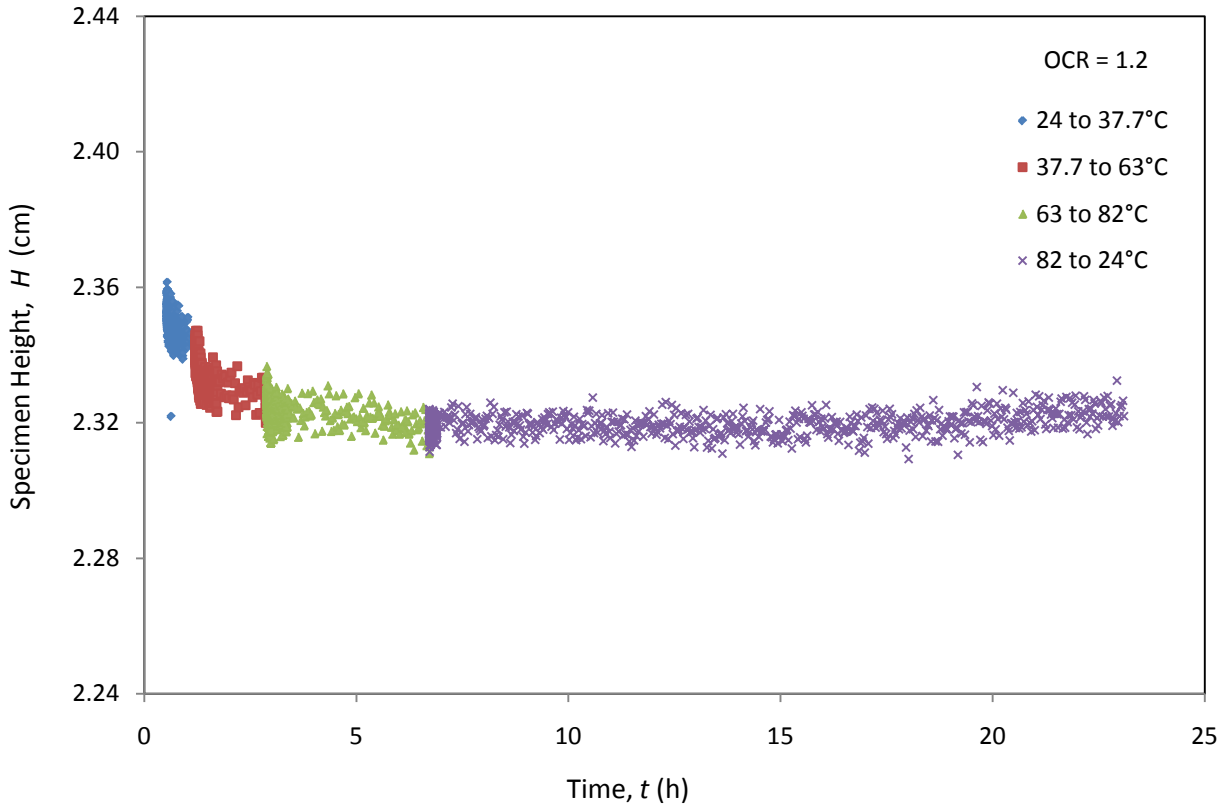

Fig. 6.11: Specimen height versus time for TC2 test

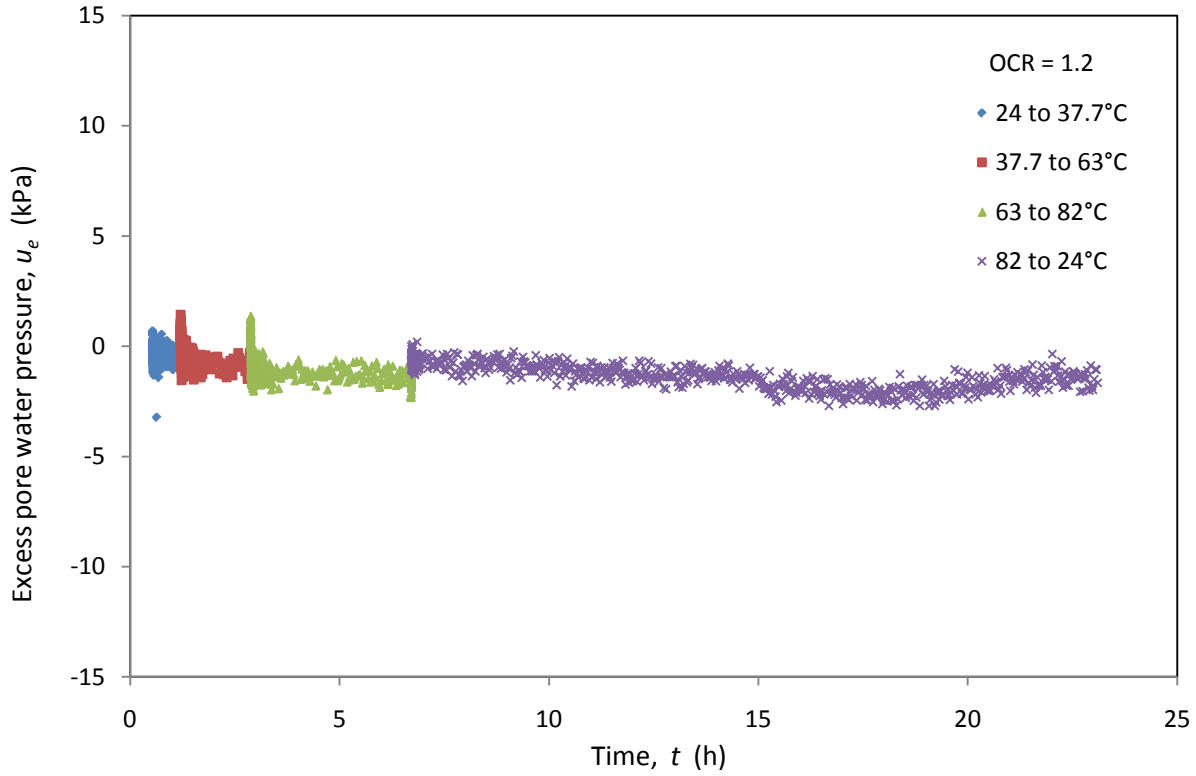

Fig. 6.12: Changes in excess pore water pressure with time for TC2 test

Table 6.4: Summary of results for TC2 test

Thermal increment/decrement	Heating rate (°C/min)		Initial temperature (°C)	Final temperature (°C)		Void ratio
	Target	Measured		**Target**	Measured	
Initial Stress	**N.A.**	**N.A.**	**N.A.**	**N.A.**	**N.A.**	0.724
1	**2.72**	1.78	24	**37.8**	37.7	0.718
2	**2.72**	2.88	37.7	**65.6**	63	0.705
3	**2.72**	2.00	63	**85**	82	0.697
4	-	-	82	-	24	0.701

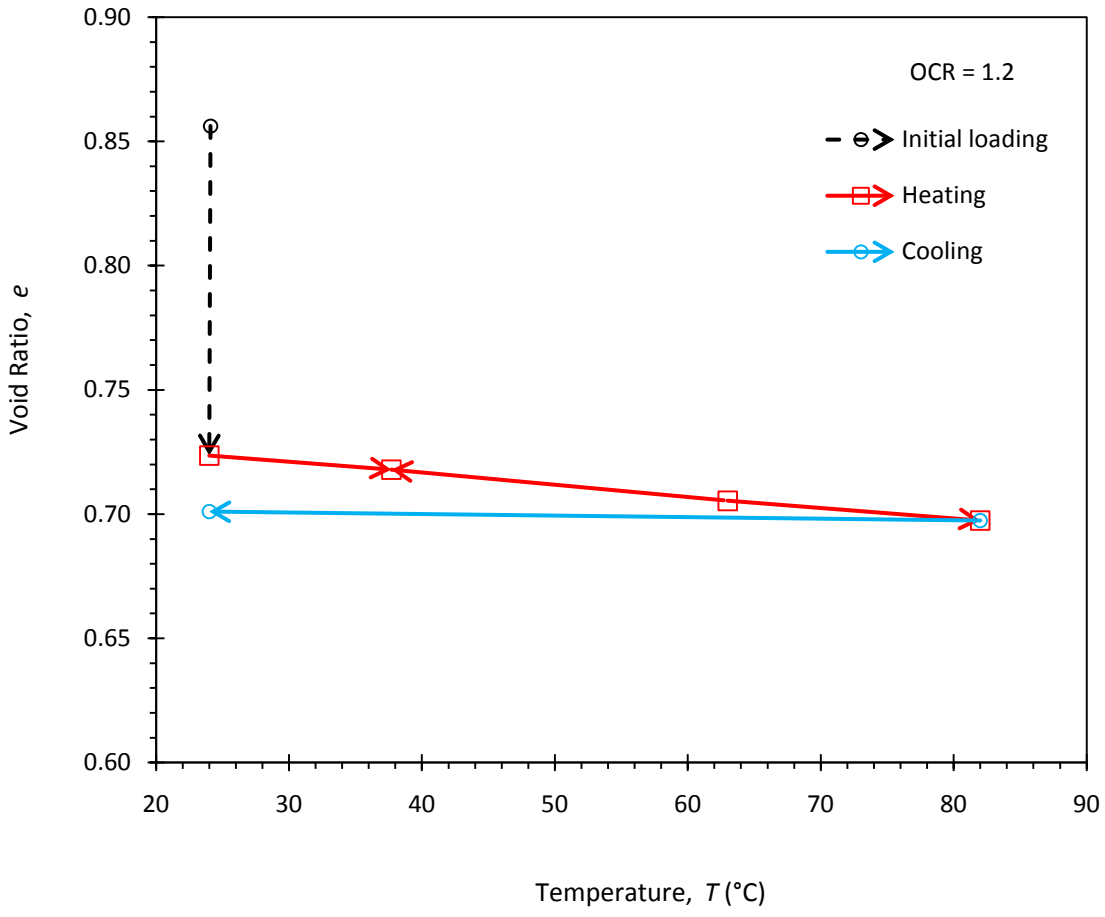

Fig. 6.13: Variations in void ratio with temperature at OCR = 1.2 for TC2 test

6.5. Thermal Consolidation (TC3) Test

The thermomechanical loading paths followed in the thermal consolidation (TC3) test are shown in Fig. 6.14. The specimen was heated in three increments at a relatively low rate, after which it was cooled, and then subsequently heated in a single stage at a relatively fast rate. Similar to the TC2 test, the TC3 test was carried out under an effective stress of 267 kPa at which point the soil has an overconsolidation ratio (OCR) value of 1.2. The vertical effective stress as measured by the load cell throughout testing period is presented in Fig. 6.15. The change in the measured temperature of the specimen with time for the TC3 test is shown in Fig. 6.16.

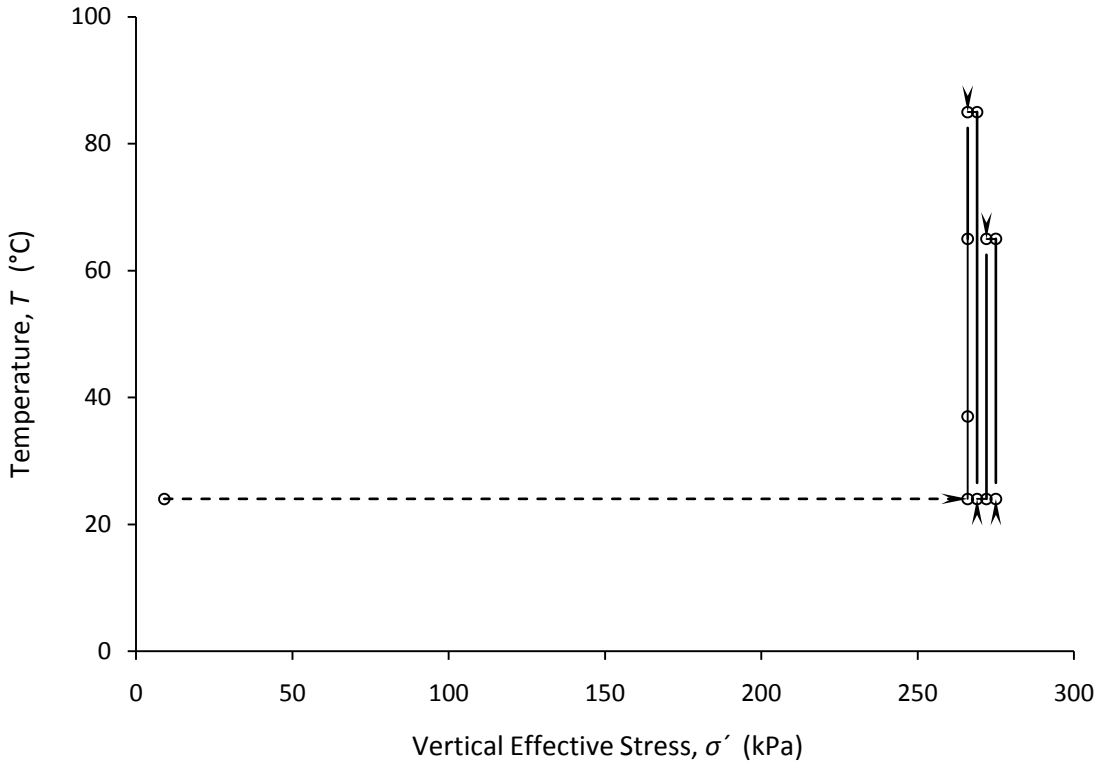

Fig. 6.14: Loading and heating paths followed in the thermal consolidation (TC3) test

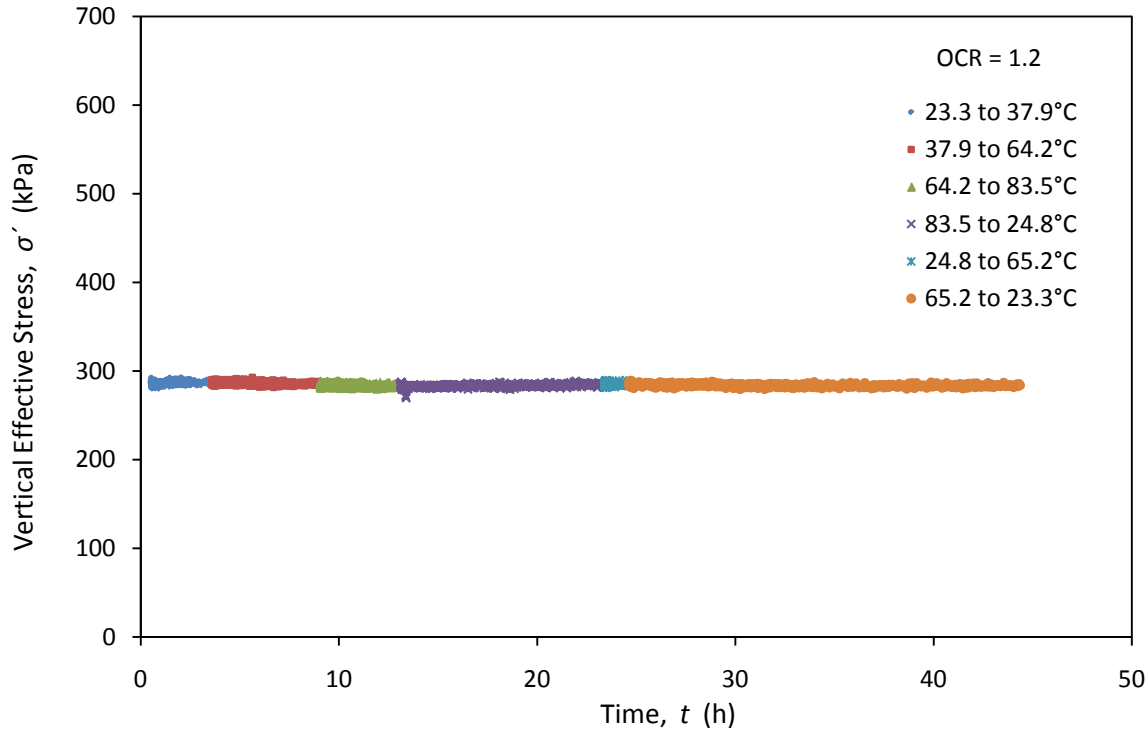

Fig. 6.15: Vertical Effective Stress versus time for TC3 test

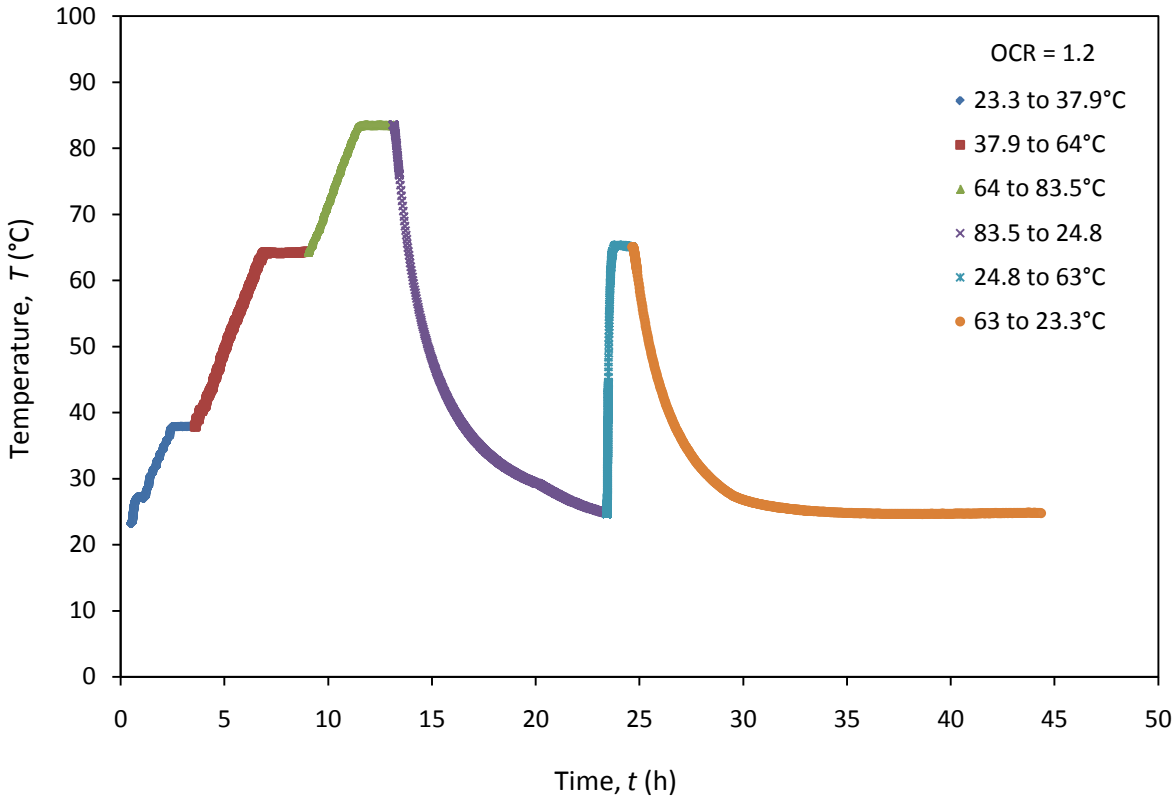

Fig. 6.16: Temperature versus time for TC3 test

The compiled data from the TC3 test in terms of changes in specimen height and pore water pressure with time are presented in Fig. 6.17 and Fig. 6.18, respectively. Similar to the TC2 test, a decrease in volume was noted during the initial heating stages of this test at a heating rate of approximately 0.14 °C/min (Fig. 6.17). A negligible change in volume was also noted during subsequent cooling. This observation may indicate that the heating tests presented in Sections 6.3 and 6.4 may actually be classified as slow heating tests (the rate of heating in these tests was approximately 2.72 °C/min) because they both showed the same volume change response noted as the initial heating stages of TC3 test. This may mean that pore water pressures were allowed to dissipate faster than heat equilibration, leading to initial contraction phases followed by expansion phases. However, the specimen showed a slight initial expansion during subsequent heating at a high rate of 5.1 °C/min followed by a contraction phase, resulting in relatively less significant net contraction.

The initial and final values of the target and measured temperatures for each thermal loading and unloading step in the TC3 test are summarized in Table 6.10. Heating rates of each heating increment performed in this test are also included in the table. The calculated void ratios at the end of each thermal loading increment are also listed in the same table. The variations in void ratio with temperature increment at the different rates applied in this test are shown in Fig. 6.19. A decrease in volume was noted during the initial slow heating stages, followed by a negligible volume change after cooling. The subsequent fast heating resulted in a relatively less contraction. Subsequent cooling resulted in a negligible change in volume.

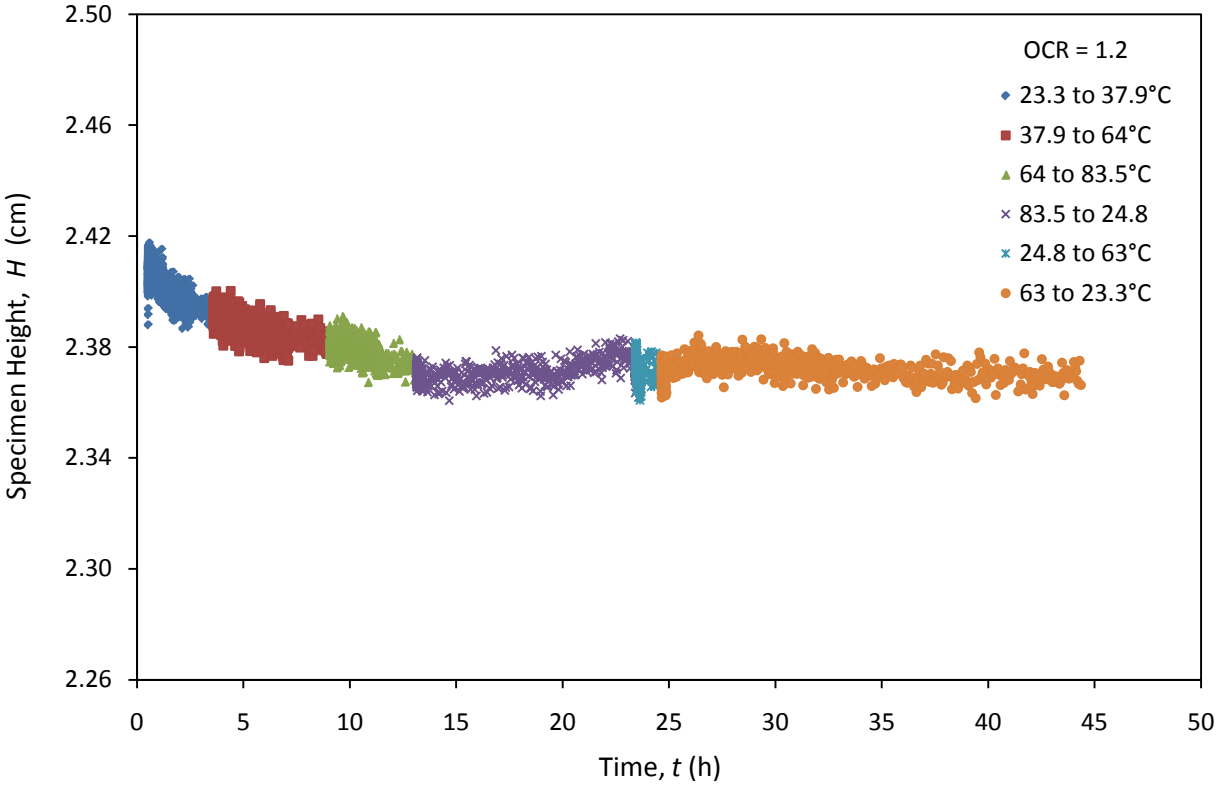

Fig. 6.17: Specimen height versus time for TC3 test

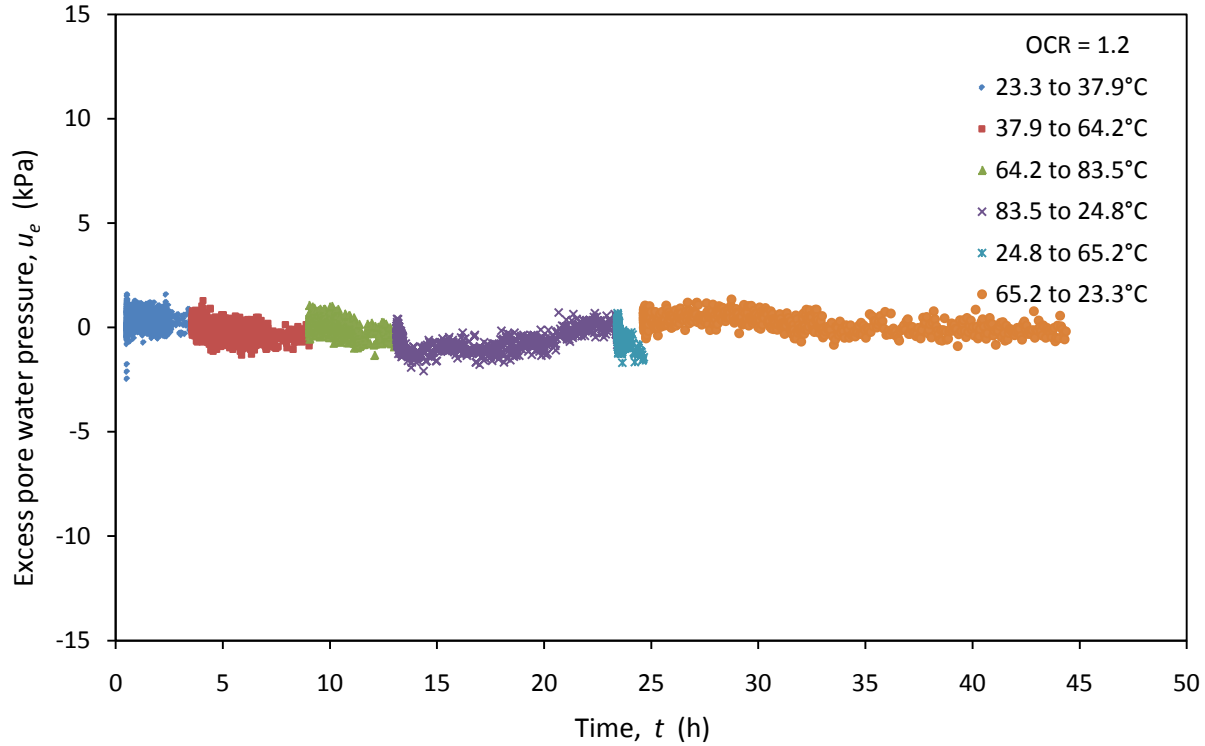

Fig. 6.18: Changes in excess pore water pressure with time for TC3 test

Table 6.5: Summary of results for TC3 test

Thermal increment/decrement	Heating rate (°C/min)		Initial temperature (°C)	Final temperature (°C)		Void ratio
	Target	Measured		**Target**	Measured	
Initial Stress	**N.A.**	**N.A.**	**N.A.**	**N.A.**	**N.A.**	0.737
1	**0.14**	0.128	23.3	**37.8**	37.9	0.730
2	**0.14**	0.139	37.9	**65.6**	64.2	0.722
3	**0.14**	0.139	64.2	**85**	83.5	0.715
4	-	-	83.5	-	24.8	0.717
5	**5.5**	5.1	24.8	**65.6**	65.2	0.713
6	-	-	65.2	-	23.3	0.714

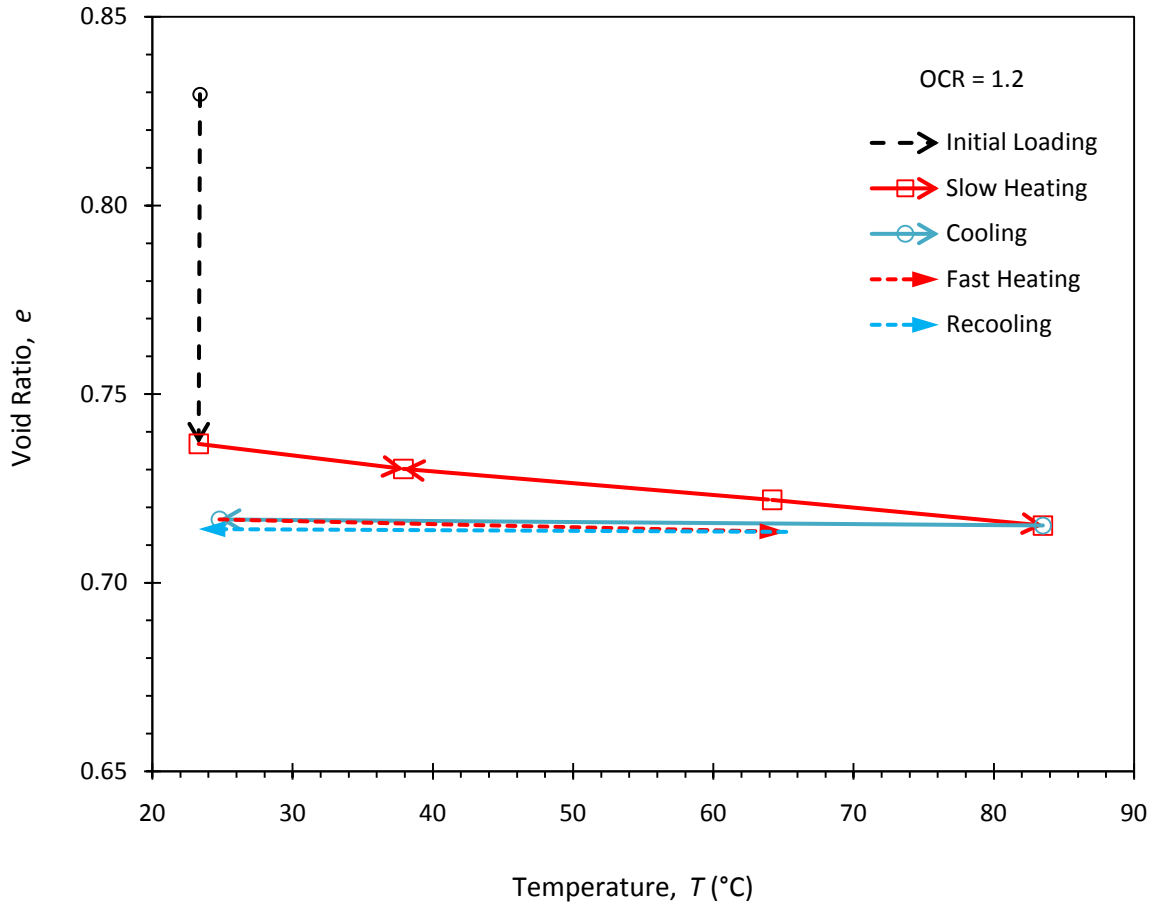

Fig. 6.19: Variations in void ratio with temperature at OCR = 1.2 for TC3 test

7. DISCUSSION OF RESULTS

7.1. Overview

The volume change during thermal consolidation test is attributed to two phenomena: thermal expansion and excess pore water pressure dissipation. When a soil specimen is heated from an external source, heat will diffuse through the soil at a rate associated with the applied rate of heating and the thermal conductivity of the soil, k_t. The temperature increase induced in the soil during heating will lead to thermal expansion of the water and solid grains (referred to as thermal expansion). However, even in fully drained conditions, some excess pore water pressure will be generated due to the difference in the coefficients of thermal expansion of the water and the soil grains (Campanella and Mitchel 1968). This excess pore water pressure will dissipate over time depending on the hydraulic conductivity of the soil, k_h, and will lead to a change in volume (i.e. thermal consolidation). Therefore, there are two different processes leading to two separate volume change processes during heating: the expansion due to the thermal expansion of the soil constituents (or simply thermal expansion); and the consolidation due to the dissipation of excess pore water pressure. The relative rates of these two volume change process can result in different final magnitudes of volume change.

The impacts of different heating rates on thermally induced volume change can be explained using an analogy obtained from drained triaxial testing of saturated soils developed by Gibson and Henkel (1954). For a given soil, the total amount of consolidation will depend on the magnitude of the excess pore water pressure generated due to heating. The magnitude of excess pore water pressure depends on the rate of heating. Specifically, if the heating process is fast, it will be similar to undrained loading of the soil, leading to a large increase in excess pore water pressure. This large increase in pore water pressure will correspond to a large gradient for flow

from the specimen. In addition, because the specimen acts as if it were undrained, the hydraulic conductivity does not change significantly. The combination of a high hydraulic gradient and a high hydraulic conductivity will result in a large amount of thermally induced consolidation. In analogy to mechanical loading, more rapid heating will result in larger excess pore water pressure (partially undrained case, Fig. 71(a), leading to more consolidation over a longer time during its dissipation. Slow heating will result in relatively less excess pore water pressure (drained case, Fig. 7.1(b), and ultimately less consolidation. This is the first effect mechanism for the rate of heating on the magnitude and rate of thermal volume change accompanied by dissipation of pore water pressure.

The thermal expansion due to heating will continue to occur until a state of heat equilibrium is reached in the soil. The time it will take for the soil to reach this state of uniform temperature is governed by the thermal conductivity (which is a unique value for the specific soil) and the rate with which the temperature increment is applied (input and output). In other words, applying the same amount of temperature change with different rates of heating will result in different periods for the thermal expansion to occur. Then, faster heating will result probably in thermal expansion over shorter period of time (uniform temperature reached faster). The combination of the two mechanisms of the heating rate on both the thermal consolidation (contraction) and the thermal expansion, through influencing the dissipation of excess pore water pressure and heat diffusion, respectively, are shown in Figure 7.2. The relative impacts of thermal expansion and thermal consolidation for the two types of testing are shown in this figure.

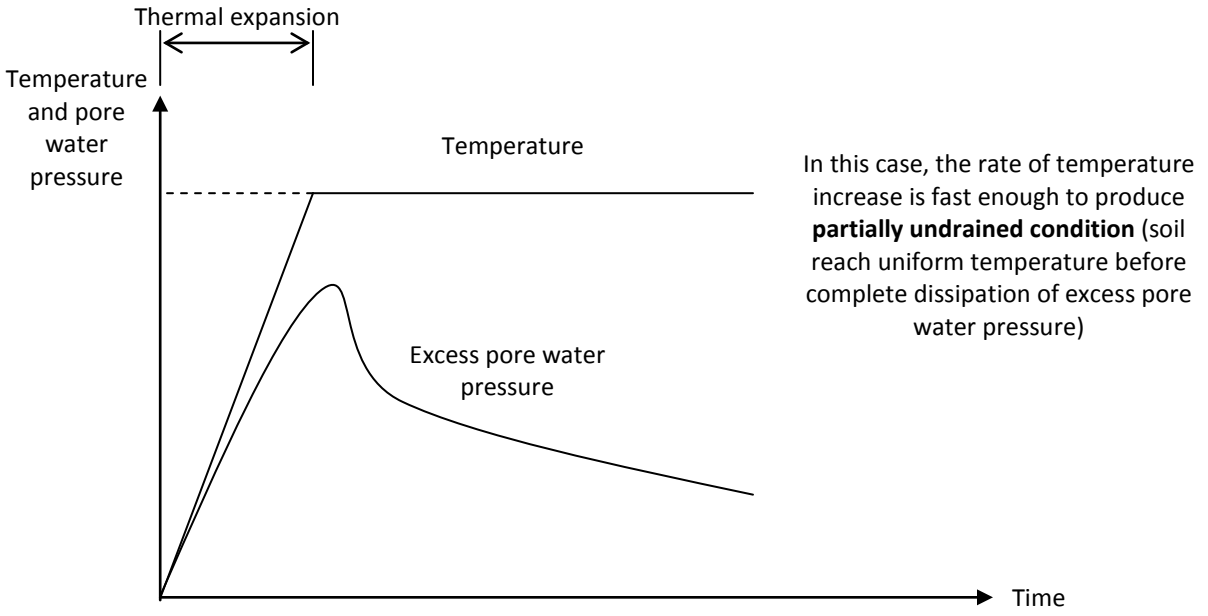

(a)

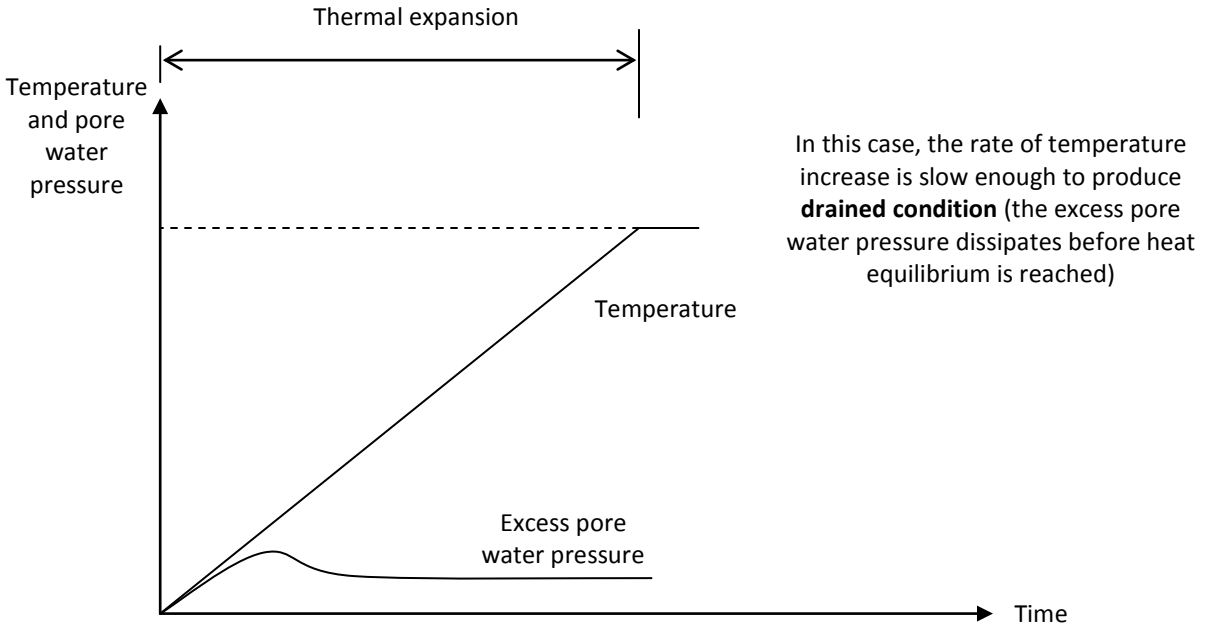

(b)

Fig. 7.1: Effect of rate of heating on the development of excess pore water pressure during drained thermal consolidation tests (a) Slow heating; (b) Fast heating

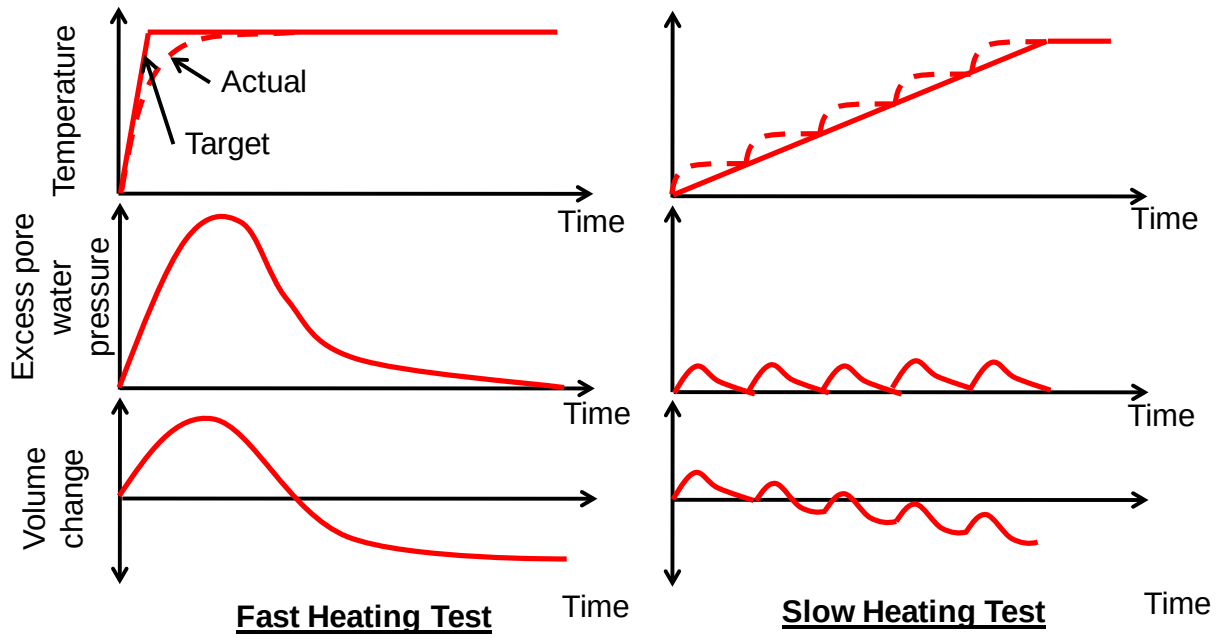

Fig. 7.2: Impact of fast and slow heating on the volume change of saturated soils

Delage et al. (2000) observed that the two phenomena of heat diffusion and pore water pressure dissipation are occurring during thermal consolidation, as discussed above, and that these phenomena can be uncoupled. In drained thermal consolidation tests, the heat equilibrium is usually reached much faster than pore water pressure dissipation in soils of low hydraulic conductivity (e.g. clays), since k_h (or c_v)is small as compared to k_t (a, the thermal diffusivity) (Delage et al. 2000). During the heating phase, an increase in volume occurs due to the undrained thermal expansion of water and solid particles (Fig. 7.3). The amount of water drained due to dissipation of pore water pressure during the heating phase is negligible. After equilibration of the specimen's temperature, the specimen will decrease in volume due to the dissipation of the pore water pressure over time in a process similar to a consolidation at a constant temperature. This case can be referred to as partially undrained [see Fig. 7.1(b)].

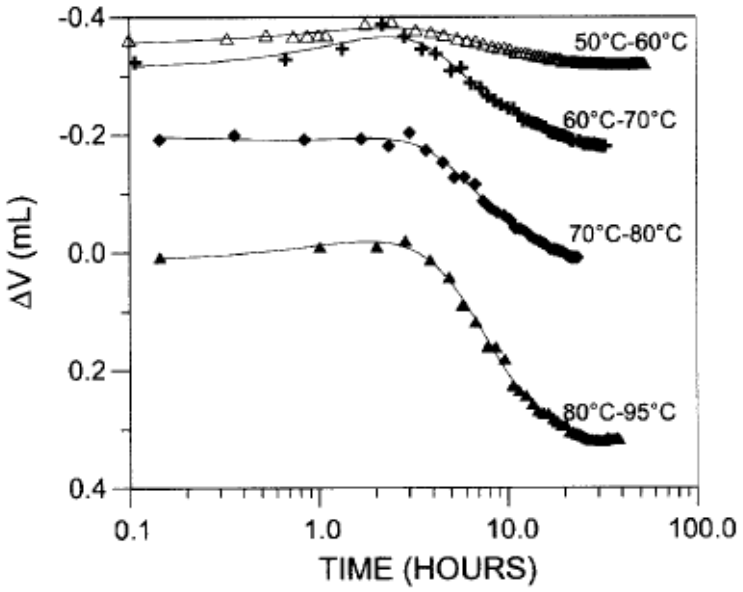

Fig. 7.3: Time rate of thermal consolidation for a compacted clay (Delage et al. 2000)

An opposite situation happens in soils of high hydraulic conductivity (e.g. sands) since k_h is much larger than k_t; the pore water pressure dissipates faster than the diffusion of heat. Excess pore water pressure is dissipated first resulting in a contraction accompanied by draining of water, and the thermal expansion of the solid particles occurs afterward. This case can be referred to as drained [see Fig. 7.1 (a)]. For any specific type of soil, thermal diffusion is influenced by the rate of temperature change induced. The higher the rate of induced temperature change, the faster the rate of heat transfer. Therefore, the rate of heating have a very significant effect on dictating drainage conditions during thermal consolidation tests, especially in soils of medium hydraulic conductivities (e.g. silts) where this effect could result in changes not only in the amount of volume change but also in its direction (i.e. expansion or contraction). In other word, any of the two cases discussed above (drained and partially undrained) could occur during thermal consolidation in effect of different rates of heating. In this section, the response of the specimens to the temperature changes and to the different rates of heating was explained based on the above discussion.

7.2. Thermal Consolidation (TC1) Test

As a result of the small OCR value of the specimen tested in the TC1 test (OCR = 1.2), this specimen behaved as normally consolidated. Despite the scatter in the data presented in the curve of change in specimen height versus time for this test (Fig. 6.5), the two phenomena (i.e. the heat diffusion and pore water pressure dissipation) can be observed. The rate of heating used in this test (2.72°C/min) was relatively low, resulting in a drained condition. The excess pore water pressure generated at the very beginning of each temperature increment dissipated very quickly before heat equilibrium was reached. This results in a contraction in the early stage of each increment. This contraction was followed by a less significant thermal expansion phase due to the thermal expansion of the solid particles, a proof of a drained condition similar to the one presented in Fig. 7.1 (a).

7.3. Thermal Consolidation (TC2) Test

Similar behavior to the TC1 test is observed for TC2 test, which was performed at the same rate of heating (2.72°C/min). The rate of heating was slow resulting in a quick dissipation of the excess pore water pressure before the specimen reaches a uniform temperature. From Fig. 6.11, an initial contraction can be observed in each heating increment. This initial contraction represents the consolidation due to the fast dissipation of the excess pore water pressure. After the pore water pressure reached a steady state value and the water drained out of the specimen, the expansion of the solid particles continued to occur until the specimen reached a state of heat equilibrium. The expansion of the solid grains can be observed from Fig. 6.11 after the end of the contraction phase, specifically in the third heating increment. This is again a drained condition in the effect of the low rate of heating used in this test. This effect was not clear in the first two increments (Fig. 6.11).

7.4. Thermal Consolidation (TC3) Test

The results of the first part of the TC3 test, which performed using a lower heating rates than the two previous tests (0.14°C/min), was similar to the TC1 and TC2 tests. The three heating increments performed in this test under a low rate of 0.14°C/min showed a considerable initial contraction (Fig. 6.17). The initial contraction is due to the fast dissipation of the excess positive pore water pressure which confirms a drained condition. However, the expansion phase was not clear. The overall change in volume observed in each increment of the three tests (i.e. TC1, TC2, and the slow stages of TC3), was a decrease in volume (see Figures 6.7, 6.13, 6.19). This is in full agreement with the observations made by Plum and Esrig (1969) (Fig. 2.9), and Baldi et al. (1988) (Fig. 2.10) for normally consolidated and slightly overconsolidated soils. A subsequent cooling of the soil resulted in almost negligible volume change which might be attributed to the fact that the measured changes in height during cooling were very small such that they fall within the accuracy of the LVDT.

The most interesting part of this test was the last stage of temperature increase which was performed at much higher rate of 5.5 °C/min compared to all of the other heating stages in the thermal consolidation tests. Under this increment, the specimen showed a different behavior. Heat equilibrium was reached faster than pore water pressure dissipation resulting in an initial dilation phase followed by a contraction phase, as shown in Fig. 6.17. The dilation occurred due to the undrained thermal expansion of water and solid particles. The amount of water drained due to dissipation of pore water pressure during the heating phase was negligible. After equilibration of the specimen's temperature, the specimen decreased in volume due to the dissipation of the pore water pressure. The rate of heating used in this increment was fast enough to produce partially undrained condition similar to that observed by Delage et al. (2000) (Fig. 7.3).

In contrast to what one would expect for a partially undrained specimen (specimen heated very fast) (more rapid heating will result in larger excess pore water pressure), the specimen showed a relatively smaller excess pore water pressure (Fig. 6.18) and exhibited less contraction (Fig. 6.19)during the fast heating increment than the three initial slow heating increments. The smaller amount of the excess pore water pressure can be attributed to the increase in the OCR value due to the heating-cooling cycle imposed to the specimen before this increment. This cycle of heating and cooling has caused the soil to behave as if it were overconsolidated, which is in agreement with the observations from Plum and Esrig (1969) and from Sultan et al. (2002) (see Figures 2.5 and 2.6). Specifically, Hueckel and Pellegrini (1992) observed from cyclic undrained heating and cooling tests on saturated clays that a substantial "negative pore-pressure difference" may be induced in clay upon the completion of the thermal cycle (subsequent cooling produces a drop in water pressure). Similar conclusion was previously made by Campanella and Mitchell (1968). Abuel-Naga et al. (2007) reported a similar behavior that the thermally induced pore water pressure under undrained heating condition is a function of the applied mean effective stress during heating phase as well as a function of stress history during cooling phase, as shown in Figures 7.4 and 7.5. In Fig. 7.4, it is shown that the rate of the thermally induced pore water pressure is stress history dependent (OCR) and tends to decrease as OCR increases.

Overall, the observed slight decrease in volume during the fast heating increment following a heating-cooling cycle is in agreement with the observations of Plum and Esrig (1969) and Baldi et al. (1988) regarding the transitional behavior form contraction to expansion as OCR value increases (see Figures 2.9 and 2.10)

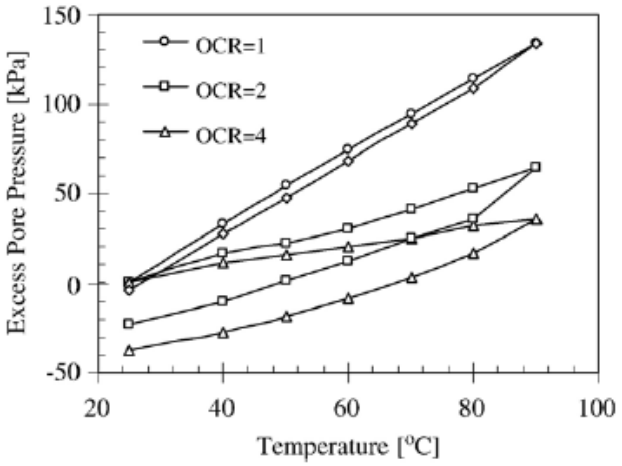

Fig. 7.4: Thermally induced pore water pressure at different OCR values (Abuel-Naga et al. 2007)

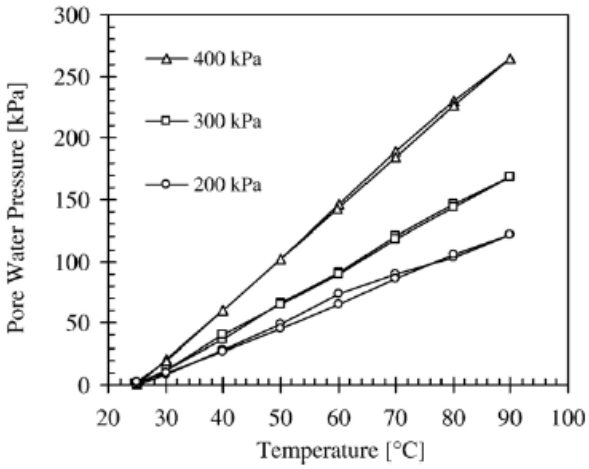

Fig. 7.5: Thermally induced pore water pressure of normally consolidated specimens at different preconsolidation pressures (Abuel-Naga et al. 2007)

Subsequent cooling after this fast heating stage led to a negligible change in volume similar to those observed in the previous tests. The slopes of the void ratio-temperature curve (Fig. 6.19) in the two cooling stages of this test were similar confirming the independency of the slope of cooling of the OCR value. Similar observations were made by Sultan et al. (2002). The response of the specimens to the different rates used in the different stages during the thermal consolidation tests indicates that only the thermal loading stage at the end of TC3 test with a heating rate of 5.5 °C/min can be classified as a fast heating test.

8. CONCLUSIONS

This study involved the use of a temperature-regulated oedometer cell to evaluate the impact of the rate of heating on the thermally induced volume change in saturated, compacted silts. It was found that the impact of heating rates on the thermally induced volume change in soils lies is the difference between the drained and undrained behavior of soils. Specifically, when a soil is heated in undrained conditions, the particles and water will expand at the same rate as the rate of heating. However, the difference in the coefficients of thermal expansion of the soil particles and the water during heating will result in the generation of excess pore water pressures. If drainage is allowed to occur, these excess pore water pressures will dissipate, leading to a time-dependent consolidation. The dissipation of thermally induced excess pore water pressure was found to depend on the rate of heating as well as the hydraulic conductivity of the soil. If the rate of heating is slow, the excess pore water pressures will be able to dissipate at a constant rate, leading to a corresponding volume change. As the volume changes, the hydraulic conductivity will change, leading to slower dissipation. Depending on the rate of heating, the rate of consolidation may be faster than the rate of thermal expansion of the soil particles and water. If a soil is heated quickly, the particles and water will expand much faster than the dissipation of excess pore water pressure. In this case, the thermally induced excess pore water pressures will be generated instantaneously and a consolidation process similar to the conventional theory of consolidation will occur. Because the excess pore water pressures will be generated nearly instantaneously, the hydraulic conductivity will remain at the initial value because of the lack of volume change. The combination of a high gradient and a high hydraulic conductivity will result in more volume change. In this case, the amount of thermal consolidation will be greater than the thermal expansion, leading to a greater net volume change than in the case of slow heating.

REFERENCES

Abdel-Hadi, O. N., and Mitchell, J. K. 1981. Coupled heat and water flows around buried cables. Journal of the Geotechnical Engineering Division, ASCE. 107(11): 1461–1487.

Abuel-Naga, H. M., Bergado, D. T., and Bouazza, A. 2007. Thermally induced volume change and excess pore water pressure of soft Bangkok clay. Engineering Geology, 89: 144–154.

Baldi, G., Hueckel, T., and Pellegrini, R. 1988. Thermal volume changes of the mineral-water system in low-porosity clay soils. Canadian Geotechnical Journal, 25: 807–825.

Boudali, M., Leroueil, S., and Srinivasa, M. B. R. 1994. Viscous behavior of natural clays. *In* Proceedings of the 13th International Conference on Soil Mechanics and Foundation Engineering, New Delhi, 1: 411–416.

Brandl, H. (2006). "Energy Foundations and other Thermo-Active Ground Structures." Géotechnique. 56(2), 81-122.

Campanella, R. G., and Mitchell, J. K. 1968. Influence of temperature variations on soil behavior. Journal of the Soil Mechanics and Foundation Engineering Division, ASCE, 94(SM3): 709–734.

Cekerevac, C., and Laloui, L. 2004. Experimental study of thermal effects on the mechanical behavior of a clay. International Journal for Numerical Analytical Methods Geomechanics, 28: 209–228.

Cekerevac, C., and Laloui, L., and Vulliet, L. 2005. A Novel Triaxial Apparatus for Thermo-Mechanical Testing of Soils. Geotechnical Testing Journal, 28(2): 1–10.

Cui, Y. J., Sultan, N., and Delage, P. 2000. A thermomechanical model for clays. Canadian Geotechnical Journal, 37(3): 607–620.

Cui, Y. J., Le, T. T., Tang, A. M., Delage, P., and Li, X. L. 2009. Investigating the time-dependent behavior of Boom clay under thermomechanical loading. Géotechnique, 59(4): 319–329.

Delage, P., Sultan, N., and Cui, Y. J. 2000. On the thermal consolidation of Boom clay. Canadian Geotechnical Journal, 37: 343–354.

Demars, K. R., and Charles, R. D. 1982. Soil volume changes induced by temperature cycling. Canadian Geotechnical Journal. 19: 188–194.

Energy Information Agency (EIA). (2008). Annual Energy Review. Report No. DOE/EIA-0384(2008).

Eriksson, L. G. 1989. Temperature effects on consolidation properties of sulphide clays. *In* Proceedings of the 12th International Conference on Soil Mechanics and Foundation Engineering, Rio de Janeiro, 3: 2087–2090.

Finn, F. N. 1951. The effects of temperature on the consolidation characteristics of remolded clay. Symposium on Consolidation Testing of Soils, ASTM, Special Technical Publication, No. 126: 65–72.

Gibson, R.E. and Henkel, D.J. 1954. Influence of duration of tests at constant rate of strain on measured 'drain' strength. Geotechnique. 4, 6-15.

Gray, H. 1936. Progress report on the consolidation of fine-grained soils. *In* Proc. of the 1st Int. Conf. on Soil Mechanics and Foundation Engineering, Cambridge, Mass., 138–141.

Hillel, D. 1998. Environmental Soil Physics. Academic Press, San Diego, California, p. 49.

Hueckel, T., and Baldi, M. 1990. Thermoplasticity of saturated clays: experimental constitutive study. Journal of Geotechnical Engineering, 116(12): 1778–1796.

Hueckel, T., and Pellegrini, R. 1992. Effective stress and water pressure in saturated clays during heating-cooling cycles. Canadian Geotechnical Journal, 29: 1095–1102.

Konrad, J.-M. & Morgenstern, N.R. (1980). A mechanistic theory of ice lens formation in fine-grained soils. Can. Geotech. J. 17, No. 4, 473–486.

Lamond,J. F., and Pielert, J. H., ed. 2006. Significance of tests and properties of concrete and concrete-making materials. ASTM International, New Jersey, p. 426.

Lide, D. R., ed. 2010. CRC Handbook of Chemistry and Physics, 90th Edition (Internet Version), CRC Press/Taylor and Francis, Boca Raton, Florida, p. 6-140.

McGinley, J. M. 1983. The effects of temperature on the consolidation process of saturated fine-grained soils. M.S. thesis, Department of Civil, Environmental and Architectural Engineering, University of Colorado, Boulder, Colorado.

McKinstry, H. A. 1965. Thermal expansion of clay minerals. The American Mineralogist, 50: 212–222.

Mitchell, J. K., and Soga, K. 2005. Fundamentals of soil behavior. John Wiley & Sons, Inc., 3rd ed., New Jersey.

Passwell, R. E. 1967. Temperature effects on clay soil consolidation. Journal of the Soil Mechanics and Foundation Engineering Division, ASCE, 93(SM3): 9–22.

Plum, R. L., and Esrig, M. I. 1969. Some temperature effects on soil compressibility and pore water pressure. *In* Effects of temperature and heat on engineering behavior of soils. Highway Research Board, Washington, DC. Special Report, No. 103: 231–242.

Slegel, D. L., and Davis, L. R. 1977. Transient heat and mass transfer in soils in the vicinity of heated porous pipes. Journal of Heat Transfer, 99: 541–621.

Sultan, N. 1997. Etude du comportement thermo-mécanique de l'argile de Boom: expériences et modélisation. Ph.D. thesis, Ecole Nationale des Ponts et Chaussées, Paris.

Sultan, N., Delage, P., and Cui, Y. J. 2002. Temperature effects on the volume change behavior of Boom clay. Engineering Geology, 64: 135–145.

Tidfors, M., and Sällfors, G. 1989. Temperature effect on preconsolidation stress. Geotechnical Testing Journal, 12(1): 93–97.

Towhata, I., Kuntiwattanakul, P., Seko, I., and Ohishi, K. 1993. Volume change of clays induced by heating as observed in consolidation tests. Soils and Foundations, 33(4): 170–183.

Uchaipichat, A., and Khalili, N. 2009. Experimental investigation of thermo-hydro-mechanical behavior of an unsaturated silt. Géotechnique, 59 (4): 339–353